(12) INTERNATIONAL APPLICATION PUBLISHED UNDER THE PATENT COOPERATION TREATY (PCT)

(19) World Intellectual Property Organization
International Bureau

(43) International Publication Date
12 March 2020 (12.03.2020)

WIPO | PCT

(10) International Publication Number
WO 2020/051541 A1

(51) International Patent Classification:
A61K 47/64 (2017.01) *A61K 47/66* (2017.01)
A61K 47/65 (2017.01)

(21) International Application Number:
PCT/US2019/050077

(22) International Filing Date:
06 September 2019 (06.09.2019)

(25) Filing Language: English

(26) Publication Language: English

(30) Priority Data:
62/728,582 07 September 2018 (07.09.2018) US

(71) Applicant: **DUKE UNIVERSITY** [US/US]; 2812 Erwin Road, Suite 306, Durham, NC 27705 (US).

(72) Inventors: **YOUSEFPOUR, Parisa**; c/o Duke University, P.O. Box 90271, Durham, NC 27708-0281 (US). **CHILKOTI, Ashutosh**; 1001 Gloria Avenue, Durham, NC 27701 (US).

(74) Agent: **ZERN, Blaine, J.** et al.; Michael Best & Friedrich LLP, 100 Eaat Wisconsin Avenue, Suite 3300, Milwaukee, WI 53202-4108 (US).

(81) Designated States *(unless otherwise indicated, for every kind of national protection available)*: AE, AG, AL, AM, AO, AT, AU, AZ, BA, BB, BG, BH, BN, BR, BW, BY, BZ, CA, CH, CL, CN, CO, CR, CU, CZ, DE, DJ, DK, DM, DO, DZ, EC, EE, EG, ES, FI, GB, GD, GE, GH, GM, GT, HN, HR, HU, ID, IL, IN, IR, IS, JO, JP, KE, KG, KH, KN, KP, KR, KW, KZ, LA, LC, LK, LR, LS, LU, LY, MA, MD, ME, MG, MK, MN, MW, MX, MY, MZ, NA, NG, NI, NO, NZ, OM, PA, PE, PG, PH, PL, PT, QA, RO, RS, RU, RW, SA, SC, SD, SE, SG, SK, SL, SM, ST, SV, SY, TH, TJ, TM, TN, TR, TT, TZ, UA, UG, US, UZ, VC, VN, ZA, ZM, ZW.

(84) Designated States *(unless otherwise indicated, for every kind of regional protection available)*: ARIPO (BW, GH, GM, KE, LR, LS, MW, MZ, NA, RW, SD, SL, ST, SZ, TZ, UG, ZM, ZW), Eurasian (AM, AZ, BY, KG, KZ, RU, TJ, TM), European (AL, AT, BE, BG, CH, CY, CZ, DE, DK, EE, ES, FI, FR, GB, GR, HR, HU, IE, IS, IT, LT, LU, LV, MC, MK, MT, NL, NO, PL, PT, RO, RS, SE, SI, SK, SM, TR), OAPI (BF, BJ, CF, CG, CI, CM, GA, GN, GQ, GW, KM, ML, MR, NE, SN, TD, TG).

(54) **Title:** NANOPARTICULATE DRUG DELIVERY SYSTEMS

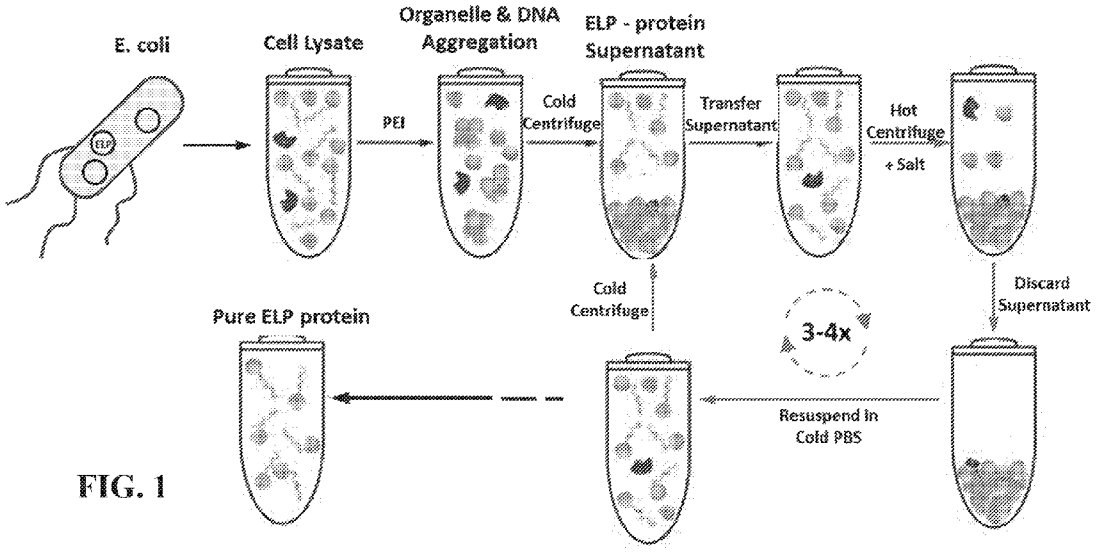

FIG. 1

(57) **Abstract:** Described herein are compositions that include an assembly of self-assembling conjugates. The self-assembling conjugates may include a polypeptide having a transition temperature (17) above 50 °C when the polypeptide is not attached to the conjugate, an albumin binding domain (ABD) attached to a first end of the polypeptide, and at least one molecule attached to a second end of the polypeptide through a cysteine group, wherein the molecule has an octanol- water distribution coefficient (logD) of greater than or equal to 1.5 at a pH of 7.4 when the molecule is not attached to the conjugate. Also described herein are methods of using the compositions.

WO 2020/051541 A1

[Continued on next page]

Published:

— *with international search report (Art. 21(3))*
— *before the expiration of the time limit for amending the claims and to be republished in the event of receipt of amendments (Rule 48.2(h))*
— *with sequence listing part of description (Rule 5.2(a))*

NANOPARTICULATE DRUG DELIVERY SYSTEMS

CROSS-REFERENCE TO RELATED APPLICATIONS

[0001] This application claims priority to U.S. Provisional Application No. 62/728,582 filed on September 7, 2018, which is incorporated fully herein by reference.

SEQUENCE LISTING

[0002] The sequence listing is filed with the application in electronic format only and is incorporated by reference herein. The sequence listing text file "028193-9286-WO01_As_Filed_ Sequence_Listing.txt" was created on September 6, 2019, and is 2,971 bytes in size.

TECHNICAL FIELD

[0003] The present disclosure relates to novel nanoparticulate drug delivery systems.

STATEMENT REGARDING FEDERALLY-SPONSORED RESEARCH OR DEVELOPMENT

[0004] This invention was made with government support under grant number R01EB000188 and R01EB007205 awarded by the National Institutes of Health and DCI/NCSU Consortium for Canine Comparative Oncology grant (2016) The government has certain rights in the invention.

BACKGROUND OF THE INVENTION

[0005] Self-nature of cancer cells and therefore off-target toxicity is the main challenge undermining the efficacy of chemotherapeutic agents. Because of their size, nano-sized carriers in the past decades have provided the opportunity to improve the selectivity of the anti-cancer agents by taking advantage of physiological and anatomical differences between the tumor cells and normal cells. This physical selectivity occurs through a phenomenon known as the enhanced permeation and retention (EPR) effect, caused by the leaky angiogenic vessels and poor lymphatic drainage in tumor tissues. In addition, many anticancer small molecules drugs suffer from poor bioavailability resulting from low water solubility and short plasma half-life. Nanocarriers are sized above the renal filtration cutoff of 5-6 nm and avoid the renal clearance and increase the half-life of their cargo drugs.

[0006] Nanocarriers can solubilize hydrophobic drugs via chemical conjugation or physical entrapment of drugs in their hydrophobic cores. Recently, self-assembling micelles have become

popular pharmaceutical nanocarriers for the delivery of poorly water-soluble anticancer drugs on account of their relatively high drug loading and uncomplicated preparation conditions. However, self-assembling micelles are unstable after injection into the human body due to dilution in the blood stream. Furthermore, micelles can be recognized and taken up by the macrophages of the reticuloendothelial system (mainly the liver and the spleen), which leads to their removal from the systematic circulation. Therefore, there remains a need for new nanoparticulate drug delivery systems that can overcome these disadvantages yet provide efficacy for delivery of poorly water-soluble anti-cancer agents.

BRIEF SUMMARY OF THE INVENTION

[0007] In one aspect, disclosed are compositions comprising an assembly of self-assembling conjugates, each self-assembling conjugate comprising a polypeptide having a transition temperature (T_t) above 50 °C when the polypeptide is not attached to the conjugate; an albumin binding domain (ABD) attached to a first end of the polypeptide; and at least one molecule attached to a second end of the polypeptide through a cysteine group, wherein the molecule has an octanol-water distribution coefficient (logD) of greater than or equal to 1.5 at a pH of 7.4 when the molecule is not attached to the conjugate, wherein the conjugate has a T_t above 40 °C at a concentration of 100μM.

[0008] In another aspect, disclosed are compositions comprising an assembly of self-assembling conjugates, each self-assembling conjugate comprising a polypeptide having a transition temperature (T_t) above 50 °C when the polypeptide is not attached to the conjugate; an albumin binding domain (ABD) attached to a first end of the polypeptide, wherein the ABD attached to the polypeptide lowers the T_t of the polypeptide no more than 5 °C relative to the polypeptide's T_t when the polypeptide is not attached to the ABD or the conjugate; and at least one molecule attached to a second end of the polypeptide through a cysteine group, wherein the molecule has an octanol-water distribution coefficient (logD) of greater than or equal to 1.5 at a pH of 7.4 when the molecule is not attached to the conjugate.

[0009] In another aspect, the disclosure provides a method of killing multiple cancer cells comprising contacting multiple cancer cells with the compositions described herein.

[0010] In another aspect, the disclosure provides a method of treating a disease or disorder in a subject comprising administering to the subject the compositions described herein. In another

aspect, the disclosure provides a method of treating a disease or disorder in a subject comprising administering to the subject the compositions described herein wherein the disease or disorder is cancer.

[0011] In another aspect, the disclosure provides a method of localizing a molecule to a tissue or organ in a subject, the method comprising administering to the subject the compositions described herein, wherein following administration of the composition the molecule is localized in the liver at less than 30% of the injected dose/gram of tissue or organ (ID/g).

[0012] In another aspect, the disclosure provides a method of localizing a molecule to a tissue or organ in a subject, the method comprising administering to the subject the compositions described herein, wherein following administration of the composition the molecule is localized in the spleen at less than 10% of the injected dose/gram of tissue or organ (ID/g).

[0013] In another aspect, the disclosure provides a method of localizing a molecule to a tissue or organ in a subject, the method comprising administering to the subject the compositions described herein, wherein following administration of the composition the amount of the molecule localized in a tissue or organ is decreased when compared to the same molecule in a self-assembling conjugate without an albumin binding domain and wherein the tissue or organ is the kidney, liver, spleen or any combination thereof.

[0014] In another aspect, the disclosure provides a method of localizing a molecule to a tumor in a subject, the method comprising administering to the subject the compositions described herein, wherein following administration of the composition the amount of the molecule localized to the tumor is increased when compared to the same molecule in a self-assembling conjugate without an albumin binding domain.

BRIEF DESCRIPTIONS OF THE DRAWINGS

[0015] FIG. 1 shows a schematic overview of inverse transition cycling which may be used to purify elastin-like polypeptide (ELP) proteins.

[0016] FIG. 2A, FIG. 2B and FIG. 2C show the characterization of albumin binding domain (ABD)-ELP monomers. FIG. 2A shows the sodium dodecyl sulfate–polyacrylamide gel electrophoresis (SDS-PAGE) analysis of purified albumin binding domain N and H (ABDN/H-) ELP polypeptides. Successful purification of (ABDN/H-)ELPs by inverse transition cycling is confirmed by SDS-PAGE. Main band corresponds to the molecular weight of ELP (63.6 kDa),

ABDN-ELP (68.5 kDa), and ABDH-ELP (68.6 kDa) and a second faint band indicates the presence of the corresponding polypeptide dimers. FIG. 2B shows the Native-PAGE analysis of interaction of human serum albumin (HSA) and mouse serum albumin (MSA) with (ABDN/H-) ELP. For lanes 5-7 and lanes 9-11, polypeptide carriers were mixed at a molar ratio of 1:1 with MSA and HSA, respectively. FIG. 2C shows the pharmacokinetics of ELP, ABDN-ELP and ABDH-ELP carriers. Polypeptides were labeled with Alexa488 and were administered via tail vein to Balb/C mice (n = 6-7) and plasma concentrations were measured at intervals over 72 h. The data was fitted to a two-compartment model from which pharmacokinetic parameters were estimated as shown in Table 1.

[0017] FIG. 3A, FIG. 3B and FIG. 3C show the calorimetric titrations of HSA with (ABDN/H-) ELP. The experiments were performed in phosphate buffered saline (pH 7.4) at 37 °C. The solid line indicates the best-fit binding isotherm. FIG. 3A shows the titration of HSA into ELP with a binding stoichiometry N = 0.75 ± 0.16 and dissociation constant K_D = 69.03 ± 15.51 μM. FIG. 3B shows the titration of HSA into ABDN-ELP with a binding stoichiometry N = 1.04 ± 0.00 and dissociation constant K_D = 48.4 ± 3.82 nM. FIG. 3C shows the titration of HSA into ABDH-ELP with a binding stoichiometry N = 1.07 ± 0.00 and dissociation constant K_D = 4.19 ± 1.07 nM.

[0018] FIG. 4A, FIG. 4B and FIG. 4C show calorimetric titrations of MSA with (ABDN/H-) ELP. The experiments were performed in phosphate buffered saline (pH 7.4) at 37 °C. The solid line indicates the best-fit binding isotherm. FIG. 4A shows the titration of MSA into ELP with a binding stoichiometry N = 0.1525 ± 0.17 and dissociation constant K_D = 71.4 ± 12.24 μM. FIG. 4B shows the titration of MSA into ABDN-ELP with a binding stoichiometry N = 1.12 ± 0.00 and dissociation constant K_D = 66.36 ± 10.65 nM. FIG. 4C shows the titration of MSA into ABDH-ELP with a binding stoichiometry N = 1.04 ± 0.00 and dissociation constant K_D = 5.19 ± 1.85 nM.

[0019] FIG. 5 shows a schematic of intravenous administration of assemblies of self-assembling conjugates.

[0020] FIG. 6A, FIG. 6B, FIG. 6C and FIG. 6D show the *in vitro* characterization of ABD-chimeric polypeptide (CP – CP and ELP are used interchangeably herein)- Doxorubicin (DOX) micelles. FIG. 6A shows the native-PAGE analysis of the interactions of HSA and MSA with (ABDN/H-) ELP. For lanes 5-7 and lanes 9-11, polypeptide carriers were mixed at a molar ratio

of 1:1 with MSA and HSA, respectively. FIG. 6B shows the cytotoxicity of ABDN-CP-DOX vs. CP-DOX and free DOX in C26 cells after 72 h incubation. IC50 was measured as 0.09 μM for free DOX, 0.30 μM for CP-DOX, and 0.31 μM for ABDN-CP-DOX. Error bars represent standard error of the mean (n=3). FIG. 6C shows the cryo-TEM micrographs of CP–DOX (left) and ABDN-CP-DOX micelles (right). FIG. 6D shows the *in vitro* drug release profile from CP-DOX and ABDN-CP-DOX micelles. The micelles released the loaded DOX under acidic conditions at pH 5.0 corresponding to intracellular space, but remained stable at pH 7.4 corresponding to vascular and extracellular space.

[0021] FIG. 7A, FIG. 7B and FIG. 7C show the calorimetric titrations of MSA with (ABDN/H-)CP-DOX micelles. The experiments were performed in phosphate buffered saline (pH 7.4) at 37 °C. The solid line indicates the best-fit binding isotherm. FIG. 7A shows the titration of MSA into CP-DOX with a binding stoichiometry N = 0.0386 ± 0.09 and dissociation constant K_D = 91.91 ± 68.36 μM. FIG. 7B shows the titration of MSA into ABDN-CP-DOX with a binding stoichiometry N = 1.01 ± 0.00 and dissociation constant K_D = 317.56 ± 53.55 nM. FIG. 7C shows the titration of MSA into ABDH-CP-DOX with a binding stoichiometry N = 0.99 ± 0.01 and dissociation constant K_D = 66.09 ± 20.20 nM.

[0022] FIG. 8A, FIG. 8B, FIG. 8C and FIG. 8D show the thermal phase transition behavior of (ABDN/H-)ELP and (ABDN/H-)CP-DOX. The Transition temperature (T_t) of empty carriers and DOX-conjugated micelles was determined by monitoring the turbidity as a function of temperature in PBS, FBS, and MS. FIG. 8A shows that ELP and CP-DOX exhibited a lower T_t in FBS and MS than that in PBS. In addition, CP-DOX exhibited a lower and less-concentration-dependent T_t than the empty carrier ELP. ABDN-CP-DOX (FIG. 8B) and ABDH-CP-DOX (FIG. 8C) also exhibited a lower and less-concentration-dependent T_t than their corresponding empty carriers. For ABDN-ELP and ABDH-ELP, the difference in T_t in FBS and PBS was not as significant as that for ELP. ABDN-CP-DOX and ABDH-CP-DOX exhibited a higher T_t in FBS than in PBS. None of the ABDN- and ABDH-fused carriers and micelles transitioned in MS. FIG. 8D shows a summary of transition temperatures of CP, ABD-CP and DOX conjugates in PBS.

[0023] FIG. 9A and FIG. 9B show dynamic light scattering graphs for CP-ABDN-DOX (FIG. 9A) and KEKE-CP-ABDN-DOX (FIG. 9B).

[0024] FIG. 10A, FIG. 10B, FIG. 10C, FIG. 10D and FIG. 10E show the *in vivo* characterization of ABD-CP-DOX micelles. FIG. 10A shows the pharmacokinetics of ABDN-CP-DOX micelles vs CP-DOX micelles. CP-DOX and ABDN-CP-DOX micelles were administered via tail vein to Balb/C mice (n = 5-6) at 10 and 20 mg/kg body weight (BW) DOX equivalent and plasma DOX concentration was measured at intervals over 72 h. The data was fitted to a two-compartment model from which pharmacokinetic parameters were estimated as shown in Table 3. FIG. 10B and FIG. 10C show the biodistribution of ABDN-CP-DOX micelles vs CP-DOX micelles. C26 tumor cells were implanted subcutaneously and allowed to grow to approximately 75-100 mm^3. Mice were treated with free DOX, CP–DOX, and ABDN-CP-DOX all at 10 and 20 mg DOX Equiv. kg−1BW. The DOX concentration was measured in tumor and normal tissues at 2 h (FIG. 10C) and 24 h (FIG. 10B) post-administration. FIG. 10D and FIG. 10E show the anti-tumor activity of ABDN-CP–DOX micelles. C26 tumor cells were implanted subcutaneously and allowed to grow to approximately 75-100 mm^3. Mice were treated on day 0 with free DOX (10 mgkg−1 BW), CP–DOX (20 mg DOX Equiv. kg−1BW), and ABDN-CP-DOX (20 mg DOX Equiv. kg−1BW). FIG. 10D shows the tumor volume up to day 60 (mean ± SEM; n=6–10). FIG. 10E shows the cumulative survival of mice up to day 60 (n=6–10).

[0025] FIG. 11 shows a line graph of the pharmacokinetics of ABDN-CP-DOX micelles in dogs. Free DOX, CP-DOX micelles and ABDN-CP-DOX micelles were administered via the cephalic vein at 27 DOX Equiv.m^{-2} body surface area for dogs weighing greater than 10 kg and 0.9 mg DOX Equiv.kg^{-1} of body weight for dogs weighing less than 10 kg, and plasma DOX concentration was measured at intervals over 72 h. The data was fit to a two-compartment model from which pharmacokinetic parameters were estimated.

[0026] FIG. 12A, FIG. 12B, FIG. 12C, FIG. 12D, FIG. 12E, FIG. 12F and FIG. 12G show the biodistribution of ABDN-CP-DOX micelles vs CP-DOX micelles at 2 h post administration. C26 tumor cells were implanted subcutaneously and allowed to grow to approximately 75-100 mm^3. Mice were treated with free DOX at 10 $mgkg^{-1}$BW, and with CP–DOX, and ABDN-CP-DOX at 10 and 20 mg DOX Equiv. kg^{-1}BW. The DOX concentration was measured in tumor (FIG. 12A), liver (FIG. 12B), spleen (FIG. 12C), heart (FIG. 12D), lung (FIG. 12E), kidney (FIG. 12F), and muscle (FIG. 12G) at 2 h post-administration. Error bars represent standard error of the mean (n=4-7). * $P < 0.05$, ** $P < 0.01$, *** $P < 0.001$.

[0027] FIG. 13A, FIG. 13B, FIG. 13C, FIG. 13D, FIG. 13E, FIG. 13F and FIG. 13G show the biodistribution of ABDN-CP-DOX micelles vs CP-DOX micelles at 24 h post administration. C26 tumor cells were implanted subcutaneously and allowed to grow to approximately 75-100 mm^3. Mice were treated with free DOX at 10 $mgkg^{-1}BW$, and with CP–DOX, and ABDN-CP-DOX at 10 and 20 mg DOX Equiv. $kg^{-1}BW$. The DOX concentration was measured in tumor (FIG. 13A), liver (FIG. 13B), spleen (FIG. 13C), heart (FIG. 13D), lung (FIG. 13E), kidney (FIG. 13F), and muscle (FIG. 13G) at 2 h post-administration. Error bars represent standard error of the mean (n=6-8). * $P < 0.05$, ** $P < 0.01$, *** $P < 0.001$.

[0028] FIG. 14A, FIG. 14B, FIG. 14C and FIG. 14D show the anti-tumor activity of ABDN-CP–DOX micelles. C26 tumor cells were implanted subcutaneously and allowed to grow to approximately 75-100 mm^3. Mice were treated on day 0 with CP–DOX and ABDN-CP-DOX. Tumor volume up to day 60 (mean ± SEM.; n=6–10) following treatment at the dose of 10 mg and 40 mg (FIG. 14C) DOX Equiv. kg−1BW. Cumulative survival of mice up to day 60 (n=6–10) following treatment at the dose of 10 mg (FIG. 14B) and 40 mg (FIG. 14D) DOX Equiv. kg−1BW.

[0029] FIG. 15A, FIG. 15B and FIG. 15C show the dose escalation in healthy mice. Increasing concentrations of free DOX (A), CP-DOX (B), and ABDN-CP-DOX (C) were administered intravenously in healthy Balb/C mice on day 0. Concentrations include 5, 10, 15, and 20 mg Dox Equiv kg-1 BW for free DOX and 20, 40, 50, and 60 mg DOX equiv/kg BW for CP-DOX, and ABDN-CP-DOX. Non-DOX-conjugated ELP and ABDN-ELP carriers were administered at protein concentration equivalent to the protein concentration in 60 mg DOX equiv/kg BW CP-DOX and ABDN-CP-DOX treatments. Error bars represent standard error of the mean (n=5).

[0030] FIG. 16A and FIG. 16B show paclitaxel (PTX) loading of ABD-CP (FIG. 16A) and CP (FIG. 16B) by MALDI-TOF-MS.

[0031] FIG. 17A and FIG. 17B show the dynamic light scattering graphs for CP-PTX (FIG. 17A) and ABD-CP-PTX (FIG. 17B).

[0032] FIG. 18A and FIG. 18B show the static light scattering graphs for CP-PTX (FIG. 18A) and ABD-CP-PTX (FIG. 18B).

[0033] FIG. 19A and FIG. 19B show the calorimetric titration of HSA with ABD-CP-PTX and ABD-CP (FIG. 19A) and CP and CP-PTX (FIG. 19B).

[0034] FIG. 20A and FIG. 20B show the calorimetric titration of MSA with ABD-CP-PTX and ABD-CP (FIG. 20A) and CP and CP-PTX (FIG. 20B).

[0035] FIG. 21 shows *in vitro* cell line cytotoxicity of MDA-MB-231 human breast cancer cells treated with CP-PTX, ABD-CP-PTX and Free PTX. The EC_{50} represents the relative 50% cell killing dose and IC_{50} is the absolute 50% cell killing dose.

[0036] FIG. 22 shows a schematic of a self-assembling conjugate and assembly thereof.

DETAILED DESCRIPTION OF THE INVENTION

[0037] Disclosed herein are compositions for nanoparticulate delivery systems. The compositions comprise an assembly of self-assembling conjugates which provide improved pharmacokinetics and biodistribution of a molecule. The self-assembling conjugates can increase localization of a molecule to a tumor and can decrease molecule accumulation in the organs and tissues of the reticuloendothelial system and, therefore, can provide enhanced antitumor activity of a chemotherapeutic.

1. Definitions

[0038] Unless otherwise defined, all technical and scientific terms used herein have the same meaning as commonly understood by one of ordinary skill in the art. In case of conflict, the present document, including definitions, will control. Preferred methods and materials are described below, although methods and materials similar or equivalent to those described herein can be used in practice or testing of the present invention. All publications, patent applications, patents and other references mentioned herein are incorporated by reference in their entirety. The materials, methods, and examples disclosed herein are illustrative only and not intended to be limiting.

[0039] The terms "comprise(s)," "include(s)," "having," "has," "can," "contain(s)," and variants thereof, as used herein, are intended to be open-ended transitional phrases, terms, or words that do not preclude the possibility of additional acts or structures. The singular forms "a," "an" and "the" include plural references unless the context clearly dictates otherwise. The present disclosure also contemplates other embodiments "comprising," "consisting of" and "consisting essentially of," the embodiments or elements presented herein, whether explicitly set forth or not.

[0040] The modifier "about" used in connection with a quantity is inclusive of the stated value and has the meaning dictated by the context (for example, it includes at least the degree of error associated with the measurement of the particular quantity). The modifier "about" should also be considered as disclosing the range defined by the absolute values of the two endpoints. For example, the expression "from about 2 to about 4" also discloses the range "from 2 to 4." The term "about" may refer to plus or minus 10% of the indicated number. For example, "about 10%" may indicate a range of 9% to 11%, and "about 1" may mean from 0.9-1.1. Other meanings of "about" may be apparent from the context, such as rounding off, so, for example "about 1" may also mean from 0.5 to 1.4.

[0041] For the recitation of numeric ranges herein, each intervening number there between with the same degree of precision is explicitly contemplated. For example, for the range of 6-9, the numbers 7 and 8 are contemplated in addition to 6 and 9, and for the range 6.0-7.0, the number 6.0, 6.1, 6.2, 6.3, 6.4, 6.5, 6.6, 6.7, 6.8, 6.9, and 7.0 are explicitly contemplated.

[0042] As used herein, the terms "administering," "providing" and "introducing" are used interchangeably herein and refer to the placement of the compositions of the disclosure into a subject by a method or route which results in at least partial localization of the composition to a desired site. The compositions can be administered by any appropriate route which results in delivery to a desired location in the subject.

[0043] "Amino acid" as used herein refers to naturally occurring and non-natural synthetic amino acids, as well as amino acid analogs and amino acid mimetics that function in a manner similar to the naturally occurring amino acids. Naturally occurring amino acids are those encoded by the genetic code. Amino acids can be referred to herein by either their commonly known three-letter symbols or by the one-letter symbols recommended by the IUPAC-IUB Biochemical Nomenclature Commission. Amino acids include the side chain and polypeptide backbone portions.

[0044] As used herein, the term "chemotherapeutic" or "anti-cancer drug" includes any drug used in cancer treatment. Chemotherapeutics include, but are not limited to, cyclophosphamide, methotrexate, 5-fluorouracil, doxorubicin, cyclophosphamide, docetaxel, doxorubicin, daunorubicin, bleomycin, vinblastine, dacarbazine, cisplatin, paclitaxel and docetaxel.

[0045] The terms "effective amount" or "therapeutically effective amount," as used herein, refer to a sufficient amount of an agent or a composition or combination of compositions being

administered which will relieve to some extent one or more of the symptoms of the disease or condition being treated. The result can be reduction and/or alleviation of the signs, symptoms, or causes of a disease, or any other desired alteration of a biological system. For example, an "effective amount" for therapeutic uses is the amount of the composition as disclosed herein required to provide a clinically significant decrease in disease symptoms. An appropriate "effective" amount in any individual case may be determined using techniques, such as a dose escalation study. The dose could be administered in one or more administrations. However, the precise determination of what would be considered an effective dose may be based on factors individual to each patient, including, but not limited to, the patient's age, size, type or extent of disease, stage of the disease, route of administration, the type or extent of supplemental therapy used, ongoing disease process and type of treatment desired (e.g., aggressive vs. conventional treatment).

[0046] As used herein, the term "hydrodynamic radius" or "R_h" refers to the measurement from dynamic light scattering for the radius of an equivalent hard sphere diffusing at the same rate as the molecule under observation. As such, the radius reflects the apparent size of the solvated, tumbling molecule. Alternatively, the radius of gyration (R_g), is the mass weighted average distance from the core of the molecule to each mass element in the molecule.

[0047] The term "imaging agent," as used herein, refers to a molecule or compound that can be detected directly or after applying a stimulus. Imaging agents may include luminescent labels which emit radiation on exposure to an external source of radiation or other stimulus, radioactive labels, NMR-active labels, or heavy atoms.

[0048] As used herein, the term "micelle" refers to an organized auto-assembly of molecules formed in a liquid where the hydrophilic regions are in contact with the surrounding solvent and the hydrophobic regions are sequestered in the center or core of the micelle. In some embodiments, the micelle may be a nanoparticle.

[0049] As used herein, the term "nanoparticle" refers to a particle with at least one dimension less than about 100 nm. Nanoparticles include, but are not limited to, nanopowders, nanoclusters, nanocrystals, and micelles.

[0050] As used herein, the term "octanol-water distribution coefficient" refers to a measure of the degree of hydrophilicity or hydrophobicity of a chemical substance, for example a drug. The measurement is the ratio of the sum of the concentrations of all forms of the compound

(ionized plus un-ionized) in each of two immiscible phases, one hydrophobic and one hydrophilic phase, at equilibrium. The measurement is pH dependent, and the aqueous phase is usually buffered to a specific value. The larger the octanol-water distribution coefficient; the more hydrophobic the chemical substance becomes. The smaller the octanol-water distribution coefficient, the more hydrophilic.

[0051] A “peptide” or “polypeptide” is a linked sequence of two or more amino acids linked by peptide bonds. The polypeptide can be natural, synthetic, or a modification or combination of natural and synthetic. Domains are portions of a polypeptide or protein that form a compact unit and are typically 15 to 350 amino acids long.

[0052] A “subject” or “patient” may be human or non-human and may include, for example, animal strains or species used as “model systems” for research purposes, such as a mouse model as described herein. Likewise, patient may include either adults or juveniles (*e.g.*, children). Moreover, patient may mean any living organism, preferably a mammal (*e.g.*, human or non-human) that may benefit from the administration of compositions contemplated herein. Examples of mammals include, but are not limited to, any member of the Mammalian class: humans, non-human primates such as chimpanzees, and other apes and monkey species; farm animals such as cattle, horses, sheep, goats, swine; domestic animals such as rabbits, dogs, and cats; laboratory animals including rodents, such as rats, mice and guinea pigs, and the like. Examples of non-mammals include, but are not limited to, birds, fish and the like. In some embodiments of the methods and compositions provided herein, the mammal is a human.

[0053] As used herein, the term “thiol” refers to a carbon-bonded sulfhydryl (-SH) group.

[0054] As used herein, the term “transition temperature” or “T_t” refers to the temperature at which the conjugate (or polypeptide) changes from one state to another, for example, soluble to insoluble. For example, below the T_t, the conjugate may be highly soluble. Upon heating above the transition temperature, for example, the conjugate may aggregate, forming a separate phase.

[0055] As used herein, "treat," "treating" and the like mean a slowing, stopping or reversing of progression of a disease or disorder when provided a composition described herein to an appropriate subject. The terms can also mean a reversing of the progression of such a disease or disorder to a point of eliminating or greatly reducing the cell proliferation. As such, "treating" means an application or administration of the compositions described herein to a subject, where

the subject has a disease or a symptom of a disease, where the purpose is to cure, heal, alleviate, relieve, alter, remedy, ameliorate, improve or affect the disease or symptoms of the disease.

2. Self-Assembling Conjugates

[0056] Provided herein are compositions comprising an assembly of self-assembling conjugates. The disclosed assembly of self-assembling conjugates can encapsulate drugs, while also being able to bind albumin. The ability of the self-assembling conjugate (and assembly thereof) to bind albumin can improve pharmacokinetic properties of the drug, which can ultimately be useful for drug delivery applications.

[0057] The ability of the assembly to encapsulate drugs and bind albumin can be attributed to the different components of the self-assembling conjugate (also referred to as "conjugate" herein). For example, each self-assembling conjugate independently comprises a polypeptide having a transition temperature (T_t) above 50 °C when the polypeptide is not attached to the conjugate (e.g., when the polypeptide is an individual molecule relative to part of the conjugate); an albumin binding domain (ABD) attached to a first end of the polypeptide; and at least one molecule attached to a second end of the polypeptide through a cysteine group, wherein the molecule has an octanol-water distribution coefficient (logD) of greater than or equal to 1.5 at a pH of 7.4 when the molecule is not attached to the conjugate, wherein the conjugate has a T_t above 40 °C at a concentration of 100μM.

[0058] In some embodiments, the assembly of self-assembling conjugates comprises a polypeptide having a T_t above 50 °C when the polypeptide is not attached to the conjugate; a ABD attached to a first end of the polypeptide, wherein the ABD attached to the polypeptide lowers the T_t of the polypeptide no more than 5 °C relative to the polypeptide's T_t when the polypeptide is not attached to the ABD or the conjugate; and at least one molecule attached to a second end of the polypeptide through a cysteine group, wherein the molecule has an octanol-water distribution coefficient (logD) of greater than or equal to 1.5 at a pH of 7.4 when the molecule is not attached to the conjugate.

[0059] The assembly of self-assembling conjugates can comprise a plurality of conjugates. For example, the assembly of self-assembling conjugates may include about 10 to about 200 self-assembling conjugates per assembly, such as about 10 to about 100 self-assembling conjugates per assembly, about 50 to about 200 self-assembling conjugates per assembly, about

10 to about 75 self-assembling conjugates per assembly, about 15 to about 60 self-assembling conjugates per assembly, or about 20 to about 60 self-assembling conjugates per assembly.

a) Polypeptide

[0060] The self-assembling conjugate may include a polypeptide. The polypeptide can have a T_t, which makes it thermally responsive. In some embodiments, the polypeptide comprises one or more thermally responsive polypeptides. The unconjugated polypeptide (e.g., the polypeptide as an individual molecule not conjugated to the ABD domain or molecule) may have phase transition behavior, wherein the unconjugated polypeptide changes phase at its T_t. Phase transition may refer to the aggregation of the polypeptide, which may occur sharply and in some instances reversibly at or above the T_t. The T_t of the polypeptide can be adjusted by varying the amino acid sequence of the polypeptide, by varying the length of the polypeptide, or a combination thereof. The T_t of the unconjugated polypeptide may be above 50 °C, such as above 55 °C, above 60 °C, or above 65 °C. In some embodiments, the T_t of the unconjugated polypeptide may be below 80 °C, below 75 °C, or below 70 °C. In addition, the T_t of the unconjugated polypeptide may instill phase transition behavior to the self-assembling conjugate. Accordingly, the T_t of the unconjugated polypeptide may affect the T_t of the conjugate.

[0061] Thermally responsive polypeptides may include, for example, elastin-like polypeptides (ELP). In some embodiments, the polypeptide is an ELP. "ELP" refers to a polypeptide comprising the pentapeptide repeat sequence $(VPGXG)_n$ (SEQ ID NO:1), wherein X is any amino acid except proline and n is an integer greater than or equal to 1. In some embodiments, the polypeptide comprises an amino acid sequence of $(X^1GVPG)_x$ (SEQ ID NO:2), wherein X^1 is an amino acid or a combination of amino acids and x is an integer from 40 to 400. In some embodiments, x is an integer from 40 to 300, from 40 to 200, from 40 to 100, from 100 to 200, from 100 to 300, from 100 to 400, from 200 to 300, from 200 to 400, or from 300 to 400. In some embodiments, X^1 is A, V, G, or a combination thereof. In some embodiments, the polypeptide comprises an amino acid sequence of $(X^1GVPG)_m$ (SEQ ID NO:3), wherein X^1 is A or V:A:G at a ratio of 1:7:8 and m is 160. In some embodiments, the polypeptide is an amino acid sequence of $(X^1GVPG)_m$ (SEQ ID NO:3), wherein X^1 is A or V:A:G at a ratio of 1:7:8 and m is 160.

[0062] In some embodiments, the polypeptide comprises a short cysteine containing sequence that can be used for fluorophore labeling, dug conjugation, or a combination thereof. In some embodiments, the short cysteine containing sequence is on the C-terminus of the polypeptide. In some embodiments, the short cysteine containing sequence is on the N-terminus of the polypeptide. In some embodiments, the polypeptide comprises an amino acid sequence of $(CGG)_z$ (SEQ ID NO:4), wherein z is an integer greater than 1. In some embodiments, z is an integer from 1 to 40, from 1 to 30, from 1 to 20, or from 1 to 10. In some embodiments, z is an integer from 5 to 10. In some embodiments, the polypeptide comprises an amino acid sequence of $(CGG)_8$ (SEQ ID NO:5) at its C-terminus.

b) Albumin Binding Domain

[0063] The self-assembling conjugate may include an albumin binding domain (ABD). The albumin binding domain can bind albumin *in vivo* or *in vitro*. The ABD may be attached to the C-terminus or the N-terminus of the polypeptide. In some embodiments, the ABD is attached to the N-terminus of the polypeptide. In some embodiments, the ABD comprises a 46 amino acid polypeptide (SEQ ID NO:6) derived from bacterial protein G (also referred to as "ABDN"). In some embodiments, the ABD may be SEQ ID NO:6. The albumin binding domain may be from any animal species, including but not limited to, human and rodent.

[0064] In some embodiments, the ABD may comprise an engineered variant of ABDN (SEQ ID NO:7) (also referred to as "ABDH"). In some embodiments, the ABD may be SEQ ID NO:7. In some embodiments, the ABD may be an engineered variant of ABDN that exhibits a different binding affinity for albumin compared to ABDN. For example, ABDH exhibits higher affinity for albumin compared to ABDN.

[0065] As described above, the unconjugated polypeptide can have phase transition behavior. Attachment of the ABD to the end of the polypeptide may affect the phase transition behavior of the polypeptide. In some embodiments, the ABD attached to the polypeptide lowers the T_t of the polypeptide no more than 5 °C relative to the polypeptide's T_t when the polypeptide is not attached to the ABD or the conjugate, such as no more than 4.5 °C relative to the polypeptide's T_t when the polypeptide is not attached to the ABD or the conjugate, no more than 4 °C relative to the polypeptide's T_t when the polypeptide is not attached to the ABD or the conjugate, no more than 3.5 °C relative to the polypeptide's T_t when the polypeptide is not attached to the

ABD or the conjugate, or no more than 3 °C relative to the polypeptide's T_t when the polypeptide is not attached to the ABD or the conjugate. In some embodiments, the ABD attached to the polypeptide lowers the T_t of the polypeptide no more than 5 °C relative to the polypeptide's T_t when the polypeptide is not attached to the ABD or the conjugate. The T_t of the polypeptide (and conjugate) can be adjusted by varying the amino acid sequence of the ABD, by varying the length of the ABD, or a combination thereof.

c) Molecule

[0066] The self-assembling conjugate may include a molecule. The molecule may be located in the core of the assembly of self-assembling conjugates. The molecule may be characterized by its octanol-water distribution coefficient (logD), where a larger value indicates greater hydrophobicity. For example, the molecule may have a log(D) of greater than or equal to 1.5 at a pH of 7.4, greater than or equal to 2 at a pH of 7.4, greater than or equal to 3 at a pH of 7.4, greater than or equal to 4 at a pH of 7.4, or greater than or equal to 5 at a pH of 7.4. In some embodiments, the molecule has a logD of about 1.5 to about 5 at a pH of 7.4.

[0067] The molecule may be a drug molecule, such as a chemotherapeutic. Such chemotherapeutic agents are well known in the art and may include, for example, doxorubicin, paclitaxel, gemcitabine, docetaxel, taxol, SN-38, irinotecan and letrozole. In some embodiments, the chemotherapeutic is doxorubicin or paclitaxel.

[0068] The molecule may be an imaging agent. Imaging agents include luminescent labels which emit radiation on exposure to an external source of radiation or other stimulus, e.g. fluorescent materials or fluorophores, chemiluminescent materials, electroluminescent materials, phosphorescent materials, quantum dots and thermoluminescent materials. Examples of fluorophores include fluoresceins, xanthenes, cyanines, naphthalenes, coumarins, oxadiazoles, pyrenes, oxazines, acridines, arylmethines, Alexa Fluors and tetrapyrroles.

[0069] Other imaging agents include radioactive labels, including positron emitting nuclei such as ^{18}F, ^{64}Cu or ^{124}I which can be detected by imaging techniques such as positron emission topography (PET). Other radioactive labels such as ^{14}C, ^{3}H, or iodine isotopes such as ^{123}I and ^{131}I, which can be detected using autoradiographic analysis or scintillation detection for example, can also be used. Imaging agents may include those which can be detected by magnetic resonance techniques, for example magnetic resonance imaging (MRI) or nuclear magnetic

resonance (NMR) detectors, the agents typically comprising one or more NMR-active nuclei that are not generally found in concentrated form elsewhere in the organism or biological sample, for example, ^{13}C, ^{2}H (deuterium) or ^{19}F. Further imaging agents include those which are effective contrast agents for X-ray photographic techniques or computed tomography (CT) imaging techniques generally comprising atoms with large nuclei, for example atoms with atomic number of 35 or more, preferably 40 or more and even more preferably 50 or more, for example iodine or barium.

[0070] The self-assembling conjugate may include varying amounts of the molecule. In some embodiments, the self-assembling conjugate may include at least one molecule. In some embodiments, the self-assembling conjugate may include about 1 to about 15 molecules. In some embodiments, the self-assembling conjugate may include about 2 to about 12 molecules, about 3 to about 10 molecules, or about 5 to about 8 molecules.

[0071] In some embodiments, the molecule is attached to the polypeptide through a thiol group. The thiol group may react with many chemical groups known in the art including, but not limited to, haloacetyls, maleimides, hydrazides, aziridines and acryloyls. The attachment of the molecule to the polypeptide may be through a hydrazide linkage. In some embodiments, the molecule is attached to the polypeptide through a pH dependent linker.

d) Phase transition

[0072] As mentioned above, the self-assembling conjugate can have phase transition behavior. The self-assembling conjugate can have a T_t that is the same or different than that of the polypeptide. As described above with respect to the polypeptide, the conjugate may also have phase transition behavior wherein the conjugate changes phase at its T_t. Phase transition may refer to the aggregation of the conjugate(s), which may occur sharply and in some instances reversibly at or above the T_t. The T_t of the conjugate may be dependent on the T_t of the unconjugated polypeptide. In addition, the T_t of the conjugate may be affected by the ABD and/or the molecule. Accordingly, the conjugate can have a varying T_t depending on the components/domains that it comprises. For example, the conjugate can have a T_t above 40 °C, above 45 °C, above 50 °C, or above 60 °C. In some embodiments, the conjugate can have a T_t below 80 °C, below 75 °C, below 70 °C, or below 65 °C.

[0073] The conjugate may undergo phase transition at varying concentrations. For example, the conjugate may phase transition at a concentration of about 5 μM to about 1 M, such as about 10 μM to about 500 μM, about 15 μM to about 250 μM, about 20 μM to about 150 μM, or about 25 μM to about 100 μM. In some embodiments, the conjugate phase transitions at a concentration that is suitable for administration to a subject. In some embodiments, the conjugate can have a T_t above 40 °C at a concentration of 100 μM, a T_t above 45 °C at a concentration of 100 μM, a T_t above 50 °C at a concentration of 100 μM, or a T_t above 60 °C at a concentration of 100 μM.

[0074] Phase transition behavior may also enable purification of the conjugate using inverse transition cycling, thereby eliminating the need for chromatography. "Inverse transition cycling" refers to a protein purification method for polypeptides having phase transition behavior, and the method may involve the use of the conjugate's reversible phase transition behavior to cycle the solution through soluble and insoluble phases, thereby removing contaminants and eliminating the need for chromatography.

e) Nanoparticles

[0075] The assembly of self-assembling conjugates may self-assemble into a variety of shapes and sizes. In some embodiments, the assembly of self-assembling conjugates may be a nanoparticle. The nanoparticle may be rod-shaped or spherical, or the composition may include combinations of differently shaped nanoparticles. In some embodiments, the molecule is located in the core of the nanoparticle. In some embodiments, the ABD is located on the periphery of the nanoparticle. In some embodiments, the nanoparticle is a micelle.

[0076] The nanoparticle may have a varying average hydrodynamic radius. In some embodiments, the nanoparticle can have an average hydrodynamic radius of about 10 nm to about 100 nm, such as about 25 nm to about 75 nm, or about 40 nm to about 60 nm. In some embodiments, the nanoparticle may have an average hydrodynamic radius of greater than 10 nm, greater than 20 nm, greater than 30 nm, greater than 40 nm, or greater than 50 nm. In some embodiments, the nanoparticle may have an average hydrodynamic radius of less than 100 nm, less than 90 nm, less than 80 nm, less than 70 nm, less than 60 nm, or less than 50 nm.

[0077] The nanoparticle may also be described by its average radius of gyration. For example, the nanoparticle may have an average radius of gyration of about 10 nm to about 100

nm, such as about 25 nm to about 75 nm or about 40 nm to about 60 nm. In some embodiments, the nanoparticle may have an average radius of gyration of greater than 10 nm, greater than 20 nm, greater than 30 nm, greater than 40 nm, or greater than 50 nm. In some embodiments, the nanoparticle may have an average radius of gyration of less than 100 nm, less than 90 nm, less than 80 nm, less than 70 nm, less than 60 nm, or less than 50 nm.

3. Methods of Use

a) Method of Killing Cancer Cells

[0078] The present disclosure also provides a method of killing multiple cancer cells. The method may include contacting multiple cancer cells with the composition as detailed herein to the subject. The cancer cells may be in an *in vitro* environment or an *in vivo* environment. In some embodiments, the cancer cells are in a subject. Many different types of cancer cells may be killed by chemotherapeutics. The compositions as detailed herein may be used to deliver chemotherapeutics to any cancer cell type.

b) Method of Treating a Disease or Disorder

[0079] The present disclosure also provides methods of treating a disease or disorder. The methods comprise administering an effective amount of the composition as detailed herein to the subject.

[0080] In some embodiments, the disease or disorder is cancer. Many different cancer types and subtypes may be treated by chemotherapeutics. The compositions as detailed herein may be used to deliver chemotherapeutics to any cancer type or subtype. In some embodiments, the cancer may be a carcinoma, sarcoma, lymphoma, leukemia, melanoma, mesothelioma, multiple myeloma, or seminoma. In certain embodiments, the cancer is leukemia. The cancer may be a cancer of the bladder, blood, bone, brain, breast, cervix, colon/rectum, endometrium, head and neck, kidney, liver, lung, muscle tissue, ovary, pancreas, prostate, skin, spleen, stomach, testicle, thyroid, or uterus.

[0081] The disease or disorder may be a cancer comprising solid tumors. Examples of cancers that comprise solid tumors include, but are not limited to, pancreatic, bladder, non-small cell lung cancer (NSCLC), breast, and ovarian cancers.

c) Method of Localizing a Molecule

[0082] The present disclosure also provides methods of localizing a molecule to a tissue or organ in a subject. In some embodiments, the methods comprise administering to the subject the composition as described herein, wherein following administration of the composition the molecule is localized in the liver at less than 30% of the injected dose/gram of tissue or organ (ID/g). In some embodiments, following administration of the composition the molecule is localized in the liver at about 1% to about 30% of the injected dose/gram of tissue or organ (ID/g).

[0083] In some embodiments, the methods comprise administering to the subject the composition as described herein, wherein following administration of the composition the molecule is localized in the spleen at less than 10% of the injected dose/gram of tissue or organ (ID/g). In some embodiments, following administration of the composition the molecule is localized in the spleen at about 1% to about 10% of the injected dose/gram of tissue or organ (ID/g).

[0084] In some embodiments, the methods comprise administering to the subject the composition as described herein, wherein following administration of the composition the amount of the molecule localized in a tissue or organ is decreased when compared to the same molecule in a self-assembling conjugate without an albumin binding domain and wherein the tissue or organ is the kidney, liver, spleen or any combination thereof. The amount of the molecule localized in a tissue or organ may be decreased at least two-fold when compared to the same molecule in a self-assembling conjugate without an albumin binding domain and wherein the tissue or organ is the kidney, liver, spleen or any combination thereof. In some embodiments, the amount of the molecule localized in a tissue or organ may be decreased about two-fold to about ten-fold when compared to the same molecule in a self-assembling conjugate without an albumin binding domain and wherein the tissue or organ is the kidney, liver, spleen or any combination thereof.

[0085] The present disclosure also provides methods of localizing a molecule to a tumor in a subject. In some embodiments, the methods comprise administering to the subject the composition as described herein, wherein following administration of the composition the amount of the molecule localized to the tumor is increased when compared to the same molecule in a self-assembling conjugate without an albumin binding domain. The amount of the molecule localized to the tumor may be increased at least two-fold when compared to the same molecule

in a self-assembling conjugate without an albumin binding domain. In some embodiments, the amount of the molecule localized to the tumor may be increased about two-fold to about 20-fold when compared to the same molecule in a self-assembling conjugate without an albumin binding domain.

4. Administration

[0086] The disclosed compositions may be incorporated into pharmaceutical compositions suitable for administration to a subject (such as a patient, which may be a human or non-human) well known to those skilled in the pharmaceutical art. The pharmaceutical composition may be prepared for administration to a subject. Such pharmaceutical compositions can be administered in dosages and by techniques well known to those skilled in the medical arts taking into consideration such factors as the age, sex, weight, and condition of the particular subject, and the route of administration.

[0087] The pharmaceutical compositions may include pharmaceutically acceptable carriers. The term "pharmaceutically acceptable carrier," as used herein, means a non-toxic, inert solid, semi-solid or liquid filler, diluent, encapsulating material or formulation auxiliary of any type. Some examples of materials which can serve as pharmaceutically acceptable carriers are sugars such as, but not limited to, lactose, glucose and sucrose; starches such as, but not limited to, corn starch and potato starch; cellulose and its derivatives such as, but not limited to, sodium carboxymethyl cellulose, ethyl cellulose and cellulose acetate; powdered tragacanth; malt; gelatin; talc; excipients such as, but not limited to, cocoa butter and suppository waxes; oils such as, but not limited to, peanut oil, cottonseed oil, safflower oil, sesame oil, olive oil, corn oil and soybean oil; glycols, such as propylene glycol; esters such as, but not limited to, ethyl oleate and ethyl laurate; agar; buffering agents such as, but not limited to, magnesium hydroxide and aluminum hydroxide; alginic acid; pyrogen-free water; isotonic saline; Ringer's solution; ethyl alcohol, and phosphate buffer solutions, as well as other non-toxic compatible lubricants such as, but not limited to, sodium lauryl sulfate and magnesium stearate, as well as coloring agents, releasing agents, coating agents, sweetening, flavoring and perfuming agents, preservatives and antioxidants can also be present in the composition, according to the judgment of the formulator. The route by which the composition is administered and the form of the composition will dictate the type of carrier to be used.

[0088] The composition can be administered prophylactically or therapeutically. In prophylactic administration, the composition can be administered in an amount sufficient to induce a response. In therapeutic applications, the composition can be administered to a subject in need thereof in an amount sufficient to elicit a therapeutic effect. An amount adequate to accomplish this is defined as "therapeutically effective dose." Amounts effective for this use will depend on, e.g., the particular composition of the conjugate regimen administered, the manner of administration, the stage and severity of the disease, the general state of health of the patient, and the judgment of the prescribing physician.

[0089] The compositions can be administered by methods well known in the art as described in Donnelly et al. (*Ann. Rev. Immunol.* 1997, *15*, 617-648); Felgner et al. (U.S. Patent No. 5,580,859, issued Dec. 3, 1996); Felgner (U.S. Patent No. 5,703,055, issued Dec. 30, 1997); and Carson et al. (U.S. Patent No. 5,679,647, issued Oct. 21, 1997), which are all incorporated by reference herein in their entirety. One skilled in the art would know that the choice of a pharmaceutically acceptable carrier, including a physiologically acceptable compound, depends, for example, on the route of administration.

[0090] The compositions can be delivered via a variety of routes. Typical delivery routes include parenteral administration, e.g., intradermal, intramuscular or subcutaneous delivery. Other routes include oral administration, intranasal, intravaginal, transdermal, intravenous, intraarterial, intratumoral, intraperitoneal, and epidermal routes. In some embodiments, the conjugate is administered intravenously, intraarterially, or intraperitoneally to the subject.

[0091] The composition may conveniently be presented in a single dose or as divided doses administered at appropriate intervals, for example, as two, three, four or more sub-doses per day. The sub-dose itself may be further divided, e.g., into a number of discrete loosely spaced administrations.

[0092] As will be readily apparent to one skilled in the art, the useful in vivo dosage to be administered and the particular mode of administration will vary depending upon the age, weight, the severity of the affliction, and subjects treated, the particular compounds employed, and the specific use for which these compounds are employed. The determination of effective dosage levels, that is the dosage levels necessary to achieve the desired result, can be accomplished by one skilled in the art using routine methods, for example, human clinical trials, in vivo studies and in vitro studies.

[0093] Dosage amount and interval may be adjusted individually to provide plasma levels of the molecule which are sufficient to maintain the modulating effects, or minimal effective concentration (MEC). The MEC will vary for each molecule but can be estimated from in vivo and/or in vitro data. Dosages necessary to achieve the MEC will depend on individual characteristics and route of administration. However, assays well known to those in the art can be used to determine plasma concentrations. Dosage intervals can also be determined using MEC value. Compositions should be administered using a regimen which maintains plasma levels above the MEC for 10-90% of the time, preferably between 30-90% and most preferably between 50-90%. In cases of local administration or selective uptake, the effective local concentration of the drug may not be related to plasma concentration.

[0094] It should be noted that the attending physician would know how to and when to terminate, interrupt, or adjust administration due to toxicity or organ dysfunctions. Conversely, the attending physician would also know to adjust treatment to higher levels if the clinical response were not adequate (precluding toxicity). The magnitude of an administrated dose in the management of the disorder of interest will vary with the severity of the symptoms to be treated and the route of administration. Further, the dose, and perhaps dose frequency, will also vary according to the age, body weight, and response of the individual patient. A program comparable to that discussed above may be used in veterinary medicine.

[0095] A therapeutically effective amount of the composition disclosed herein may be administered alone or in combination with a therapeutically effective amount of at least one additional therapeutic agents. In some embodiments, effective combination therapy is achieved with a single composition or pharmacological formulation that includes both agents, or with two distinct compositions or formulations, administered at the same time, wherein one composition includes a compound of this invention, and the other includes the second agent(s). Alternatively, in other embodiments, the therapy precedes or follows the other agent treatment by intervals ranging from minutes to months.

[0096] A wide range of second therapies may be used in conjunction with the compositions of the present disclosure. The second therapy may be a combination of a second therapeutic agent or may be a second therapy not connected to administration of another agent. Such second therapies include, but are not limited to, surgery, immunotherapy, radiotherapy, or a second chemotherapeutic agent.

5. Examples

[0097] It will be readily apparent to those skilled in the art that other suitable modifications and adaptations of the present disclosure described herein are readily applicable and appreciable, and may be made using suitable equivalents without departing from the scope of the present disclosure or the aspects and embodiments disclosed herein. Having now described the present disclosure in detail, the same will be more clearly understood by reference to the following examples, which are merely intended only to illustrate some aspects and embodiments of the disclosure, and should not be viewed as limiting to the scope of the disclosure. The disclosures of all journal references, U.S. patents, and publications referred to herein are hereby incorporated by reference in their entireties.

Example 1: Materials and Methods

[0098] *(ABDN/H-)ELP biosynthesis and purification.* (ABDN/H-) ELPs were expressed from the cloned gene in E. coli cells as described previously. The amino acid sequence of ABDN is LAEAKVLANRELDKYGVSDYYKNLINNAKTVEGVKALIDEILAALP (SEQ ID NO:6). The amino acid sequence of ABDH is LAEAKVLANRELDKYGVSDFYKRLINKAKTVEGVEALKLHILAALP (SEQ ID NO:7). The genes encoding the (ABDN/H-) ELPs were assembled by recursive directional ligation (Pre-RDL) in a modified pET plasmid in NEB 5-alpha cells (Invitrogen Corporation, Carlsbad, CA), and were extracted using the QIAprepTM spin miniprep kit (Qiagen; Germantown, MD) (Novagen, Madison, WI). Genes encoding ABDs and the multi-cysteine drug conjugation tail were appended respectively to the N-terminus and C-terminus of the (ABDN/H-) ELPs gene by Pre-RDL. 5'-phosphorylated oligonucleotides encoding ABDs and cysteine rich tail were purchased from Integrated DNA technologies (Coralville, IA) and were annealed and ligated into the vector containing the CP (also referred to as ELP herein) gene using T4 DNA ligase (Invitrogen; Carlsbad, CA) for 1 hr at room temperature, transformed into chemically competent NEB 5-alpha cells. Transformants were selected on TB-agar plates containing 100 μg mL-1kanamycin and positives were confirmed by bidirectional DNA sequencing. Plasmids were transformed into expression host BLR(DE3)TM cells (Novagen, Madison, WI). To express (ABDN/H-) ELPs, transformed cells were used to start 50 ml Terrific Broth (TB) seed cultures containing kanamycin (100 μg/ml) at 250 rpm and 37 °C. These cultures were used to inoculate

1 liter of TB medium, and the culture was grown under the same conditions. At mid-log phase cells were induced with 1 mM IPTG and incubated at 37 °C overnight with shaking. Cells were harvested after 10-12 hours, re-suspended in 2.5 mL PBS per liter culture, and disrupted by ultrasonication (Misonix; Farmingdale, NY). Polyethyleneimine (20% v/v, 2 mL per liter culture) was added to remove nucleic acids nucleoproteins. (ABDN/H-)ELPs were purified from the clarified supernatant using two cycles of inverse transition cycling, as shown in FIG. 1. In the first inverse transition cycle, (ABDN/H-)ELP solutions were incubated for 10 min at 50 °C, followed by 10 min on ice, and were centrifuged at 4 °C (13,000 rpm, 10 min). The (ABDN/H-) ELP supernatant was supplemented with sodium chloride to a final concentration of ~2.5 M and were heated to 37 °C to initiate the inverse phase transition; (ABDN/H-)ELP coacervates were collected by centrifugation (14,000 rpm, 10 min, 30-35 °C) and were resuspended in tris(2-carboxyethyl)phosphine hydrochloride (TCEP; Pierce Biotechnology, Rockford, IL) (TCEP, 30 mM, pH adjusted to 7.0). Second cycle was performed same as the first one except that 0.5 M final concentration of sodium chloride was used for triggering the phase transition of ELP. After inverse transition cycling purification, (ABDN/H-)ELP purity was determined by SDS-PAGE electrophoresis. The purified CPs were then dialyzed against water and lyophilized.

[0099] *DOX Drug conjugation and determination.* DOX (Carbosynth, Berkshire, UK) was covalently conjugated to cysteine residues of $(Cys\text{-}Gly\text{-}Gly)_8$ (SEQ ID NO:5) segment of the CP via the pH sensitive linker 3,3'-N-[ε-Maleimidocaproic acid] hydrazide (EMCH, Pierce Biotechnology, Rockford, IL). The conjugation reaction included two steps. In the first step, DOX was conjugated by its carbonyl group to EMCH. In the second step, activated DOX was coupled to the cysteine thiols of (ABDN/H-)ELPs via a hydrazine bond. To perform the first step, 220 mg of DOX was reacted with 114 mg of EMCH 100 mL anhydrous methanol with 100 μL of tri-fluoroacetic acid for 16 hrs in dark and at room temperature. In the second step, the reaction solution was concentrated to 20 mL using rotary evaporation and was added dropwise to (ABDN/H-)ELP suspended in 10 mL reaction buffer (0.1 M Na PO4, 1 mM EDTA, pH 7.0) and 3 mM TCEP. The reactants were stirred for 20 hrs in the dark and at room temperature. Unreacted DOX was removed by Amicon ultra-15 centrifugal filter units (MWCO 10 kDa, Millipore) and with 30% acetonitrile and 70% PBS as the eluent. Following removal of unreacted DOX, acetonitrile was removed by Amicon filtration against PBS. To calculate the conjugation efficiency, a small fraction of the CP-DOX was Amicon filtered against water, and

lyophilized. The lyophilized CP-DOX was weighed and dissolved in PBS. The concentration of CP and DOX was calculated by gravimetry and spectrophotometry at 488nm, using an extinction coefficient of 11500 $M^{-1}cm^{-1}$, respectively. The conjugation number was defined as the concentration of DOX divided by the concentration of CP.

[00100] *Synthesis of paclitaxel-levulinic acid (PTX-LEV) and conjugation of paclitaxel with CP.* As shown in Scheme 1, PTX-LEV was synthesized as described previously (Bhattacharyya et al. Nat Commun. 2015; 6: 7939, which is incorporated by reference herein in its entirety).

Scheme 1

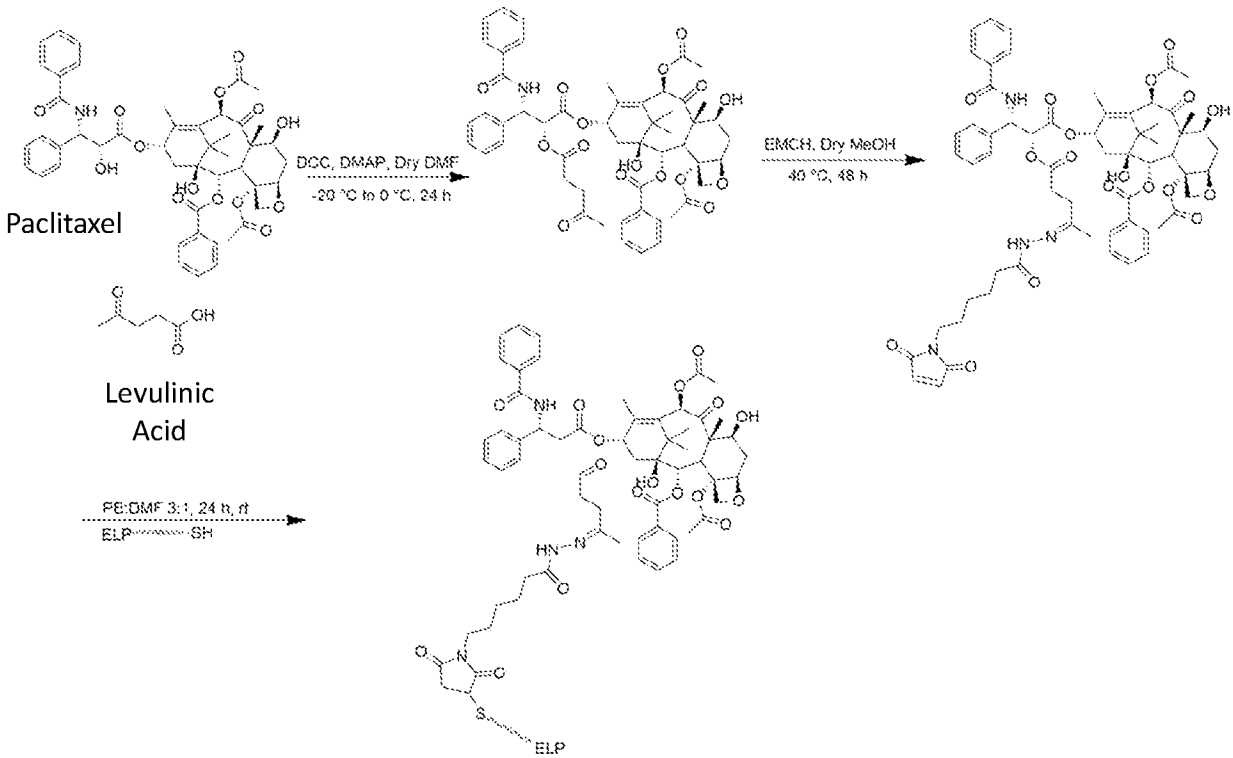

[00101] Briefly, levulinic acid (0.08 g, 0.7 mmol) and N,N'-Dicyclohexylcarbodiimide (DCC) (0.145 g, 0.7 mmol) was dissolved in dry Dimethylformamide (DMF) and mixed to each other, stirred for 30 mins at −20 °C. PTX (0.5 g, 0.58 mmol) and 4-Dimethylaminopyridine (DMAP) (0.5 g, 0.58 mmol) were dissolved in dry DMF and were added to the above mixture. The reaction mixture was left stirred for 24 h at 4 °C. The reaction mixture was filtered and the DMF was evaporated to dryness. The compound was purified with column chromatography with silica gel and 1.5% methanol (MeOH) in chloroform as eluent. Retention Factor (R_f): 0.48 in EtOAc/Hexane=2:1. PTX-LEV (0.05 g, 0.05 mmol) and N-ε-Maleimidocaproic acid hydrazide (EMCH) (0.018 g, 0.07 mmol) was dissolved in dry MeOH and left stirring in the dark for 36 h

at 45 °C. After that, the MeOH was evaporated to dryness and the compound was purified with silica gel column chromatography with 2-2.5 % MeOH in chloroform as eluent. PTX-LEV-EMCH was immediately used for next step. Rf: 0.6 in 10 % MeOH in $CHCl_3$. ESI-MS: 1159 [M+H]. ^1H NMR (400 MHz, DMSO-d6): δ 10.24 (s, 1H, 12′), 9.28 (d, 1H, -HNBz), 7.97/7.7/7.67 (5H, aromatic: O–Bz), 7.82/7.48 (5H, aromatic: N–Bz), 7.44/7.17 (5H, aromatic: Ph3′-), 6.99 (s, 2H, 12′), 6.27 (s, 3H, 10-$OCOCH_3$), 5.97 (m, 1H, 13), 5.4 (d, 1H, 2), 5.25 (dd, 1H, 3′), 4.91 (m, 1H, 5), 4.61 (d, 2H, 2′), 4.09 (m, 1H, 7), 3.99 (dd, 2H, 4-CCH_2O), 3.57 (m, 1H, 3), 3.37 (m, 2H, 5′), 3.33(s, 3H, 10-$OCOCH_3$), 3.17 (t, 2H, 4′), 3.16 (t, 3H, 11′), 2.6 (m, 2H, 6), 2.35 (m, 2H, 7′), 2.25 (s, 3H, 6′), 2.1 (s, 3H, 4-$OCOCH_3$), 1.82 (s, 3H, 8-CH_3), 1.75 (d, 2H, 14), 1.48 (s, 3H, 12-CH_3), 1.49 (m, 2H 8′), 1.23 (m, 2H, 10′), 0.992/ 1.01 (s, 3H, 15-2CH_3s), 0.84 (m, 2H, 9′). ^{13}C NMR: (125 MHz, DMSO-d6): δ 207.8, 202.35, 190.22, 174.52, 171.78, 171.05, 169.59, 166.279, 165.19, 155.51, 139.41, 134.43, 131.51, 129.92, 129.55, 128.64, 128.25, 127.56, 127.42, 127.23, 83.55, 80.18, 76.61, 75.20, 74.69, 70.67, 70.36, 65.31, 57.35, 54.47, 46.02, 42.87, 36.48, 34.40, 33.49, 32.97, 31.97, 29.75, 27.79, 26.30, 25.84, 24.65, 22.38, 21.36, 20.64, 16.76, 13.92, 9.72. HRMS (ESI): m/z calcd for $C_{62}H_{71}N_4O_{18}$ ($[M + H]^+$): 1159.476341, found: 1159.47380.

[00102] Prior to conjugation with activated PTX, purified CP was suspended in reaction buffer (0.1 M NaPO4, 1 mM ethylenediaminetetraacetic acid (EDTA), pH 7.0) and reduced with 1 mL of Tris(2-carboxyethyl)phosphine hydrochloride (TCEP) at neutral pH (100 mM, pH 7.0) at ~5x excess to thiol. Excess TCEP was removed from the solution by initiating the phase transition with sodium chloride (2.5 M) and centrifugation at 4,000 rpm at 25 °C for 10 minutes. The CP pellet obtained by centrifugation was re-suspended in ~2 mL of reaction buffer. Purified PTX-LEV-EMCH was re-suspended in ~2 mL of DMF and slowly transferred to the stirring CP solution. 1 mL of pH neutral TCEP (100 mM) was added and the reactants were stirred for 16 hrs at 20 °C in the dark. After reaction, the unreacted PTX-LEV-EMCH precipitate was separated by centrifugation at 13,000 rpm at 10 °C for 10 minutes. The supernatant was further purified by diluting it in 20% acetonitrile in PBS and centrifuging the solution in an Amicon Ultra-15 Centrifugal Filter Units (MWCO: 10 kDa, Millipore) at 2,500 rpm at 10 °C. The CP-PTX solution was washed twice with NH_4HCO_3 solution (pH 7.4) and then freeze dried.

[00103] *pH dependent drug release.* To study pH dependent drug release from CP-DOX micelles, the fraction of unbound drug was determined as a function of time at physiological pH

7.4 and acidic pH 5.0. CP-DOX micelles in PBS (400uM DOX equivalent) were diluted 1:1 v/v into either pH 5.0 (0.1 M Na acetate) or pH 7.4 (0.1 M NaH_2PO_4). Samples were incubated at 37 °C for 0.0, 0.25, 25, 0.5, 1, 2, 4, 6, or 24 hr and were neutralized by addition of pH 7.4 (0.1 M NaH_2PO_4). 25 uL of sample at each time point was injected into LC10 HPLC (Shimadzu Scientific Instruments; Columbia, MD) with Shodex OHPak SB-804 column (New York, NY) and acetonitrile: PBS (7:3) as the mobile phase at an isocratic flow rate of 0.5 mL min^{-1}. Eluting peaks were detected with a UV-Visible detector set at 490 nm. Free DOX at various known concentrations were injected as standard. HPLC data was quantified by integrating the area under the peak corresponding to the free drug. The concentrations of unbound DOX in samples were calculated using the regression coefficients obtained from the linear regression analysis of the calibration curve ($r^2 = 0.998$, $F_{1,11} = 4{,}932$, $p = 6x10^{-16}$). The cumulative percent released drug (F%, released) at each time point was defined as the concentration of unbound DOX at that time point divided by total DOX concentration times 100. For pH 5.0 samples, data points were fit by nonlinear regression to a first order release model: $F\%, released = a[1-exp(-ln(2)\ t / t_{1/2})]$ (1) where t is the time (hrs) after incubation, $t_{1/2}$ is the half-life (hrs) of release, and a (%) is the maximum extent of drug release. DOX release at pH 7.4 was negligible and no correlation with time was observed.

[00104] *Thermal Turbidimetry.* Thermal profiles of CPs and CP conjugates were determined by measuring the transition temperature (T_t) over a range of concentrations (5, 10, 25, 50, and 100 uM) in PBS, FBS, and MS using a Cary UV-visible spectrophotometer equipped with temperature controller (Agilent Technologies, CA, USA). T_t values were determined by measuring the turbidity at wavelength 350 nm for CP monomers and 650 nm for CP-DOX conjugates by raising the temperature at 1 °C/min. The transition temperature was defined as the maximum first derivative of the optical density.

[00105] *Light Scattering.* Dynamic and static light scattering measurements were performed using an ALV/CGS-3 goniometer system (Germany). CP monomers and conjugates were prepared in PBS at 25 μM and filtered through 0.22 μm Millex-GV filters into a 10 mm disposable borosilicate glass tube (Fischer). To study the effect of albumin binding on micellar self-assembly, mouse albumin was added to the samples at 1:1 albumin-CP molar ratio in PBS. Measurements were obtained at 25 °C and 37 °C for angles between 30–150° at 5° increments with each angle consisting of 3 runs and 10 s each at each run. Hydrodynamic radius (R_h) was

determined by dynamic light scattering. The radius of gyration (R_g) and the average molecular weight of the particle (MW) were calculated from the slope and intercept of a partial Zimm plot, respectively, using ALV/Dynamic and Static FIT and PLOT software and according. The micelle aggregation number N_{agg}, or the number of polypeptide chains per nanoparticle, was calculated by dividing the micelle molecular weight by the molecular weight of the polypeptide monomer.

[00106] *Interaction with albumin.* Interaction of CP monomers and micelles with human and mouse albumin was analyzed by isothermal titration calorimetry (ITC). ITC was conducted using a VP-ITC instrument ((MicroCal LLC, Northampton, MA, USA). Aliquots of 5 uL of 500 uM albumin in PBS were titrated via a 250 µl syringe into CP or CP-DOX at 50 µM concentration, stirring at 300 rpm at 37 °C. For background correction, PBS (in the cell) was titrated with albumin (in the syringe) at the same concentrations and conditions. Background was subtracted from the final curves and the binding and thermodynamic parameters – binding constant (K_D), number of binding sites (n), and enthalpy (ΔH) – were computed by non-linear fitting to an independent-binding site model using Origin Lab software (USA) for the VP-ITC calorimeter.

[00107] For PTX conjugates, ITC was conducted using a Nano ITC system (TA Instruments, Utah, USA). Aliquots of 10 uL of 500 uM albumin in PBS were titrated via a 250 µl syringe into CP-PTX at 50 uM concentration, stirring at 300 rpm at 37 °C. For background correction, PBS (in the cell) was titrated with albumin (in the syringe) at the same concentrations and conditions. Background was subtracted from the final curves and the binding and thermodynamic parameters – binding constant (K_D), number of binding sites (n), and enthalpy (ΔH) – were computed by non-linear fitting to an independent-binding site model using TA Instruments NanoAnalyze software.

[00108] *SDS- and Native-PAGE characterization.* SDS-PAGE was used to analyze the purity and apparent molecular weight of purified ABD-ELP monomers and their interaction with albumin, respectively. Native-PAGE analysis was used to visualize the interaction of CP monomers and micelles with albumin. ABD-ELP monomers were loaded at around 20 ug (10 uL loading volume) on 4-20% Mini-PROTEAN ® TGX Stain-Free™ Gel (BioRad, Hercules, CA). Electrophoresis was performed in Tris-glycine buffer (25 mM Tris, 192 mM glycine, 0.1% SDS, pH 8.3) containing 0.1% SDS at 180 V for 30 min. For Native-PAGE, ABD-ELP monomers and micelles were mixed at equal molarity with albumin and were loaded (20 ug per protein) on the gel. Native electrophoresis was run under the same conditions and with the same stacking gel

and running buffer as SDS-PAGE, except that no SDS was used. The gels were silver-stained for the protein portion.

[00109] *Size and morphology of CP conjugated micelles.* The radius and the aggregation number of the self-assembled micelles were determined, in the presence and absence of albumin, by dynamic and static light scattering at 37 °C using an ALV/CGS-3 goniometer system (Germany). Freeze fracture electron microscopy was performed to visualize the micelles and estimate their radius and morphology.

[00110] *Cell culture and tumor inoculation.* The C26 murine colon adenocarcinoma cell line was used to evaluate the potency of DOX both *in vitro* and *in vivo*. Cells were grown at 37 °C with 5% carbon dioxide in T-75 flasks in a humidified incubator. Culture medium included RPMI-1640 (R8758; Sigma, St. Louis, MO), supplemented with 10% fetal bovine serum (F0392; Sigma, St. Louis, MO), 4.5 g L-1 D-glucose (G8769; Sigma), 10 mM HEPES (15630-080; Invitrogen; Carlsbad, CA), penicillin, streptomycin and 1 mM sodium pyruvate (11360-070, Invitrogen). Cells were passaged every 2-3 days by enzymatic detachment with 0.05% trypsin + 0.5 mM EDTA (25300-054; Invitrogen). After 5 min at 37 °C trypsin was removed from detached cells by centrifugation at 400 g for 4 min, and cells were re-suspended in 10 mL media. 500 uL of cells were transferred to a new T-75 flask containing 15 mL medium. For *in vivo* implantation, detached cells were washed twice in Minimum Essential Medium (MEM, 51200-038; Invitrogen; Carlsbad, CA). Tumor inoculation was performed by injecting $4x10^5$ cells in 30 µl of medium into the right flank. Tumors were allowed to grow for 8-10 days to a size of around 75 mm^3. All animals were treated in accordance with National Institute of Health Guide for Supplemental methods and data the Care and Use of Laboratory Animals under protocols approved by the Duke University Institutional Animal Care and Use Committee.

[00111] *In vitro Cytotoxicity. In vitro* cytotoxicity of the ABDN-CP-DOX versus that of naked CP-DOX and free DOX was determined using the calorimetric MTS assay. C26 murine colon adenocarcinoma cells were seeded (5000 cells/well) in a 96-well plate. After 24 h, cells were treated in triplicate with 3-fold serial dilutions of drugs beginning with 100 uM. After 72 h incubation, 20 µL of CellTiter 96 AQueousTM (Promega; Madison, WI) 3-(4,5-dimethlthiazol-2-yl)-5-(3-carboxymethoxphenyl)-2-(4-sulfophenyl)-2H-tetrazolium (MTS) reagent was added to each well followed by 3 h incubation at 37 °C. The absorbance at 490 nm was determined using a Victor3 TM microplate reader (Perkin Elmer; Waltham, MA). For each plate, blank wells

(with no cells) were defined as 0% viability and wells treated with PBS were defined as 100% viability. The background absorbance at 490 nm was corrected by subtracting the average absorbance of the blank wells from each well. The percent viability was defined as the absorbance of each well normalized to the absorbance of wells treated with PBS. Inhibitory concentration (IC 50) values were calculated using a four-parameter logistic fit in the Prism program (GraphPad Software, San Diego, CA, USA).

[00112] *In vitro* cytotoxicity of the ABDN-CP-PTX versus that of naked CP-PTX and free PTX was determined using the calorimetric MTS assay. MDA-MB-231 human breast cancer cells were seeded (3000 cells/well) in a 96-well plate. After 24 h, cells were treated in triplicate with 3-fold serial dilutions of drugs beginning with 100 uM. After 72 h incubation, 20 μL of CellTiter 96 AQueousTM (Promega; Madison, WI) 3-(4,5-dimethlthiazol-2-yl)-5-(3-carboxymethoxphenyl)-2-(4-sulfophenyl)-2H-tetrazolium (MTS) reagent was added to each well followed by 3 h incubation at 37 °C. The absorbance at 490 nm was determined using a Victor3 TM microplate reader (Perkin Elmer; Waltham, MA). For each plate, blank wells (with no cells) were defined as 0% viability and wells treated with PBS were defined as 100% viability. The background absorbance at 490 nm was corrected by subtracting the average absorbance of the blank wells from each well. The percent viability was defined as the absorbance of the each well normalized to the absorbance of wells treated with PBS. Inhibitory concentration (IC 50) values were calculated using a four-parameter logistic fit in the Prism program (GraphPad Software, San Diego, CA, USA). The MTS assay was repeated twice to ensure validity of results.

[00113] *Pharmacokinetics of ABD-ELP monomers and ABD-CP-DOX micelles.* For pharmacokinetics analysis, ABD-ELP and ELP-monomers were traced *in vivo* by fluorescent labeling. A single cysteine was added to the C-terminus of polypeptides and was reacted with Alexa 488-maleimide (Life Technologies, Carlsbad, CA, USA). 50 uL Alexa 488-maleimide at 27.75 uM in DMSO was added to the polypeptide solution in the reaction (250 uM) and was allowed to stir for 3 hr at room temperature in the dark. Unbound Alexa488 was then removed by Amicon ultra-15 centrifugal filter units (MWCO 10 kDa, Millipore) and in PBS. Alexa488 concentration and conjugation efficiency was then determined.

[00114] Alexa488 labeled polypeptides were injected intravenously into Balb/C mice and 10 uL blood samples were collected at 40 s (15 uL from the tail vein at 40 s), 15 and 30 min, 2, 4, 8, 24, 48, and 72 hrs after injection, diluted into 100 uL heparinized PBS (1,000 U mL-1), and

centrifuged (5,000 g, 5 min, 4 °C) to remove cells and debris. 125 uL of the supernatant was loaded onto a black 96-well plate (BD Biosciences) in duplicate. Free Alexa488-maleimide solutions at various known concentrations were prepared in heparinized PBS and were loaded onto the plate as standards. Alexa488 fluorescence was measured on a Wallac Victor3 TM microplate reader (Perkin Elmer; Waltham, MA). The relationship between background-corrected fluorescence and concentration of DOX standards successfully fit into a linear regression.

[00115] Pharmacokinetics profile of CP-DOX micelles was explored by intravenous injection into female Balb/C mice (10 and 20 mg DOX Equiv kg-1 BW) via the tail vein. 10 uL blood sample was collected from the tail vein at 40 s, 15 and 30 min, 2, 4, 8, 24, 48, and 72 hrs after injection, diluted into 100 uL heparinized PBS (1,000 U mL-1), and centrifuged (5,000 g, 5 min, 4 °C) to remove cells and debris. To release DOX from the micelles, 10 uL of plasma was incubated in 490 μL of acidified isopropanol (75 mM HCl, 10% water, 90% isopropanol) overnight at 4 °C in the dark. The isopropanol extract was then centrifuged (14,000 RPM, 10 min, 4 °C) and 125 uL of the supernatant was loaded onto a black 96-well plate (BD Biosciences) in duplicate. Free DOX solutions at various known concentrations were prepared in acidified isopropanol and were loaded onto the plate as standards. DOX fluorescence was measured on a Wallac Victor3 TM microplate reader (Perkin Elmer; Waltham, MA) using excitation at 485 nm and emission at 590 nm. The relationship between background-corrected fluorescence and concentration of DOX standards successfully fit into a linear regression.

[00116] *Canine pharmacokinetics and toxicities.* Healthy beagles and hounds, purchased from a commercial vendor (Covance Inc, Princeton, NJ) were used to investigate the pharmacokinetics of ABDN-CP-DOX micelles. All procedures and protocols involving care, handling, and dosing for this study were reviewed and approved by the Institutional Animal Care and Use Committee (IACUC) at North Carolina State University College of Veterinary Medicine, which is an AAALAC-accredited facility. The animals' health status were monitored daily by the animal technicians and veterinary staff, paying particular attention for signs of gastrointestinal toxicities including vomiting, diarrhea, lethargy, and inappetence. If noted, supportive care was provided. ABDN-CP-DOX, CP-DOX and DOX were infused via cephalic vein at a 10% reduced dose of the maximally tolerated dose (MTD) of native DOX in dogs, i.e. 27 DOX Equiv. m^{-2} body surface area (BSA) for dogs weighing greater than 15 kg and 0.9 mg DOX Equiv. kg^{-1} of body

weight (BW) for dogs weighing less than 15 kg. Due to the limited animal availability and the high cost of the canine experiments, pharmacokinetics were studied with 3 dogs for CP-DOX and free DOX, and with 2 dogs for ABDN-CP-DOX. 2 mL blood samples were drawn from jugular vein at 40 s, 15 and 30 min, 2, 4, 8, 24, 48, and 72 h after injection, diluted into 400 μL heparinized PBS (1000 UmL^{-1}). Sample processing and analysis were performed as with murine pharmacokinetics studies. Blood samples (2 ml) were also drawn 7 days after the injections for hematology and serum biochemistry analysis, since temporary bone marrow dyscrasias typically occur 7 days after the injection of most chemotherapeutic drugs.

[00117] *Biodistribution.* The biodistribution profile of CP-DOX micelles was explored by intravenous injection into female Balb/C mice (5 and 10 mg DOX Equiv kg-1 BW) via the tail vein. At 2 and 24 h after injection, tissues (tumor, muscle, heart, lung, liver, spleen and kidney) were removed, weighed and suspended in 1.0 mL acidified isopropanol (75 mM HCl, 10% water, 90% isopropanol). Tissues were then homogenized using 2 mm diameter zirconia beads and a MiniBeadbeater-1TM (Biospec; Bartlesville, OK) for 2 min at 5,000 beats per minute and were incubated overnight at 4 °C in the dark. The isopropanol extracts were then vortexed, and centrifuged (14,000 RPM, 10 min, 4 °C) and 125 uL of the supernatant was loaded onto a black 96-well plate (BD Biosciences) in duplicate. Free DOX solutions at various known concentrations were prepared in acidified isopropanol and were loaded onto the plate as standards. To correct for background tissue fluorescence, tissues were removed from three untreated control mice and were processed similarly. For each tissue, a background (counts per mg tissue) curve was created using 2-fold dilutions of the processed tissues in acidified isopropanol. DOX fluorescence was measured on a Victor3 TM microplate reader (Perkin Elmer; Waltham, MA) using excitation at 485 nm and emission at 590 nm. The background fluorescence was subtracted from each well and DOX concentration in each well was calculated using the DOX fluorescence standard curve.

[00118] *Maximum tolerated dose.* A dose escalation experiment was performed to determine the maximum tolerated dose (MTD) and toxicity profile of CP-DOX micelles. CP-DOX micelles were administered via tail vein into female Balb/C mice (7 weeks old) at increasing dose levels. Body weight was monitored as a measure of toxicity for up to 10 days. To rule out the possibility of CP toxicity, free CP was injected at the dose equal to the ELP dose at the highest CP-DOX

dose level i.e. 60 mg/kg BW. MTD was defined as the dose above which body weight loss exceeded 15% of the initial body weight within 10 days.

[00119] *Tumor regression and survival.* CP-DOX micelles were injected intravenously at 10, 20, and 40 mg/kg BW DOX equivalent into the female Balb/C mice (6-8 weeks old) bearing dorsal C26 tumors 8-10 days after tumor implantation when a tumor size of around 75 mm^3 was reached. Tumor size and body weight were monitored over a span of two months. Tumor volume was calculated as follows: Volume [mm^3] = length x width 2 x π / 6. Mice with a tumor volume greater 1000mm^3 or body weight loss greater than 15% were euthanized.

Example 2: Development of an albumin binding chimeric polypeptide

[00120] Albumin binding domain fused chimeric polypeptides called ABD-ELPs were designed and included three segments: 1) an ELP scaffold; 2) an albumin binding domain fused to the N-terminus; 3) a short cysteine containing sequence fused to C-terminus for fluorophore labeling and dug conjugation. Naked ELPs (i.e. ELPs) with no ABD at their N-terminus were used as controls. To ensure self-assembly into micelles upon later drug conjugation, a highly hydrophilic ELP was engineered that contained 160 repeats of the Val-Pro-Gly-X-Gly with X=Ala. (ABDN/H-)ELPs were purified from *E. coli* by inverse transition cycling (FIG. 1 and FIG. 2A) with high yield (100-200 mgL^{-1}). The binding affinity of ABDN-ELP and ABDH-ELP for human and mouse albumin was analyzed quantitatively by ITC (FIG. 3A-FIG. 3C and FIG. 4A-FIG. 4C, respectively) and qualitatively by native-PAGE (FIG. 2B). The binding data also showed that both ABDN-ELP and ABDH-ELP bind to mouse albumin with 1:1 stoichiometry and nanomolar affinity (K_D=66.36±10.65 nM for ABDN-ELP (FIG. 4B) and K_D=5.192 ±1.855 nM for ABDH-ELP (FIG. 4C)), whereas ELP controls displayed no specific affinity (FIG. 4A). The binding data showed that both ABDN-ELP and ABDH-ELP bind to human albumin with 1:1 stoichiometry and nanomolar affinity (K_D=48.4±3.82 nM for ABDN-ELP (FIG. 3B) and K_D=4.186 ±1.068 nM for ABDH-ELP (FIG. 3C)), whereas ELP controls displayed no specific affinity.

[00121] An *in vivo* pharmacokinetics study was performed by labeling (ABDN/H-)ELPs with Alexa488 and examining the concentration-time profile (FIG. 2C) following intravenous administration. Data were fitted to a two-compartment model and showed that fusion to ABDs increases the half-life of ELPs from 11.2±0.6 h to 16.8±0.5 h for ABDN-ELP and 16.9±0.3 h for

ABDH-ELP (Table 1). Despite higher binding affinity of ABDH-CP for albumin than ABDN-CP, no significance difference was observed between the half-life of ABDH-CP and ABDN-CP in vivo. Both ABDH-CP and ABDN-CP increased the half-life of CP from 11 h to 17 h (FIG. 2C, Table 1).

[00122] Furthermore, bioavailability was measured by calculating the area under the curve (AUC) and was determined to increase from 38.8±0.8 μM. h for ELP to 80.2±1.9 μM. h for ABDN-ELP and 88.3±1.3 μM. h for ABDH-ELP (Table 1). Mouse serum albumin was also labeled with Alexa488 and was administered as a positive control. The half-life of MSA was found to be 34.6±1.9 h which is in good agreement with the expected half-life for endogenous MSA (approximately 35 h).

Table 1. Pharmacokinetic parameters of ELP, ABDN-ELP, ABDH-ELP, and MSA. Values are shown as mean (SD).

Parameter	Symbol [unit]	ABDN-CP	ABDH-CP	CP	MSA
Elimination half-life	$\alpha\ t_{1/2}$ [h]	16.8 ± 0.5	16.9 ± 0.3	11.2 ± 0.6	34.6 ± 1.9
Area under the curve	AUC [μM. h]	80.2 ± 1.9	88.3 ± 1.3	38.8 ± 0.8	157.3 ± 4.3
Distribution half-life	$\beta\ t_{1/2}$ [min]	74.7 ± 17.7	93.2 ± 12.7	127.3 ± 12.8	72.7 ± 10.2
Apparent distribution volume	V_D [mL g^{-1}]	0.27 ± 0.01	0.25 ± 0.00	0.33 ± 0.01	2.78 ± 0.11
Plasma clearance	CL [mL h^{-1} g^{-1}]	0.012 ± 0.000	0.011 ± 0.000	0.026 ± 0.001	0.058 ± 0.002
Elimination rate constant	k_e [h^{-1}]	0.68 ± 0.00	0.07 ± 0.00	0.14 ± 0.01	0.05 ± 0.00
Tissue to plasma rate constant	k_{ep} [h^{-1}]	0.31 ± 0.07	0.25 ± 0.04	0.14 ± 0.02	0.24 ± 0.04
Plasma to tissue rate constant	k_{pe} [h^{-1}]	0.21 ± 0.06	0.16 ± 0.03	0.11 ± 0.02	0.30 ± 0.05

Example 3: Development of albumin binding self-assembling micelles with Doxorubicin

[00123] DOX was conjugated to cysteines included in the short cysteine containing sequence, e.g., $(Gly\text{-}Gly\text{-}Cys)_8$ (SEQ ID NO:5) appended at the C-terminus of the (ABDN/H-)ELPs via a pH-labile hydrazone bond (FIG. 6C). Drug conjugation imparts amphiphilicity and drives self-assembly of the conjugates. The conjugation efficiency was 5.1± 0.5 and 4.6± 0.6 and 4.7±0.3 doxorubicin molecules per polypeptide for CP-DOX, ABDN-CP-DOX and ABDH-CP-DOX, respectively. As with the (ABD-)ELP monomers, binding affinity of the (ABD-)CP-DOX micelles to mouse albumin was analyzed qualitatively and quantitatively by ITC (FIG. 7A- FIG. 7C) and native-PAGE (FIG. 6A). It was observed that DOX conjugated (ABDN/H-)ELPs still displayed 1:1 stoichiometry and strong sub-μM affinity for albumin (K_D=317.56±53.55 for ABDN-CP-DOX (FIG. 7B) and K_D=66.093 ±20.20nM for ABDH-CP-DOX (FIG. 7C)) though their affinity was lower than their non DOX-conjugated counterparts (FIG. 7A).

Example 4: Binding to albumin increases the transition temperature.

[00124] The effects of ABD fusion and albumin binding on the thermal behavior of (ABDN/H-)ELP monomers and (ABDN/H-)CP-DOX micelles were examined by studying the turbidity profile of these constructs in PBS, fetal bovine serum, mouse serum and human serum as a function of temperature (FIG. 8A-FIG. 8D). Fusion of ABDN/H decreased the transition temperature of ELP from 60 °C at 100 μM concentration in PBS to 57 °C and 55 °C under the same conditions for ABDN-ELP and ABDH-ELP, respectively. This decrease in transition temperature is attributed to the hydrophobic nature of ABDs. The decrease in the transition temperature is more pronounced after drug (DOX) conjugation where ABDN-CP-DOX and ABDH-CP-DOX transition at 44 °C and 40 °C compared with 47 °C for CP-DOX (FIG. 8D). Moreover, phase transition of (ABDN/H-)CP-DOX micelles occurred at a lower temperature and a less concentration dependent manner than their non-drug conjugated counterparts. The lower transition temperature and weaker concentration dependence of micelle structures with respect to monomer may be due to close proximity of the (ABD/H-)CPs in the corona of the micelles, which maximizes the local concentration of (ABD/H-)ELPs. Furthermore, ABDN/H-ELP monomers as well as ABDN/H-CP-DOX micelles showed a higher transition temperature in FBS than PBS and showed no transition in MS and HS up to 70 °C whereas naked ELP monomers

and CP-DOX micelles transitioned at a lower temperature in FBS, MS, and HS than in PBS as described previously.

[00125] Therefore, among various ABDs, only ABDs that do not lower the transition temperature of the CP-drug conjugate to 40 °C or lower will be useful for preparing albumin binding nanoparticulate systems.

Example 5: Binding to albumin does not break the micelles.

[00126] Self-assembly of CP-DOX conjugates into micelles was confirmed by light scattering and freeze-fracture transmission electron microscopy. (ABDN/H-)CP-DOX micelles showed a narrow size distribution with a hydrodynamic radius (R_h) of 36.29 nm, 59.0 nm, and 51.28 nm at 22 °C for CP-DOX, ABDN-CP-DOX, and ABDH-CP-DOX micelles, respectively, and 22.33 nm and 45.63 nm at 37 °C for CP-DOX, and ABDN-CP-DOX micelles, respectively, as measured by dynamic light scattering (DLS) (Table 2). Neither ABDN-CP-DOX nor ABDH-CP-DOX conjugates aggregate at room temperature (25 °C), however, at body temperature (37 °C), ABDH-CP-DOX conjugates show aggregates, but ABDN-CP-DOX conjugates remain aggregate-free. This was thought to be due to the initiation of thermal phase transition of ABDH-CP-DOX micelles around 37 °C due to the lower transition temperature of the ABDH-CP-DOX micelles (FIG. 8). Therefore, considering lower stability of ABDH-CP-DOX micelles at body temperature together with similar pharmacokinetics of ABDN-CP-DOX and ABDH-CP-DOX micelles, ABDN-CP-DOX micelles were preferred.

[00127] Static light scattering (SLS) provided the micelle radius of gyration (Rg) and aggregation number (N_{agg}) (Table 2). At 37 °C, R_g and N_{agg} were found to be, respectively 18.74 nm and 16.69 for CP-DOX conjugates, and 34.97 nm and 42.04 for ABDN-CP-DOX conjugate. R_g and N_{agg} could not be determined for ABDH-CP-DOX conjugate at 37 °C due to presence of aggregates. In addition, the shape factor ($p=R_g/R_h$) of the micelles was calculated as 0.839, and 0.766 for CP-DOX and ABDH-CP-DOX micelles, respectively, both of which indicated a spherical morphology. In addition, CP-DOX and ABDN-CP-DOX micelles were fast-frozen from 37 °C and were observed with freeze-fracture transmission electron microscopy (FF-TEM) (FIG. 6C). The observed images corroborated the mean size and morphology obtained by DLS. Light scattering analysis in the presence of equimolar concentration of mouse albumin showed that binding to albumin did not break the micelle structure. Binding to albumin resulted in

increasing the N_{agg} and decreasing the R_h of ABDN/H-CP-DOX micelles. In case of ABDH-CP-DOX micelles, no aggregates were detected in the presence of mouse albumin at 37 °C; this is consistent with the thermal profile data where binding to albumin prevented the phase transition and aggregation of ABDN/H-CP-DOX micelles.

Table 2. Light scattering data for (ABDN/H-) CP-DOX micelles in the presence and absence of albumin.

Sample	Temperature (°C)	N_{agg}	R_g (nm)	R_h (nm)	$\rho = R_g/R_h$
CP-DOX	22	10.92	28.05	36.29	0.773
	37	16.69	18.74	22.33	0.839
CP-DOX : MSA (1:1)	22	NM[a]	NM[a]	36.22	NM[a]
	37	NM[a]	NM[a]	30.24	NM[a]
ABDN-CP-DOX	22	34.97	36.95	59.00	0.62
	37	42.04	34.97	45.63	0.766
ABDN-CP-DOX : MSA (1:1)	22	58.63	38.44	50.21	0.766*
	37	57.89	29.52	38.23	0.777
ABDH-CP-DOX	22	17.06	34.55	51.28	0.694
	37	Agg[b]	-	-	-
ABDH-CP-DOX : MSA (1:1)	22	31.15	37.50	47.17	0.794
	37	36.14	36.75	46.919	0.783

[a] Non-measurable
[b] Aggregated

[00128] The sequence and arrangement of ABDN-CP is important for nanoparticle formation. ABDN-CP-DOX and CP-ABDN-DOX form nanoparticles, but when a small zwitterionic KEKE (SEQ ID NO:8) sequence was added to the N-terminus, KEKE-CP-ABDN-DOX did not form nanoparticles (Table 3, FIG. 9A and FIG. 9B).

Table 3. Light scattering data for ABDN-CP-DOX, CP-ABDN-DOX, and KEKE-CP-ABDN-DOX

Conjugate	R_h	Mass	Polydispersity
ABDN-CP-DOX	*See Table 2*		
CP-ABDN-DOX	45.8 nm	100%	32.2%
KEKE-CP-ABDN-DOX	7.8 nm	90.2 %	10.7 %
	68.9 nm	9.8 %	19.4 %

Example 6: Albumin binding prolongs the circulation time of monomers but not micelles.

[00129] Pharmacokinetics studies of (ABDN-)CP-DOX micelles were performed at a DOX equivalent dose of 10 and 20 mg/kg BW. DOX concentration versus time profiles of (ABDN/H-

)CP-DOX micelles were determined using intrinsic DOX fluorescence and were fitted to a two-compartment model (FIG. 10A). At the dose of 10 mg/kg BW DOX equivalent, no significant difference was observed between ABDN-CP-DOX and CP-DOX micelles as to their half-life (17.5±0.8 h for ABDN-CP-DOX and 20.1±0.6 h for CP-DOX) and bioavailability i.e. AUC (3328.5±100.3 μM. h for ABDN-CP-DOX and 2994±59.0 μM. h for CP-DOX), whereas at the dose of 10 mg/kg BW DOX equivalent, ABDN-CP-DOX micelles displayed a half-life of 18.3±0.6 h and AUC of 1400.4±34.2 μM. h while the half-life and AUC of CP-DOX micelles were measured as 9.7± 0.6 h and 724.82±33.1 μM. h, respectively (Table 4). These data are suggestive of linear pharmacokinetics for ABDN-CP-DOX and non-linear pharmacokinetics for CP-DOX.

Table 4: Pharmacokinetic parameters of CP-DOX, ABDN-CP-DOX, and ABDN-DOX. Values are shown as mean (SD)

		CP-DOX 10mg/kg	ABDN-CP-DOX 10mg/kg	CP-DOX 20mg/kg	ABDN-CP-DOX 20mg/kg
Elimination half-life	α $t_{1/2}$ [h]	9.7 ± 0.6	18.3 ± 0.6	20.1 ± 0.9	17.5 ± 0.8
Area under the curve	AUC [μM. h]	724.8 ± 33.1	1400.4 ± 34.2	2994.5 ± 59.0	3328.5 ± 100.3
Distribution half-life	β $t_{1/2}$ [min]	13.8 ± 2.4	12.4 ± 1.4	42.1 ± 5.1	71.7 ± 17.5
Apparent distribution volume	V_D [mL g^{-1}]	0.20 ± 0.01	0.34 ± 0.01	0.39 ± 0.01	0.25 ± 0.01
Plasma clearance	CL [mL h^{-1} g^{-1}]	0.023 ± 0.001	0.013 ± 0.000	0.013 ± 0.000	0.011 ± 0.000
Elimination rate constant	k_e [h^{-1}]	0.38 ± 0.04	0.10 ± 0.01	0.09 ± 0.00	0.08 ± 0.00
Tissue to plasma rate constant	k_p [h^{-1}]	0.84 ± 0.12	1.22 ± 0.13	0.35 ± 0.04	0.29 ± 0.07
Plasma to tissue rate constant	k_{ep} [h^{-1}]	1.90 ± 0.40	2.08 ± 0.27	0.58 ± 0.08	0.25 ± 0.07

[00130] The effect of albumin binding on pharmacokinetics was further investigated in dogs, as they are large, long-lived animals that share stronger similarities in their anatomy and physiology with humans than mice and are therefore a better model to understand the advantages

and limitations of new cancer therapeutics and delivery modalities. All three formulations were injected at a dose that was reduced by 10% relative to the clinical therapeutic dose of DOX. Observing the relatively small animal-to-animal variation and given the high cost of these experiments and limited animal availability, the pharmacokinetic study was closed with three dogs for CP-DOX and free DOX, and two dogs for ABDN-CP-DOX. As with the pharmacokinetics study in mice, DOX concentration in blood as a function of time following i.v. injection of free DOX, CP-DOX and ABDN-CP-DOX was measured by quantifying the intrinsic fluorescence of DOX, and the data were fitted to a two-compartment model (FIG. 11). Free DOX formulation had an elimination half-life ($t_{1/2}$) of 2.9 ± 0.8 h and an area under the curve (AUC) of 1769.1 ± 498.0 μM. h. In contrast CP-DOX micelles exhibited a three-fold longer $t_{1/2}$ of 9.8 ± 1.9 h ($P < 0.05$), and a 48-fold greater AUC of 84106.0 ± 7616.8 μM. h AUC compared to free DOX ($P < 0.05$). ABDN-CP-DOX micelles exhibited a plasma half-life of 30.8 ± 2.0 h that was three-fold greater than that of CP-DOX ($P < 0.001$), and an AUC of 509371.7 ± 43095.2 μM. h that is six-fold larger than that of CP-DOX ($P < 0.001$) (Table 5). Furthermore, despite a significant increase in the plasma half-life and AUC of ABD-CP-DOX compared to CP-DOX and free DOX, no hematology or serum chemistry abnormalities were noted with ABDN-CP-DOX and CP-DOX groups one week after infusion (Table 6 and Table 7), suggesting that these micellar formulations do not cause dose-limiting adverse effects associated with free DOX.

Table 5: Canine pharmacokinetic parameters of ABDN-CP-DOX, CP-DOX and free DOX at a dose of 27 DOX Equiv/m^{-2} body surface area (BSA) for dogs weighing greater than 10 kg and 0.9 mg DOX Equiv/kg^{-1} of body weight (BW) for dogs weighing less than 10 kg. Values are shown as mean ± SD (n= 2 for ABDN-CP-DOX, n= 3 for CP-DOX and DOX).

		Dox	CP-DOX	ABDN-CP-DOX
Elimination half-life	$\alpha\ t_{1/2}$ [h]	2.9 ± 0.8	9.8 ± 1.9	30.8 ± 2.0
Area under the curve	AUC [μM. h]	1769.1 ± 498.0	84106.0 ± 7616.8	509371.7 ± 43095.2
Distribution half-life	$\beta\ t_{1/2}$ [min]	3.6 ± 0.5	6.6 ± 1.2	102.3 ± 49.3
Apparent distribution volume	V_D [mL g^{-1}]	3.85 ± 0.26	0.27 ± 0.01	0.02 ± 0.00
Plasma clearance	CL [mL h^{-1} g^{-1}]	0.7875 ± 0.0951	0.0194 ± 0.0004	0.0003 ± 0.0000
Elimination rate constant	k_e [h^{-1}]	0.96 ± 0.13	0.15 ± 0.01	0.02 ± 0.00
Tissue to plasma rate constant	k_p [h^{-1}]	2.31 ± 0.42	2.85 ± 0.50	0.34 ± 0.17
Plasma to tissue rate constant	k_{pt} [h^{-1}]	8.51 ± 1.20	3.37 ± 0.65	0.06 ± 0.03

Table 6: Canine hematology parameters one week after administration of CP-DOX and ABDN-CP-DOX micelles. No abnormalities in blood hematology were observed in any of the animals.

Test	Unit	CP-DOX			ABDN-CP-DOX		Normal range
		Subject 1	Subject 2	Subject 3	Subject 1	Subject 2	
WBC	X10^3/µL	3.93	6.29	4.95	7.86	7.01	4.39 - 11.61
RBC	X10^6/µL	5.99	5.72	6.87	5.97	6.19	5.7 - 8.01
Hemoglobin	g/dL	13.9	13.6	16	14.7	14.6	13.8 - 20.3
Hematocrit	%	41.4	40.9	47.2	42.7	43.9	39.2 - 55.9
MCV	fL	69.1	71.6	68.7	71.7	71	61.8 - 75.1
MCH	pg	23.2	23.9	23.3	24.6	23.6	20.2 - 25.3
MCHC	g/dL	33.6	33.3	33.9	34.3	33.2	30.8 - 35.4
RDW	%	12.6	13.8	12.4	12.8	11.7	11.3 - 13.5
Platelets	X10^3/µL	369	617	342	228	208	190 - 468
MPV	fL	10.9	7.8	7.9	12.2	11.9	7.9 - 13.8
PCT	%	0.4	0.48	0.27	0.28	0.25	0.2 -0.58
Reticulocyte %	%	0.44	2.74	0.59	0.43	0.23	0.11 - 1.26
Reticulocyte #	X10^6/µL	0.026	0.156	0.041	0.025	0.014	
Reticulocyte Absolute	/µL	26000	156000	41000	25000	14000	8040 - 93730
Packed Cell-Volume	%	41	40	44	42	42	39 - 58
Plasma Protein	g/dL	5.9	6	6	6.2	5.8	5.9 - 7.3
Segmented Neutrophils	10^3/µL	3.105	4.969	3.661	5.502	4.276	2.841 - 9.112
Lymphocytes	10^3/µL	0.393	0.252	0.396	1.572	1.122	0.594-3.305
Abnormal Lymphs	10^3/µL	0.079	0.315	0.248	0.157	0.561	0.075 - 0.85
Monocytes	10^3/µL	0.197	0.692	0.198	0.314	0.21	0.03 - 1.264

Table 7: Canine serum chemistry parameters one week after administration of CP-DOX and ABDN-CP-DOX micelles. No abnormalities in blood serum chemistry were observed in any of the animals.

Test	Unit	CP-DOX			ABDN-CP-DOX		Normal range
		Subject 1	Subject 2	Subject 3	Subject 1	Subject 2	
Glucose	mg/dL	99	99	98	90	82	70 - 131
Urea Nitrogen	mg/dL	12	19	16	17	15	6 - 26
Creatinine	mg/dL	0.5	0.7	0.7	0.7	0.7	0.7 - 1.5
Phosphorus	mg/dL	3.2	4.7	4	4.1	4.7	2.5 - 5.6
Calcium	mg/dL	9.7	9.5	9.9	10.3	10.7	9.4 - 11.4
Magnesium	mg/dL	2	2.1	2	1.9	2.2	1.8 - 2.5
Protein- Total	g/dL	5.3	5.4	5.6	6	5.9	5.2 - 7.3
Albumin	g/dL	3.6	3.1	3.6	3.8	3.6	3 - 3.9
Globulin	g/dL	1.7	2.3	2	2.2	2.3	1.7 - 3.8
Alb/Glob Ratio		2.12	1.35	1.8	1.73	1.57	0.9 - 1.8
Cholesterol	mg/dL	122	160	157	153	94	124 - 344
Bilirubin- Total	mg/dL	<0.2	<0.2	<0.2	<0.2	<0.2	0 - 0.2
Alkaline Phosphatase	IU/L	29	45	59	26	31	16 - 140
ALT	IU/L	50	39	28	18	21	12-54
AST	IU/L	23	24	22	20	31	16 - 140
GGT	IU/L	6	3	3	<3	<3	0 - 6
CK	IU/L	121	152	134	141	296	43 - 234
Sodium	mmol/L	148	143	146	148	148	140 - 156
Potassium	mmol/L	4.3	4.8	4.2	4	4.4	4 - 5.3
Chloride	mmol/L	109	106	107	109	111	108 - 122
Bicarbonate	mmol/L	24	19	22	22	21	18 - 26
Anion Gap		19.3	22.8	21.2	21	20.4	11.2 - 19.9
Na / K Ratio		34.4	29.8	34.8	37	33.6	27.7 - 35.9
Osmolality-Calc.	mOsm/kg	293.1	287.2	290.5	293.8	293.4	278.7 - 311.6
Amylase	IU/L	563	1025	823	597	677	236 - 1337
Lipase	IU/L	51	208	31	57	57	12 - 147

Example 7: Albumin binding improves targeting and biodistribution profile of the micelles.

[00131] The *in vivo* distribution of CP-DOX was evaluated after intravenous injection into tumor-bearing mice at a dose of 10 mg/kg and 20 mg/kg (FIG. 10B and FIG. 10C). It was observed that 24 h following injection, ABD-CP-DOX accumulated into tumor significantly more than CP-DOX and free DOX. CP-DOX micelles mainly distributed to the organs of the reticuloendothelial system i.e. liver and spleen (FIG. 10C). Furthermore, reticuloendothelial uptake of ABD-CP-DOX micelles was significantly smaller than that of CP-DOX micelles at both 2 h and 24 h time points. Free DOX showed smaller uptake than CP-DOX micelles in liver

and spleen and ABD-CP-DOX in liver at both 2 h and 24 h time points. DOX however was distributed more to muscle, heart, lung, and kidney than CP-DOX and ABD-CP-DOX micelles.

[00132] The *in vivo* tissue distribution of CP-DOX and ABDN-CP-DOX micelles was evaluated by *i.v.* injection of a dose of 10 and 20 mg DOX Equiv.kg^{-1} into Balb/C mice bearing *s.c.* C26 tumors. Free DOX was injected at a dose of 10 mg DOX Equiv.kg^{-1}. The higher dose of 20 mg DOX Equiv.kg^{-1} was not available for this study, as DOX is known to have a maximum tolerated dose that is $\leq$ 10 mg DOX Equiv.kg^{-1}. ABDN-CP-DOX micelles showed ~2 fold significantly greater accumulation in the tumor than CP-DOX micelles at 24 h post-injection at both 10 mg DOX Equiv.kg^{-1} ($P < 0.001$) and 20 mg DOX Equiv.kg^{-1} ($P < 0.01$) doses (FIG. 13A). Furthermore, compared with CP-DOX, ABDN-CP-DOX accumulated to a significantly lower extent in the liver and spleen at 2 h post-injection (FIG. 12B-C) and had significantly lower accumulation in the liver at 24 h post-injection (FIG. 13B). Free DOX showed lower accumulation in the liver than both CP-DOX and ABDN-CP-DOX micelles ($P < 0.001$), and lower accumulation in the spleen than CP-DOX micelles. No significant difference was observed between the spleen accumulation of free DOX and ABDN-CP-DOX. Free DOX however distributed to a greater extent to the heart, lung, kidneys, and muscle than CP-DOX and ABDN-CP-DOX micelles (FIG. 12D-G, FIG. 13D-G).

[00133] Biodistribution data in mice showed that albumin binding decreased the accumulation of micelles in RES organs i.e. liver and spleen. Micelles are colloidal nanoparticles and therefore are opsonized and sequestered into the RES organs i.e. the liver and spleen. Albumin coating prevents the adsorption of other serum proteins including opsonins and results in lower RES uptake, as reported in previous studies, and is consistent with an increase in plasma half-life at higher dose. The linear pharmacokinetics of ABD-CP-DOX micelle is significant from a clinical perspective, as dosing drugs with non-linear pharmacokinetics is difficult and infuses an element of unpredictability in terms of adverse reactions of the drug. Albumin binding nanoparticles showed lower accumulation in RES organs (liver and spleen) and therefore decrease the off-site toxicities of DOX (FIG. 13B and FIG. 13C). This is important from a clinical point view, as liver toxicity is a frontline concern in nanoparticulate drug development that accounts for the costly failure of many drugs late in the pipeline.

[00134] Consistent with the lower RES organ uptake, which are well known "sinks" for nanoparticles, the tumor accumulation of ABDN-CP-DOX micelles was approximately 2.5-fold greater than compared to CP-DOX micelles at a dose of 10, and was approximately 2-fold greater at a dose of 20 mg DOX Equiv.kg^{-1} BW.

Example 8: ABD-CP-DOX micelles increase the tumoricidal effect

[00135] Anti-tumor efficacy of the ABD-CP-DOX micelles compared with CP-DOX micelles and free DOX was evaluated in a mouse C26 colon cancer model (FIG. 10D and FIG. 10F). Results of tumor measurements revealed that tumor growth was significantly slower in the ABD-CP-DOX administration group than that of CP-DOX and free DOX groups (FIG. 10D). Furthermore, at a DOX equivalent dose of 20 mg/kg BW, ABD-CP-DOX micelles prolonged the survival periods of tumor bearing mice as compared to CP-DOX micelles (FIG. 10E). 50% of tumor bearing mice treated with ABD-CP-DOX survived 60 days after treatment, whereas CP-DOX treated group showed a 39-day survival. Both micellar treatment groups showed slower tumor growth and longer survival than the free DOX treatment group.

Example 9: Development of albumin binding self-assembling micelles with Paclitaxel

[00136] Paclitaxel was conjugated to cysteine residues at the C-terminus of CP and ABD-CP via a pH-sensitive linker, as described in Example 1. Paclitaxel conjugation was confirmed by MALDI-TOF-MS. Conjugation with ABD-CP resulted in a 1700 Dalton molecule weight difference indicating the presence of 2 drugs per ABD-CP (FIG. 16A). Conjugation with CP resulted in a 2100 Dalton molecule weight difference indicating the presence of on average 2.5 drugs per CP (FIG. 16B). Following conjugation to paclitaxel both CP-PTX and ABD-CP-PTX were evaluated by dynamic light scattering to verify their hydrodynamic radii (FIG. 17A and FIG. 17B). The results for two different concentrations are shown in Table 8.

Table 8: Dynamic light scattering data for ABDN-CP-PTX and CP-PTX

Conjugate	Concentration (μM)	R_h (nm)	% Intensity	Polydispersity
CP-PTX	20	48.9 ± 2.3	99.3	40.8%
	40	52.4 ± 2.9	96.4	30.5%
ABD-CP-PTX	20	39.6 ± 2.2	95.4	24.6%
	40	44.1 ± 4.7	96.6	26.6%

Static light scattering (FIG. 18A and FIG. 18B) was used to analyze the radius of gyration, R_G, a mass density size measurement and overall molecular weight of the conjugated nanoparticle. The dynamic and static light scattering results were combined to calculate a number of chains per nanoparticle (n_{agg}, Table 9).

Table 9: Light scattering data for ABDN-CP-PTX and CP-PTX at 20 μM concentration

	DLS Analysis		SLS Analysis		
	R_h (nm)	**Polydispersity**	**R_G (nm)**	**MW_{agg}**	**N_{agg}**
CP-PTX	48.9 ± 2.3	40.8%	38.35	1.060 MDa	16.2
ABD-CP-PTX	39.6 ± 2.2	24.6%	42.83	4.548 MDa	64.5

[00137] As with the (ABD-)CP-DOX micelles, the binding affinity of ABD-CP and ABD-CP-PTX for human serum albumin (HSA) and mouse serum albumin (MSA) was analyzed quantitatively by ITC (FIG. 19A, 19B, 20A, and 20B). It was observed that PTX conjugated ABD-CP still displayed strong sub-μM affinity for both mouse and human albumin (Table 10). The binding data showed that both ABD-CP monomers and ABD-CP-PTX micelles bind to human and mouse albumin with 1:1 stoichiometry and nanomolar affinity, whereas ELP and CP-PTX controls displayed no specific affinity.

[00138] Table 10: Albumin binding affinity for ABD-CP-PTX, ABD-CP and CP-PTX.

Conjugate	Albumin	K_D (nM)	n
ABD-CP	HSA	6.47	0.95
	MSA	16.3	1.05
ABD-CP-PTX	HSA	5.58	0.92
	MSA	4.37	0.95
CP	HSA	4500	1.46
	MSA	3500	0.85
CP-PTX	HSA	N/A	N/A
	MSA	N/A	N/A

[00139] ABDN-CP fusions for conjugation with Paclitaxel showed that the T_t decreased from 60 °C for CP to 48 °C for ABDN-CP. ABDN-CP-PTX nanoparticles, showed no aggregates at 37 °C.

Example 10: *In vitro* cytotoxicity of ABDN-CP-PTX, CP-PTX, and free PTX.

[00140] *In vitro* cytotoxicity of the ABDN-CP-PTX versus that of naked CP-PTX and free PTX was determined using the calorimetric MTS assay in MDA-MB-213 human breast cancer cells (FIG. 21). This cell line was chosen because it demonstrates higher inherent resistance to Paclitaxel. The half-maximal inhibitory concentration (IC_{50}), defined as the concentration of the drug required to cause 50% decrease in viable MDA-MB-213 cells in culture, was found to be 10.9, 22.4, and 9.8 nM for ABDN-CP-PTX, CP-PTX, and free PTX, respectively (Figure 21). These IC_{50} values are similar, confirming that the anticancer activity of PTX is not markedly reduced upon conjugation to ABDN-CP or the CP.

[00141] For reasons of completeness, various aspects of the invention are set out in the following numbered clauses:

[00142] Clause 1. A composition comprising: an assembly of self-assembling conjugates, each self-assembling conjugate comprising a polypeptide having a transition temperature (T_t) above 50 °C when the polypeptide is not attached to the conjugate; an albumin binding domain (ABD) attached to a first end of the polypeptide; and at least one molecule attached to a second end of the polypeptide through a cysteine group, wherein the molecule has an octanol-water distribution coefficient (logD) of greater than or equal to 1.5 at a pH of 7.4 when the molecule is not attached to the conjugate, wherein the conjugate has a T_t above 40 °C at a concentration of 100 μM.

[00143] Clause 2. A composition comprising: an assembly of self-assembling conjugates, each self-assembling conjugate comprising a polypeptide having a transition temperature (T_t) above 50°C when the polypeptide is not attached to the conjugate; an albumin binding domain (ABD) attached to a first end of the polypeptide, wherein the ABD attached to the polypeptide lowers the T_t of the polypeptide no more than 5 °C relative to the polypeptide's T_t when the polypeptide is not attached to the ABD or the conjugate; and at least one molecule attached to a second end of the polypeptide through a cysteine group, wherein the molecule has an octanol-water distribution coefficient (logD) of greater than or equal to 1.5 at a pH of 7.4 when the molecule is not attached to the conjugate.

[00144] Clause 3. The composition of clause 1 or clause 2, wherein the ABD comprises SEQ ID NO:6.

[00145] Clause 4. The composition of any one of clauses 1-3, wherein the polypeptide comprises an amino acid sequence of $(X^1GVPG)_x$ (SEQ ID NO:2), wherein X^1 is an amino acid or a combination of amino acids and x is 40 to 400.

[00146] Clause 5. The composition of any one of clauses 1-4, wherein the polypeptide comprises an amino acid sequence of $(X^1GVPG)_m$ (SEQ ID NO:3), wherein X^1 is A or V:A:G at a ratio of 1:7:8 and m is 160.

[00147] Clause 6. The composition of any one of clauses 1-3, wherein the polypeptide comprises an amino acid sequence of $(CGG)_z$ (SEQ ID NO:4) at its C-terminus, wherein z is greater than 1.

[00148] Clause 7. The composition of clause 6, wherein the polypeptide comprises an amino acid sequence of $(CGG)_8$ (SEQ ID NO:5) at its C-terminus.

[00149] Clause 8. The composition of any one of clauses 1-7, wherein the molecule is a chemotherapeutic or an imaging agent.

[00150] Clause 9. The composition of any one of clauses 1-8, wherein about 1 to about 15 molecules are attached to the polypeptide.

[00151] Clause 10. The composition of any one of clauses 1-9, wherein the molecule is attached to the polypeptide through a thiol group.

[00152] Clause 11. The composition of any one of clauses 1-10, wherein the assembly of self-assembling conjugates is a nanoparticle.

[00153] Clause 12. The composition of any one of clauses 1-11, wherein the molecule is located in a core of the nanoparticle.

[00154] Clause 13. The composition of any one of clauses 1-12, wherein the nanoparticle has an average hydrodynamic radius of about 10 nm to about 100 nm.

[00155] Clause 14. The composition of any one of clauses 1-13, wherein the nanoparticle is a micelle.

[00156] Clause 15. A method of killing multiple cancer cells comprising contacting multiple cancer cells with the composition of any of clauses 1-14.

[00157] Clause 16. A method of treating a disease or disorder in a subject comprising administering to the subject the composition of any of clauses 1-14.

[00158] Clause 17. The method of clause 16, wherein the disease or disorder is cancer.

[00159] Clause 18. A method of localizing a molecule to a tissue or organ in a subject, the method comprising administering to the subject the composition of any of clauses 1-14, wherein following administration of the composition the molecule is localized in the liver at less than 30% of the injected dose/gram of tissue or organ (ID/g).

[00160] Clause 19. A method of localizing a molecule to a tissue or organ in a subject, the method comprising administering to the subject the composition of any of clauses 1-14, wherein following administration of the composition the molecule is localized in the spleen at less than 10% of the injected dose/gram of tissue or organ (ID/g).

[00161] Clause 20. A method of localizing a molecule to a tissue or organ in a subject, the method comprising administering to the subject the composition of any of clauses 1-14, wherein following administration of the composition the amount of the molecule localized in the tissue or organ is decreased when compared to the molecule in a self-assembling conjugate without an albumin binding domain and wherein the tissue or organ is a kidney, liver, spleen or any combination thereof.

[00162] Clause 21. The method of clause 20, wherein the amount of the molecule localized in the tissue or organ is decreased at least two-fold.

[00163] Clause 22. A method of localizing a molecule to a tumor in a subject, the method comprising administering to the subject the composition of any of clauses 1-14, wherein following administration of the composition the amount of the molecule localized to the tumor is increased when compared to the molecule in a self-assembling conjugate without an albumin binding domain.

[00164] Clause 23. The method of clause 22, wherein the amount of the molecule localized to the tumor is increased at least two-fold.

Sequences

$(VPGXG)_n$ wherein X is any amino acid except proline and n is an integer greater than or equal to 1 (SEQ ID NO:1)

$(X^1GVPG)_x$ wherein X^1 is an amino acid or a combination of amino acids and x is an integer from 40 to 400 (SEQ ID NO:2)

$(X^1GVPG)_m$ wherein X^1 is A or V:A:G at a ratio of 1:7:8 and m is 160 (SEQ ID NO:3)

$(CGG)_z$ wherein z is an integer greater than 1 (SEQ ID NO:4)

$(CGG)_8$ (SEQ ID NO:5)

LAEAKVLANRELDKYGVSDYYKNLINNAKTVEGVKALIDEILAALP (SEQ ID NO:6)

LAEAKVLANRELDKYGVSDFYKRLINKAKTVEGVEALKLHILAALP (SEQ ID NO:7)

KEKE (SEQ ID NO:8)

CLAIMS

What is claimed is:

1. A composition comprising:

an assembly of self-assembling conjugates, each self-assembling conjugate comprising

a polypeptide having a transition temperature (T_t) above 50 °C when the polypeptide is not attached to the conjugate;

an albumin binding domain (ABD) attached to a first end of the polypeptide; and

at least one molecule attached to a second end of the polypeptide through a cysteine group, wherein the molecule has an octanol-water distribution coefficient (logD) of greater than or equal to 1.5 at a pH of 7.4 when the molecule is not attached to the conjugate,

wherein the conjugate has a T_t above 40 °C at a concentration of 100 μM.

2. A composition comprising:

an assembly of self-assembling conjugates, each self-assembling conjugate comprising

a polypeptide having a transition temperature (T_t) above 50°C when the polypeptide is not attached to the conjugate;

an albumin binding domain (ABD) attached to a first end of the polypeptide, wherein the ABD attached to the polypeptide lowers the T_t of the polypeptide no more than 5 °C relative to the polypeptide's T_t when the polypeptide is not attached to the ABD or the conjugate; and

at least one molecule attached to a second end of the polypeptide through a cysteine group, wherein the molecule has an octanol-water distribution coefficient (logD) of greater than or equal to 1.5 at a pH of 7.4 when the molecule is not attached to the conjugate.

3. The composition of claim 1 or claim 2, wherein the ABD comprises SEQ ID NO:6.

4. The composition of claim 1 or claim 2, wherein the polypeptide comprises an amino acid sequence of $(X^1GVPG)_x$ (SEQ ID NO:2), wherein X^1 is an amino acid or a combination of amino acids and x is 40 to 400.

5. The composition of claim 1 or claim 2, wherein the polypeptide comprises an amino acid

sequence of $(X^1GVPG)_m$ (SEQ ID NO:3), wherein X^1 is A or V:A:G at a ratio of 1:7:8 and m is 160.

6. The composition of claim 1 or claim 2, wherein the polypeptide comprises an amino acid sequence of $(CGG)_z$ (SEQ ID NO:4) at its C-terminus, wherein z is greater than 1.

7. The composition of claim 6, wherein the polypeptide comprises an amino acid sequence of $(CGG)_8$ (SEQ ID NO:5) at its C-terminus.

8. The composition of claim 1 or claim 2, wherein the molecule is a chemotherapeutic or an imaging agent.

9. The composition of claim 1 or claim 2, wherein about 1 to about 15 molecules are attached to the polypeptide.

10. The composition of claim 1 or claim 2, wherein the molecule is attached to the polypeptide through a thiol group.

11. The composition of claim 1 or claim 2, wherein the assembly of self-assembling conjugates is a nanoparticle.

12. The composition of claim 1 or claim 2, wherein the molecule is located in a core of the nanoparticle.

13. The composition of claim 11, wherein the nanoparticle has an average hydrodynamic radius of about 10 nm to about 100 nm.

14. The composition of claim 11, wherein the nanoparticle is a micelle.

15. A method of treating a disease or disorder in a subject comprising administering to the subject the composition of claim 1 or claim 2.

16. The method of claim 15, wherein the disease or disorder is cancer.

17. A method of localizing a molecule to a tissue or organ in a subject, the method comprising administering to the subject the composition of claim 1 or claim 2, wherein following administration of the composition the amount of the molecule localized in the tissue or organ is decreased when compared to the molecule in a self-assembling conjugate without an albumin binding domain and wherein the tissue or organ is a kidney, liver, spleen or any combination thereof.

18. The method of claim 17, wherein the amount of the molecule localized in the tissue or organ is decreased at least two-fold.

19. A method of localizing a molecule to a tumor in a subject, the method comprising administering to the subject the composition of claim 1 or claim 2, wherein following administration of the composition the amount of the molecule localized to the tumor is increased when compared to the molecule in a self-assembling conjugate without an albumin binding domain.

20. The method of claim 19, wherein the amount of the molecule localized to the tumor is increased at least two-fold.

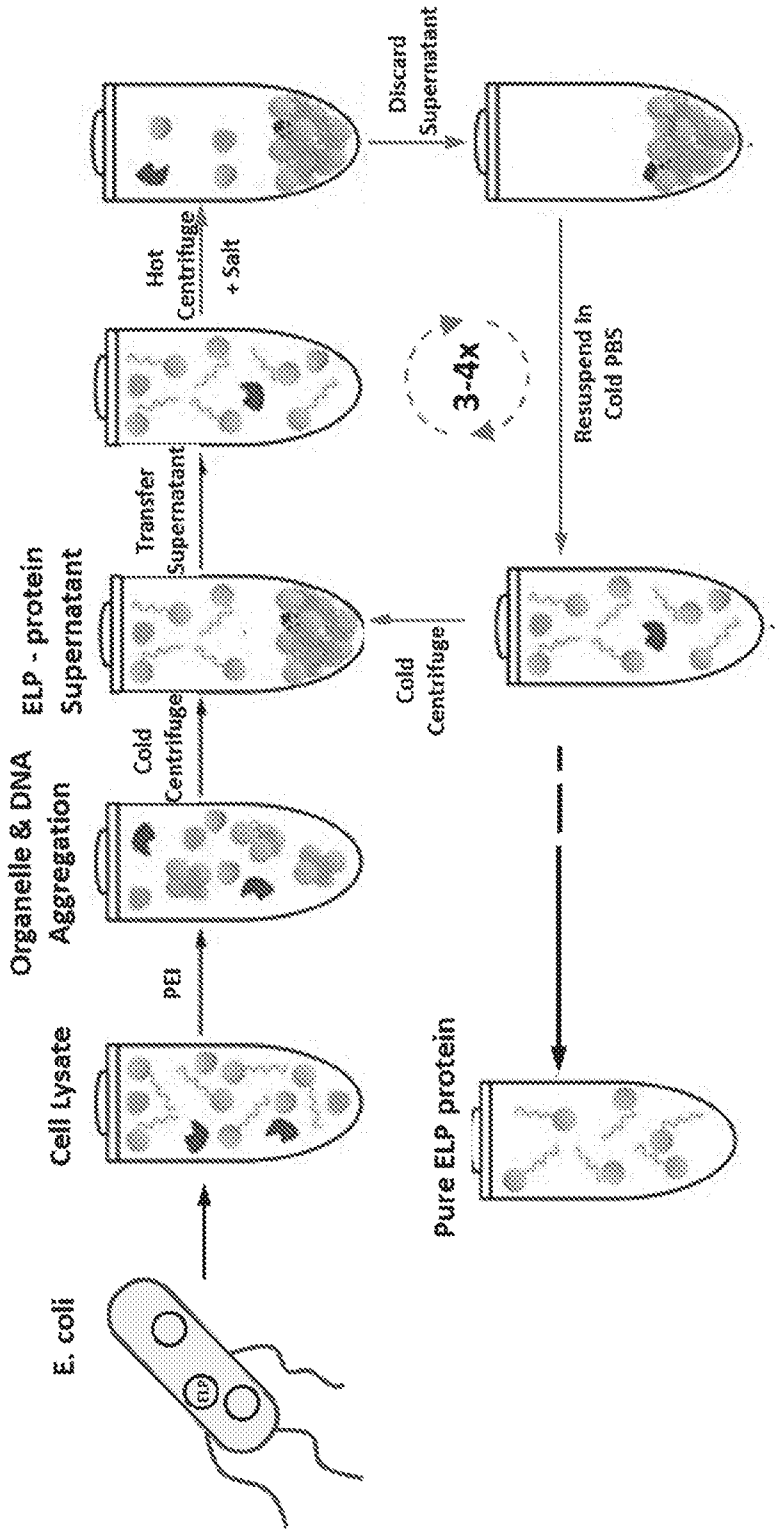
E. coli
Cell Lysate
PEI
Organelle & DNA Aggregation
Cold Centrifuge
ELP - protein Supernatant
Transfer Supernatant
Hot Centrifuge
+ Salt
Discard Supernatant
3-4x
Resuspend in Cold PBS
Cold Centrifuge
Pure ELP protein

FIG. 1

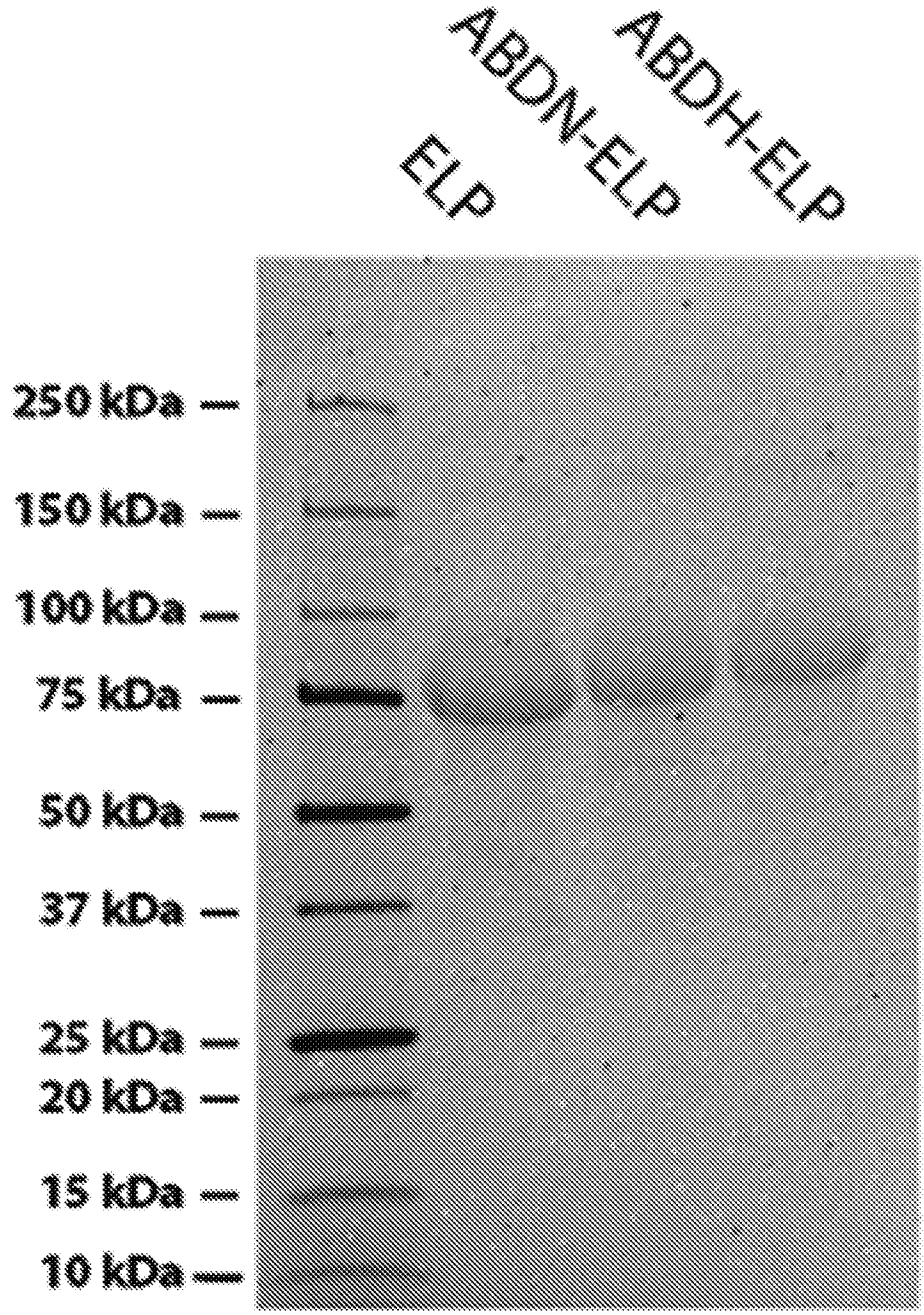
ELP
ABDN-ELP
ABDH-ELP
250 kDa
150 kDa
100 kDa
75 kDa
50 kDa
37 kDa
25 kDa
20 kDa
15 kDa
10 kDa

FIG. 2A

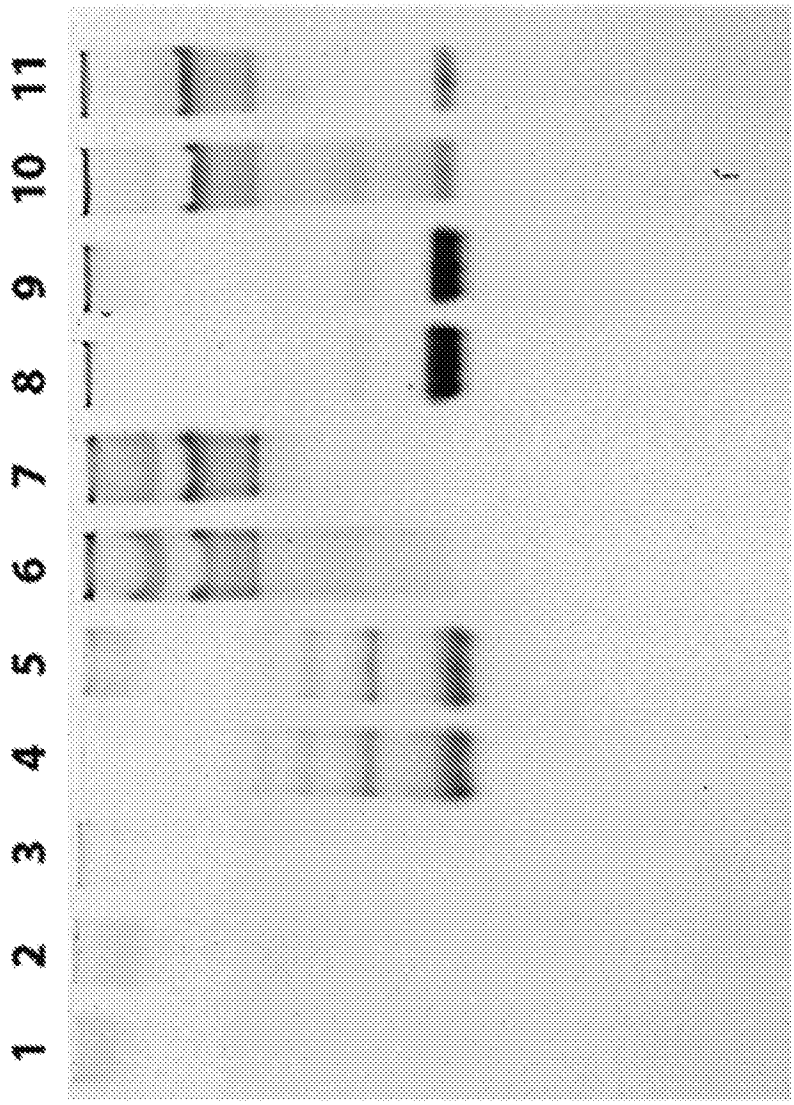
1 2 3 4 5 6 7 8 9 10 11
1: ELP
2: ABDN-ELP
3: ABDH-ELP
4: MSA
5: ELP+MSA
6: ABDN-ELP + MSA
7: ABDH-ELP + MSA
8: HSA
9: ELP+ HSA
10: ABDN-ELP + HSA
11: ABDH-ELP + HSA

FIG. 2B

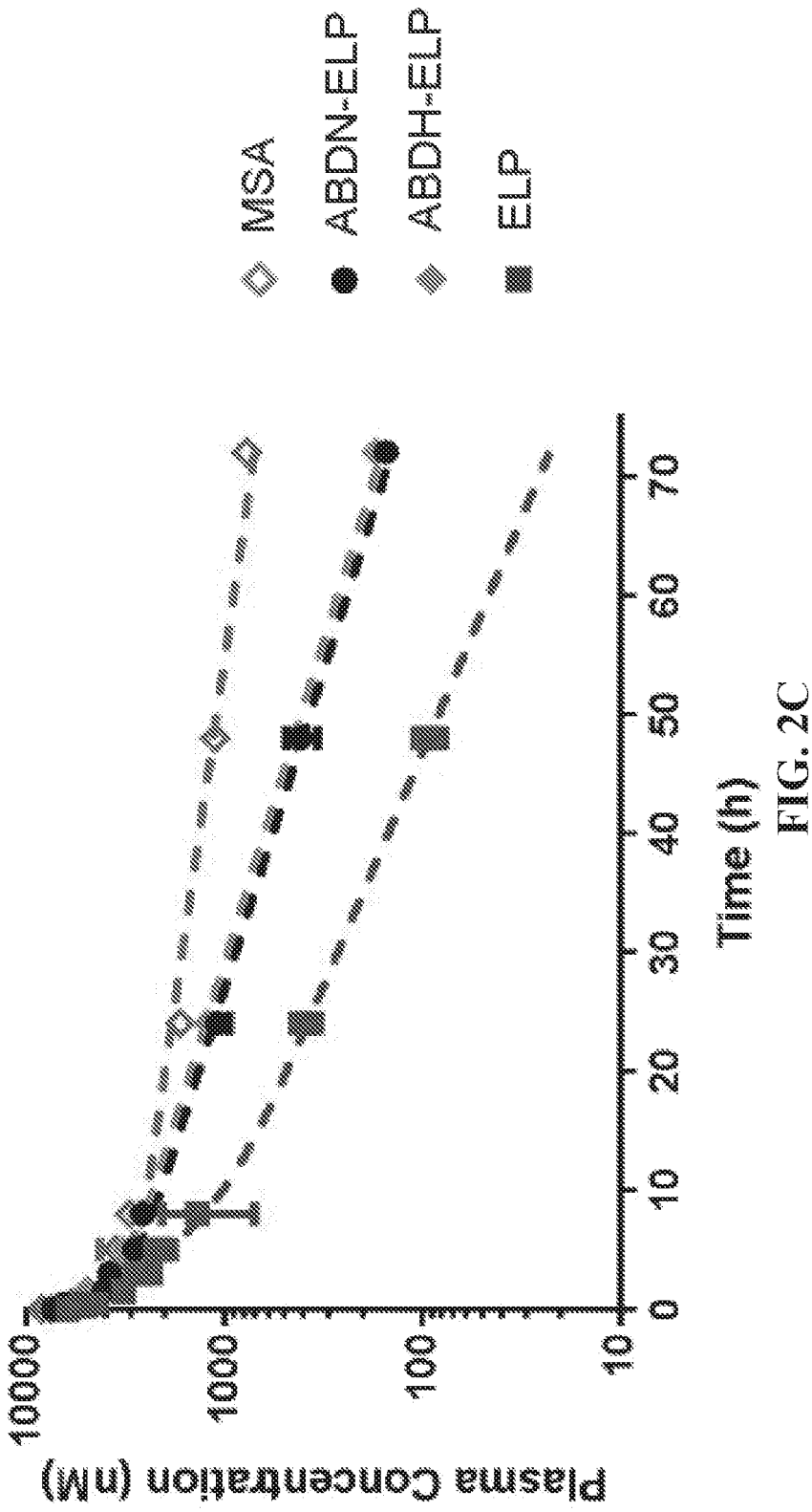
MSA
ABDN-ELP
ABDH-ELP
ELP
Plasma Concentration (nM)
10000
1000
100
10
0
10
20
30
40
50
60
70
Time (h)

FIG. 2C

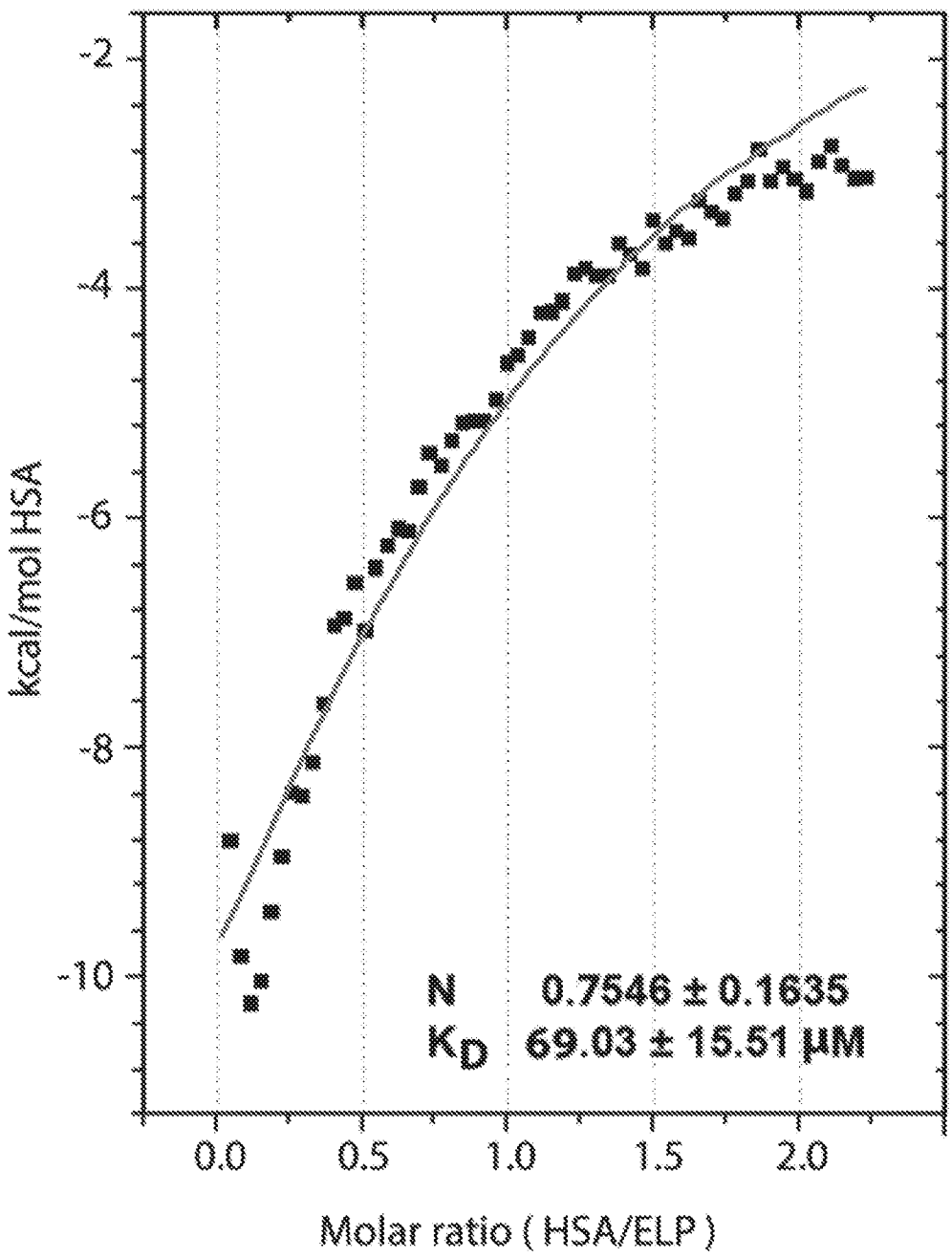
-2
-4
-6
-8
-10
kcal/mol HSA
N 0.7546 ± 0.1635
K_D 69.03 ± 15.51 μM
0.0
0.5
1.0
1.5
2.0
Molar ratio (HSA/ELP)

FIG. 3A

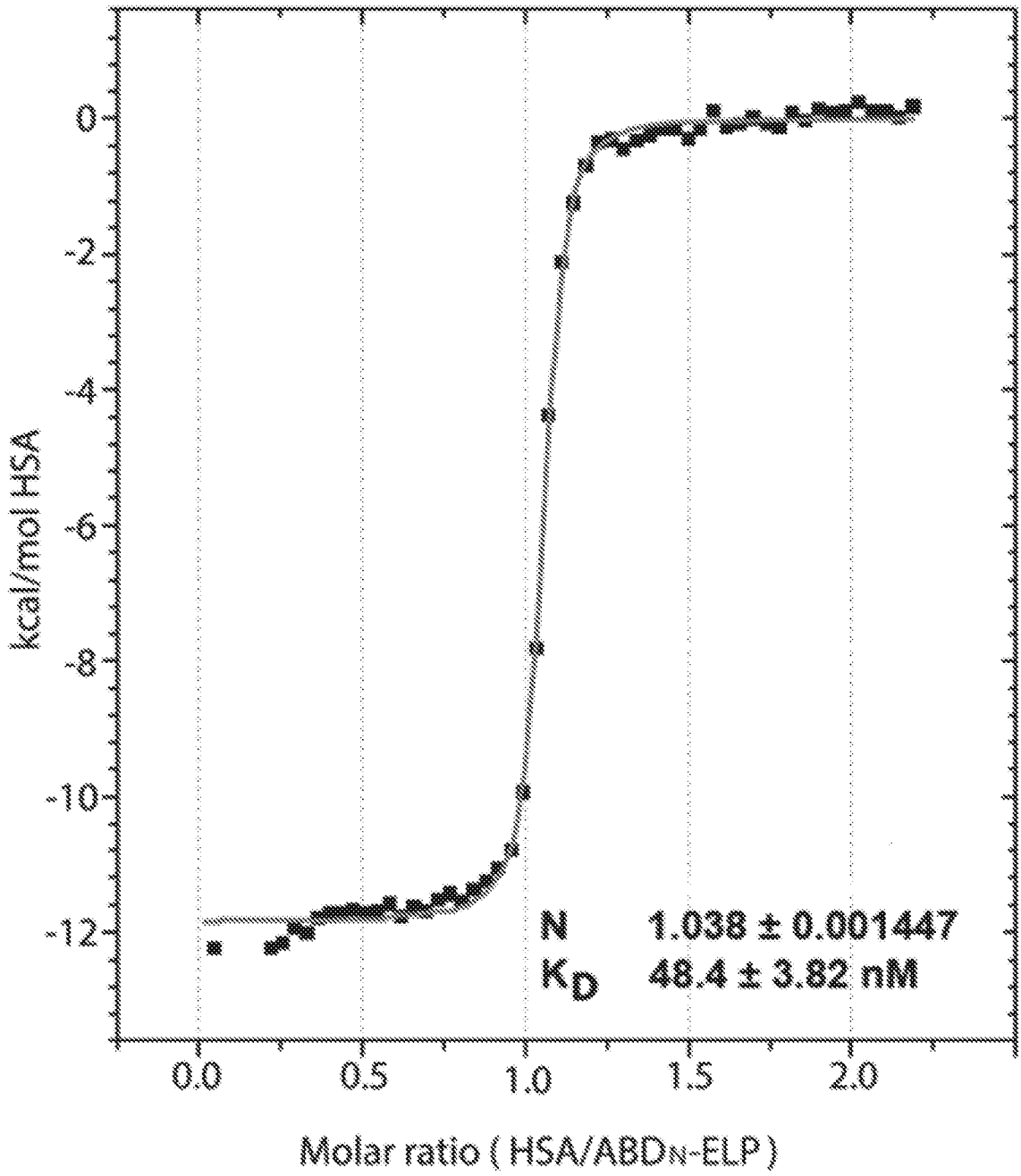
kcal/mol HSA
0
-2
-4
-6
-8
-10
-12
0.0
0.5
1.0
1.5
2.0
Molar ratio (HSA/ABDN-ELP)
N 1.038 ± 0.001447
KD 48.4 ± 3.82 nM

FIG. 3B

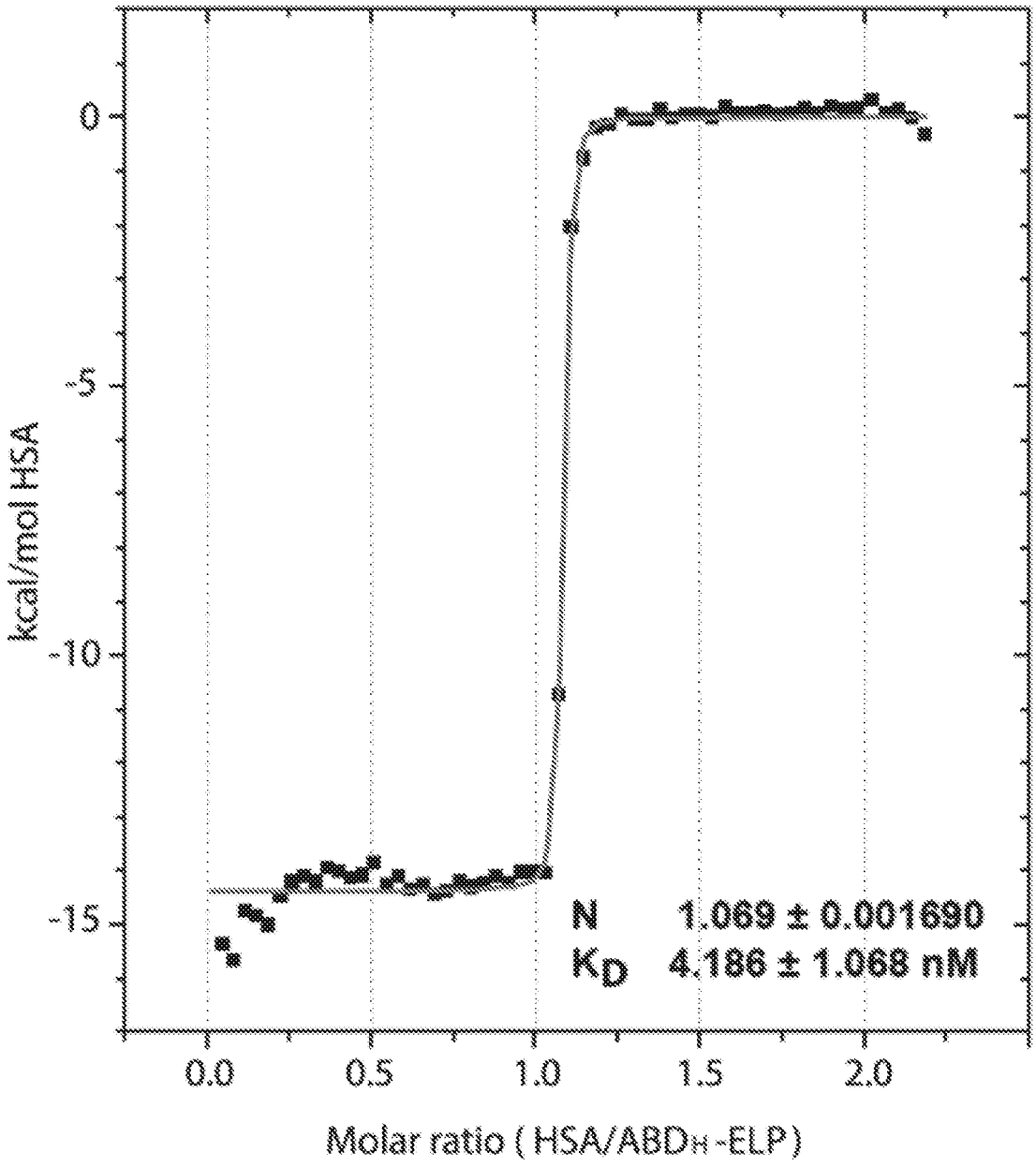
0
-5
-10
-15
kcal/mol HSA
N 1.069 ± 0.001690
K_D 4.186 ± 1.068 nM
0.0
0.5
1.0
1.5
2.0
Molar ratio (HSA/ABD_H -ELP)

FIG. 3C

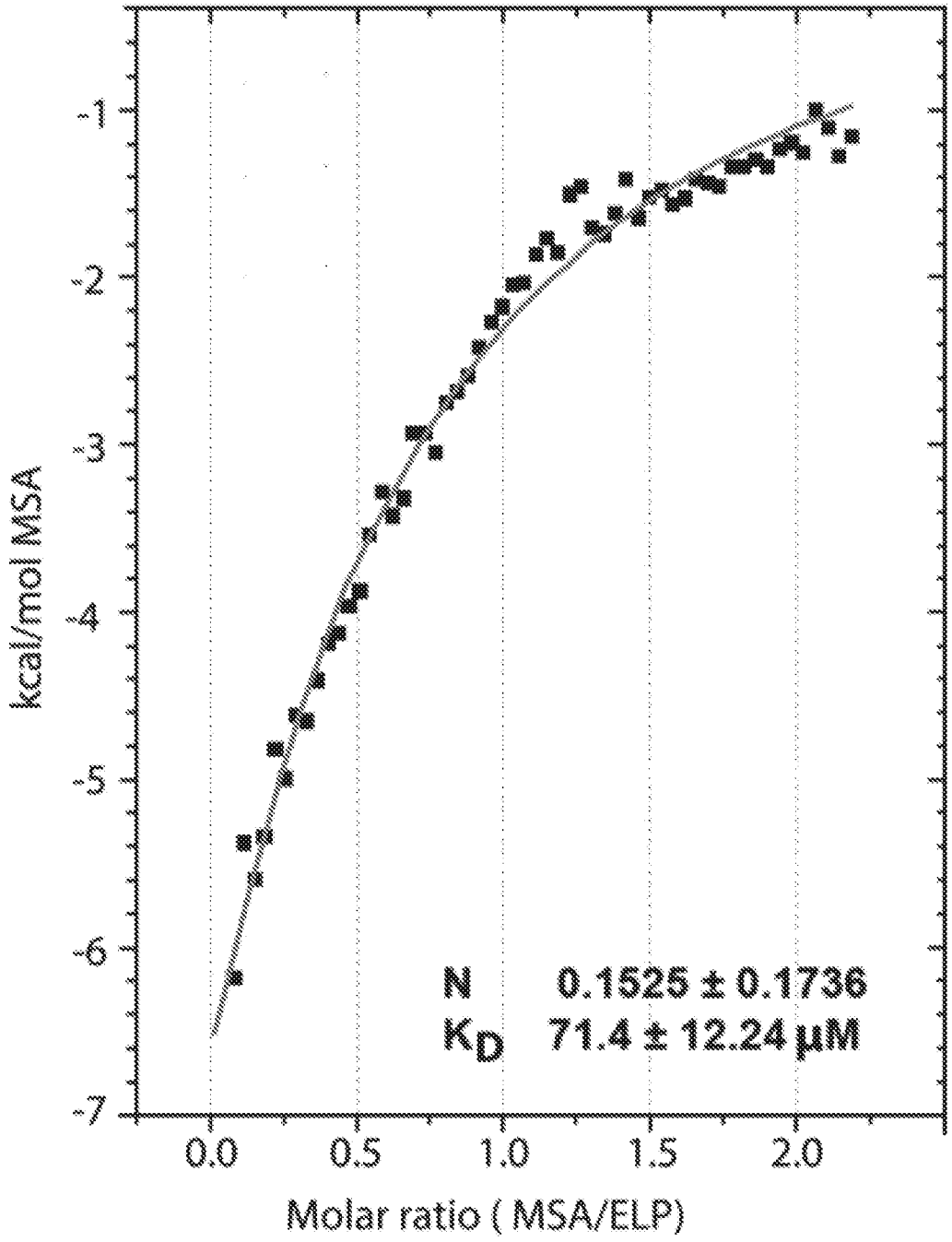
kcal/mol MSA
-1
-2
-3
-4
-5
-6
-7
0.0
0.5
1.0
1.5
2.0
Molar ratio (MSA/ELP)
N 0.1525 ± 0.1736
K_D 71.4 ± 12.24 µM

FIG. 4A

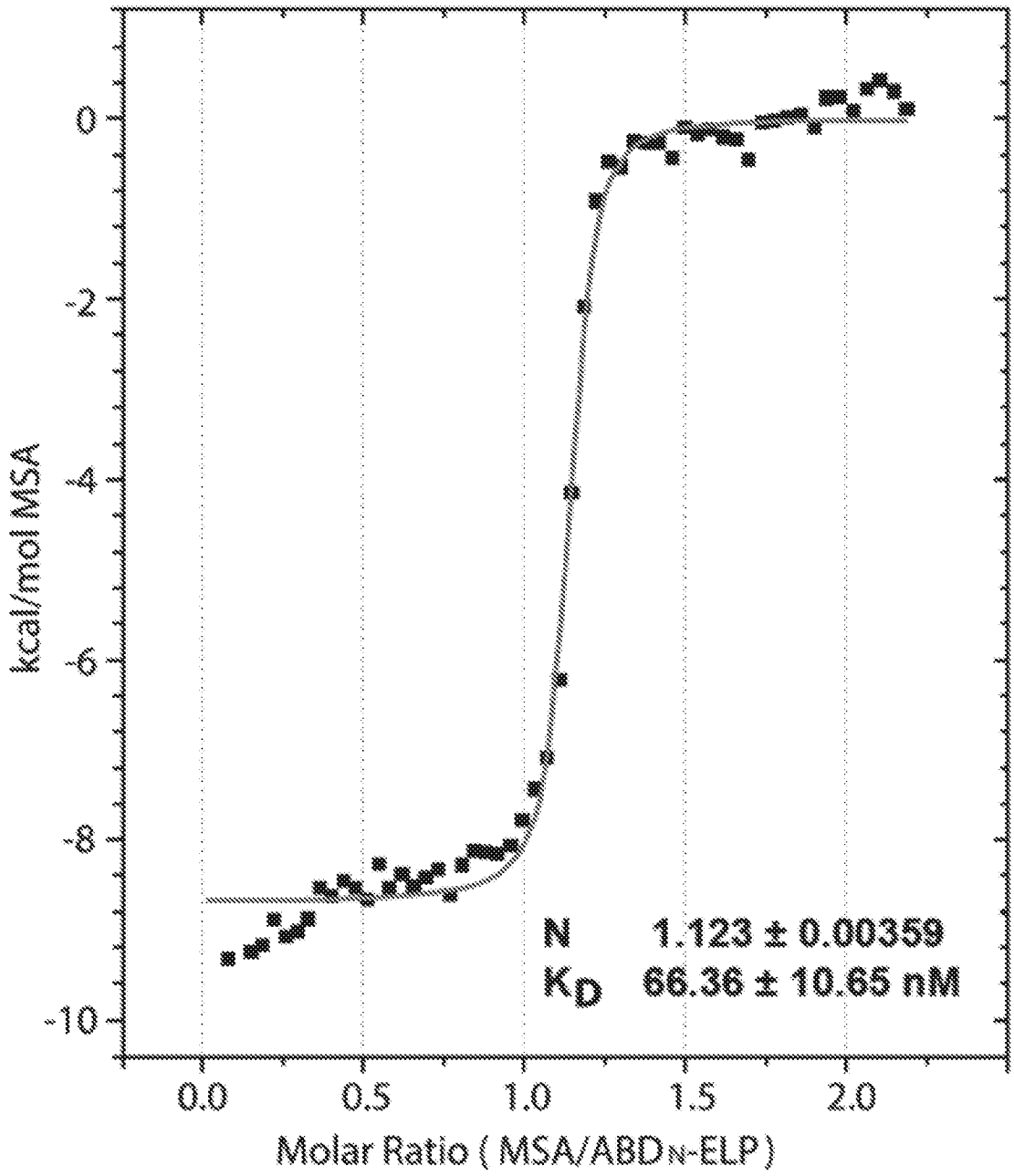
kcal/mol MSA
0
-2
-4
-6
-8
-10
0.0
0.5
1.0
1.5
2.0
Molar Ratio (MSA/ABDN-ELP)
N 1.123 ± 0.00359
KD 66.36 ± 10.65 nM

FIG. 4B

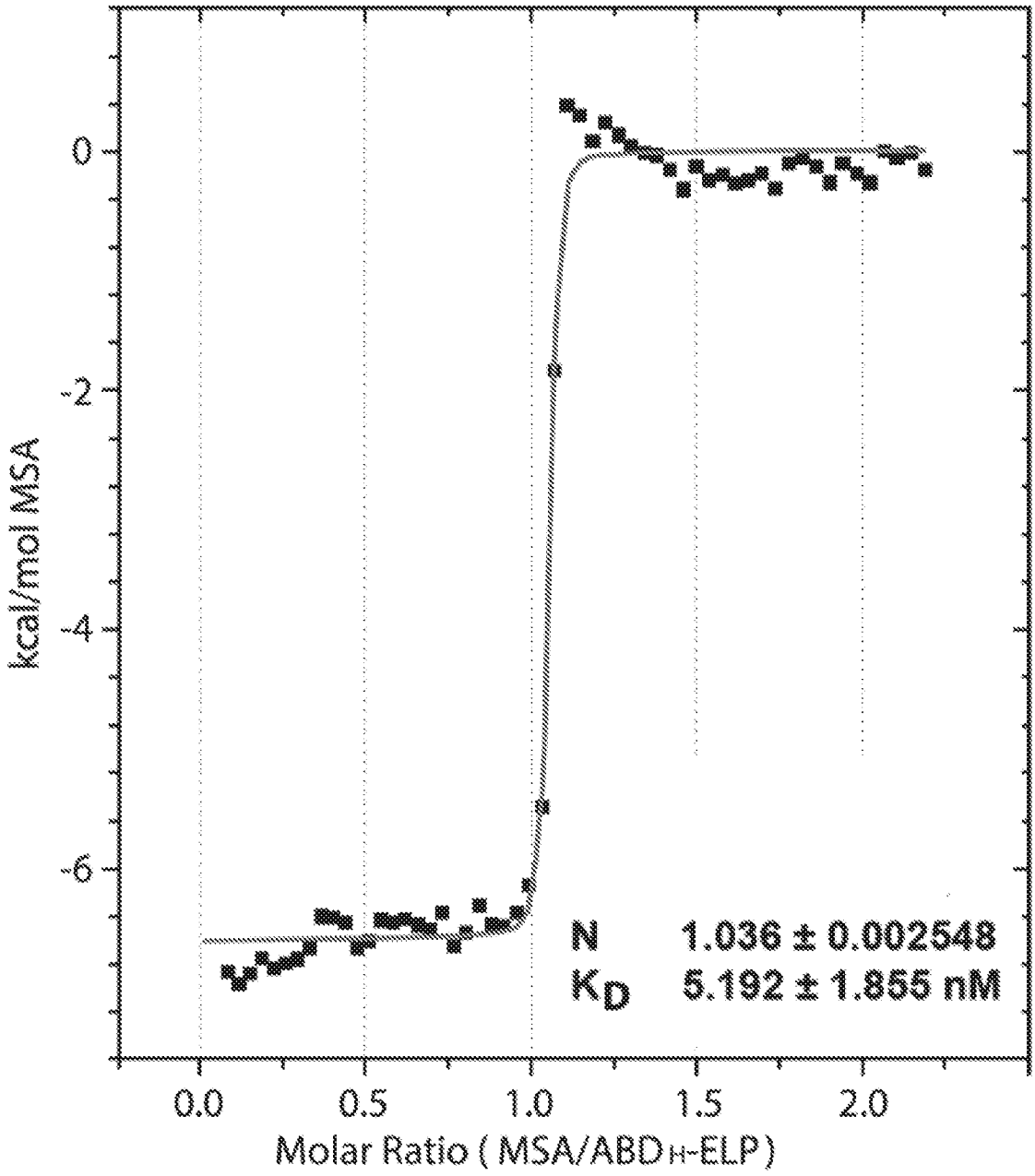
kcal/mol MSA
0
-2
-4
-6
0.0
0.5
1.0
1.5
2.0
Molar Ratio (MSA/ABDH-ELP)
N 1.036 ± 0.002548
KD 5.192 ± 1.855 nM

FIG. 4C

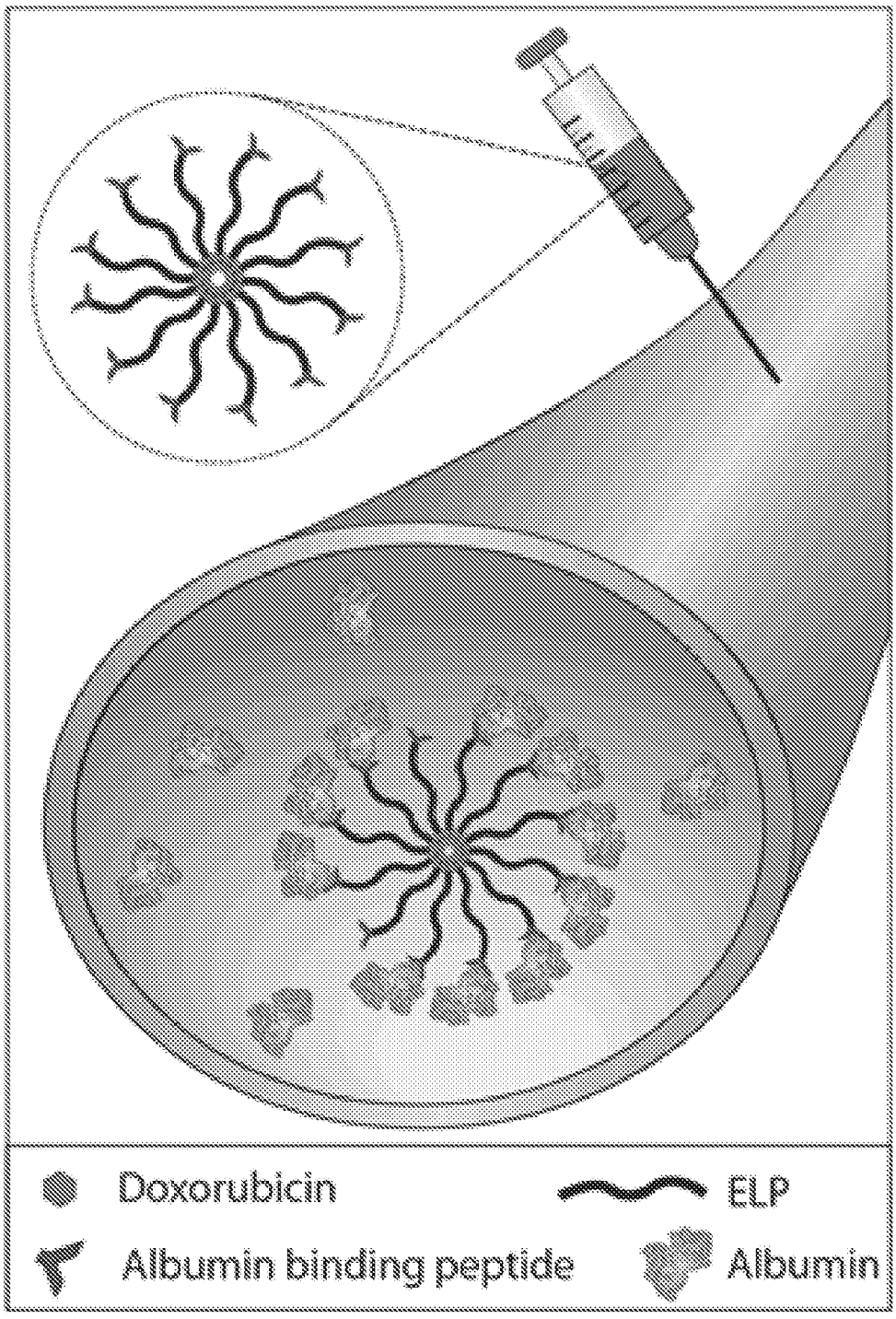

FIG. 5

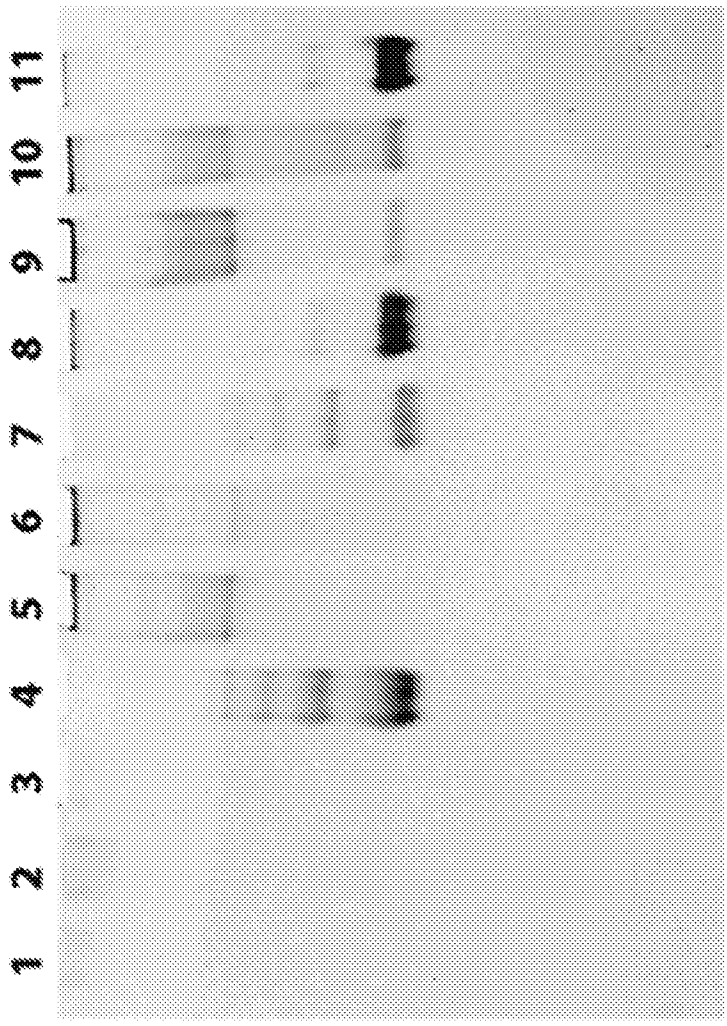
1 2 3 4 5 6 7 8 9 10 11
1: ABDH-CP-DOX
2: ABDN-CP-DOX
3: CP-DOX
4: MSA
5: ABDH-CP-DOX + MSA
6: ABDN-CP-DOX + MSA
7: CP-DOX + MSA
8: HSA
9: ABDH-CP-DOX + HSA
10: ABDN-CP-DOX + MSA
11: CP-DOX + HSA

FIG. 6A

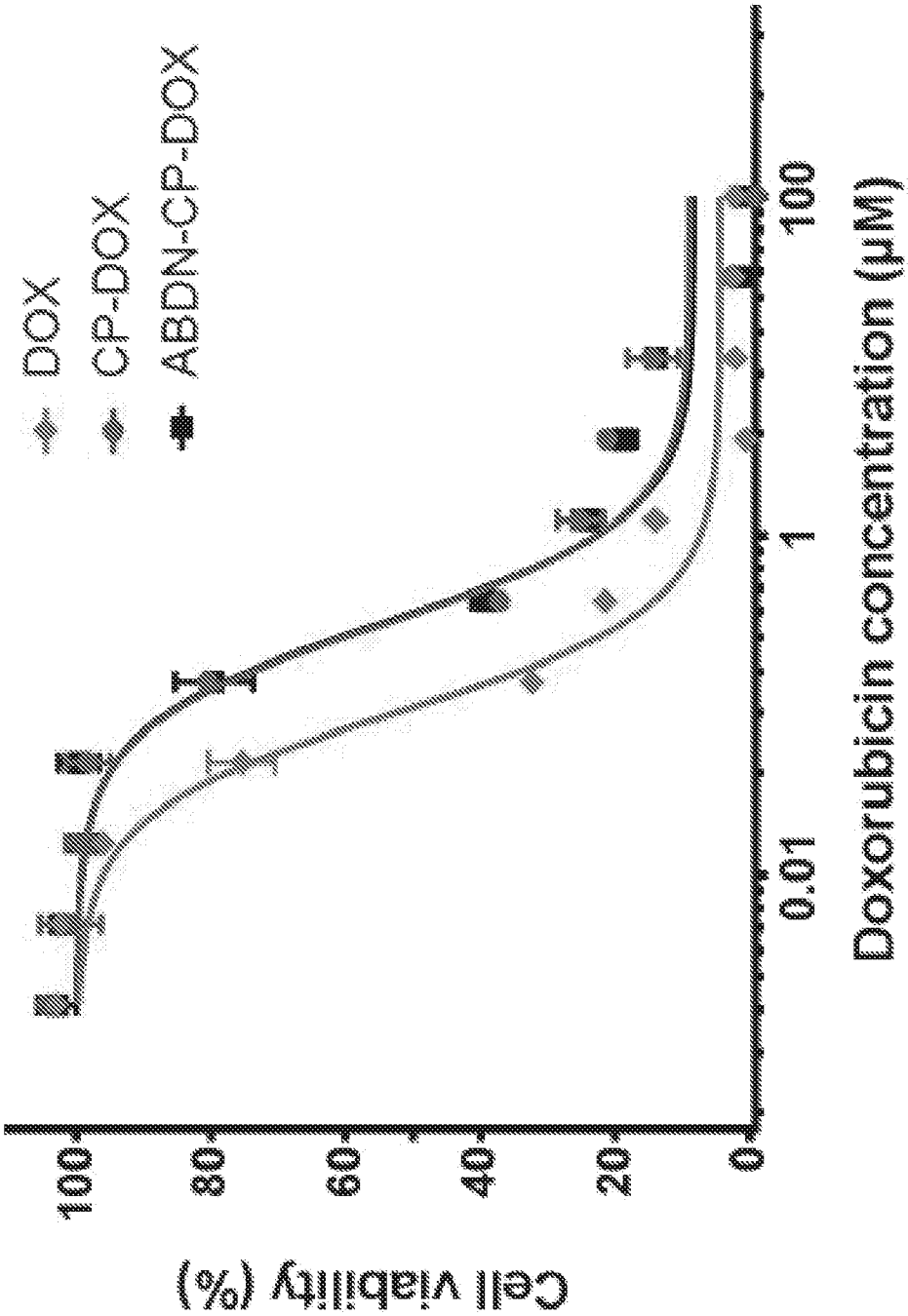
DOX
CP-DOX
ABDN-CP-DOX
Cell viability (%)
100
80
60
40
20
0
0.01
1
100
Doxorubicin concentration (μM)

FIG. 6B

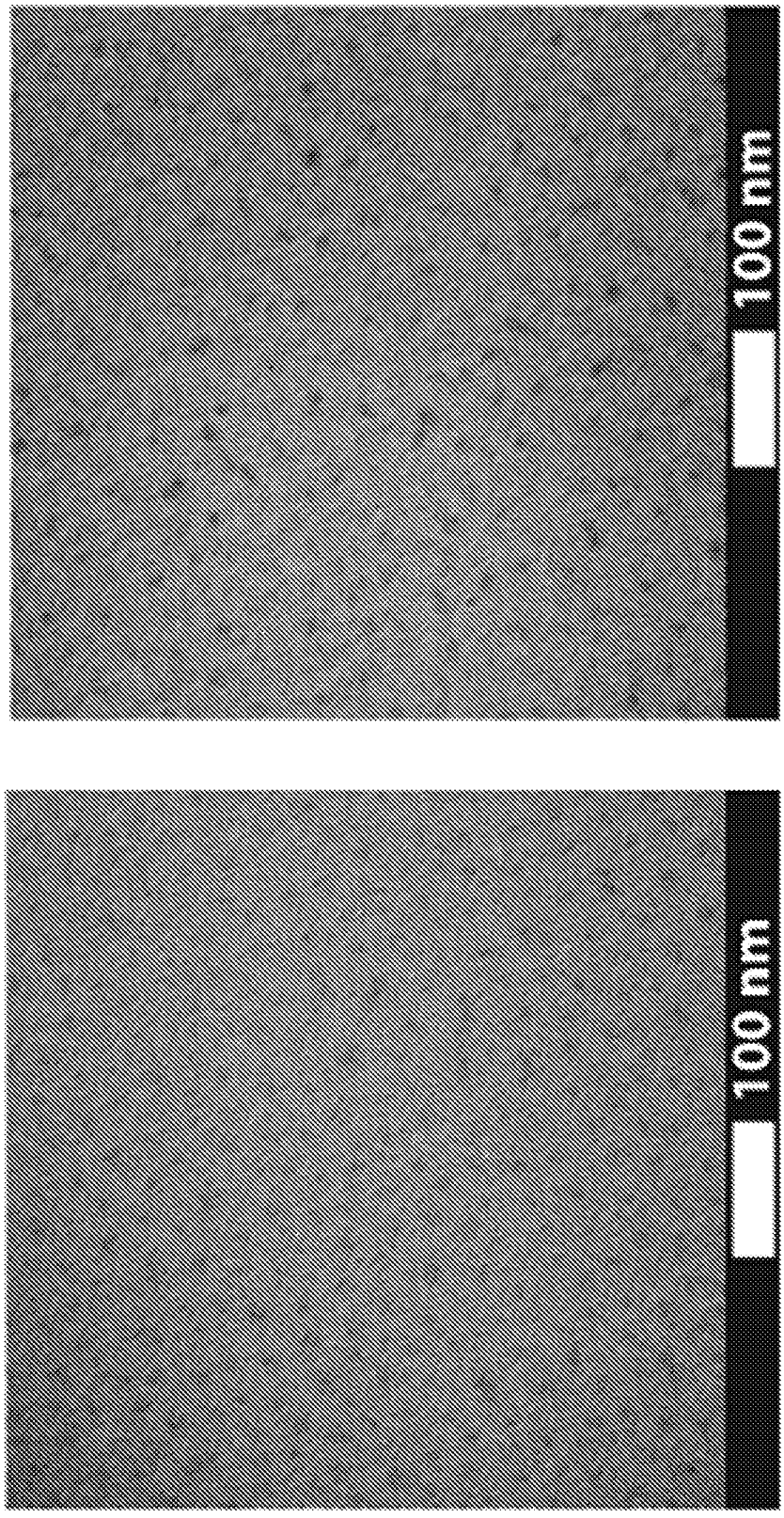

FIG. 6C

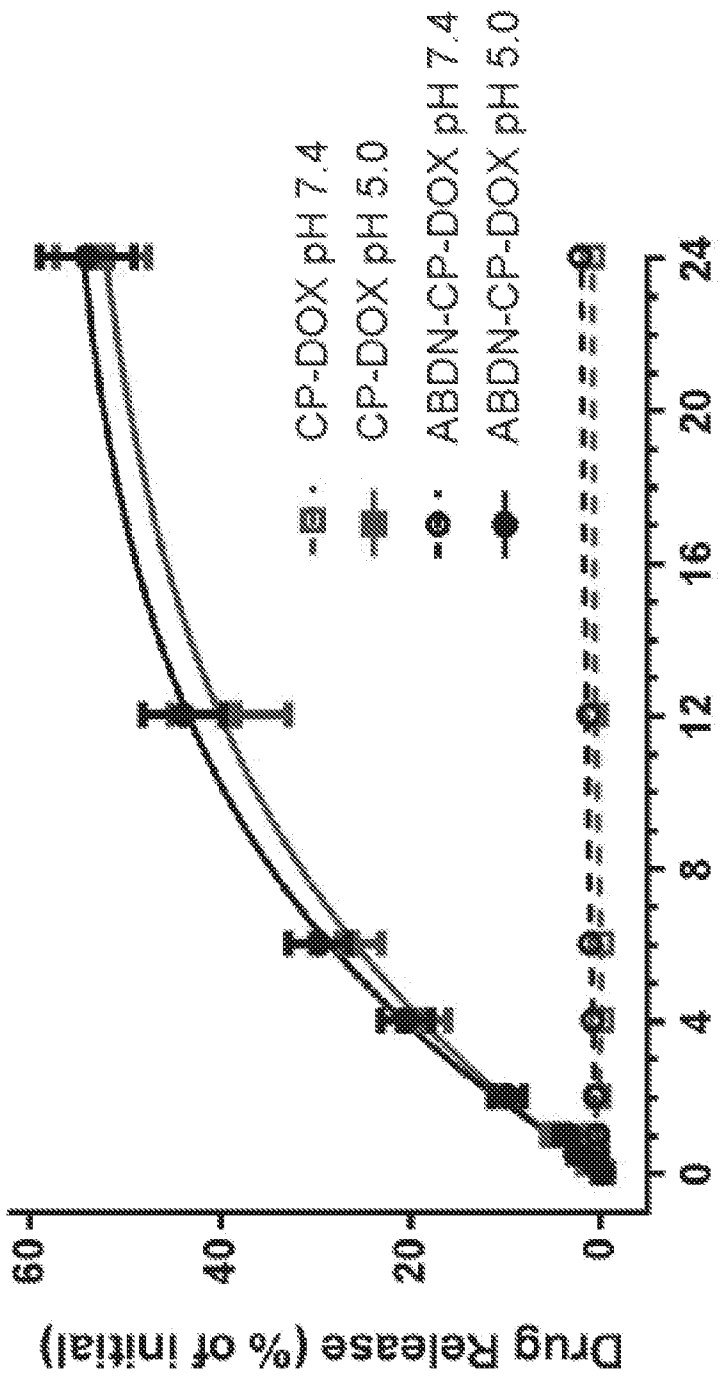
Drug Release (% of initial)
60
40
20
0
0
4
8
12
16
20
24
Time (h)
CP-DOX pH 7.4
CP-DOX pH 5.0
ABDN-CP-DOX pH 7.4
ABDN-CP-DOX pH 5.0

FIG. 6D

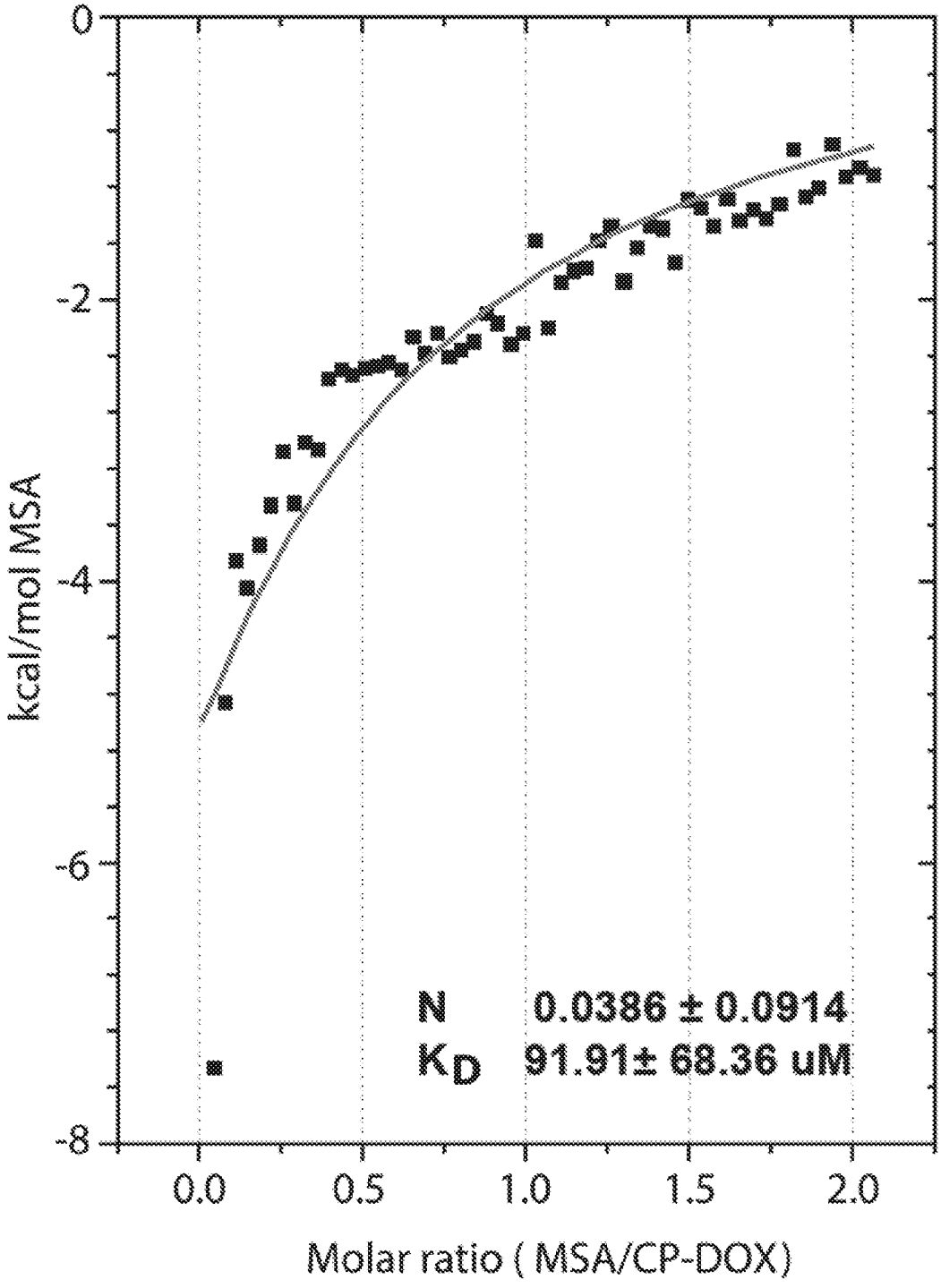
0
-2
-4
-6
-8
kcal/mol MSA
0.0
0.5
1.0
1.5
2.0
Molar ratio (MSA/CP-DOX)
N 0.0386 ± 0.0914
K_D 91.91± 68.36 uM

FIG. 7A

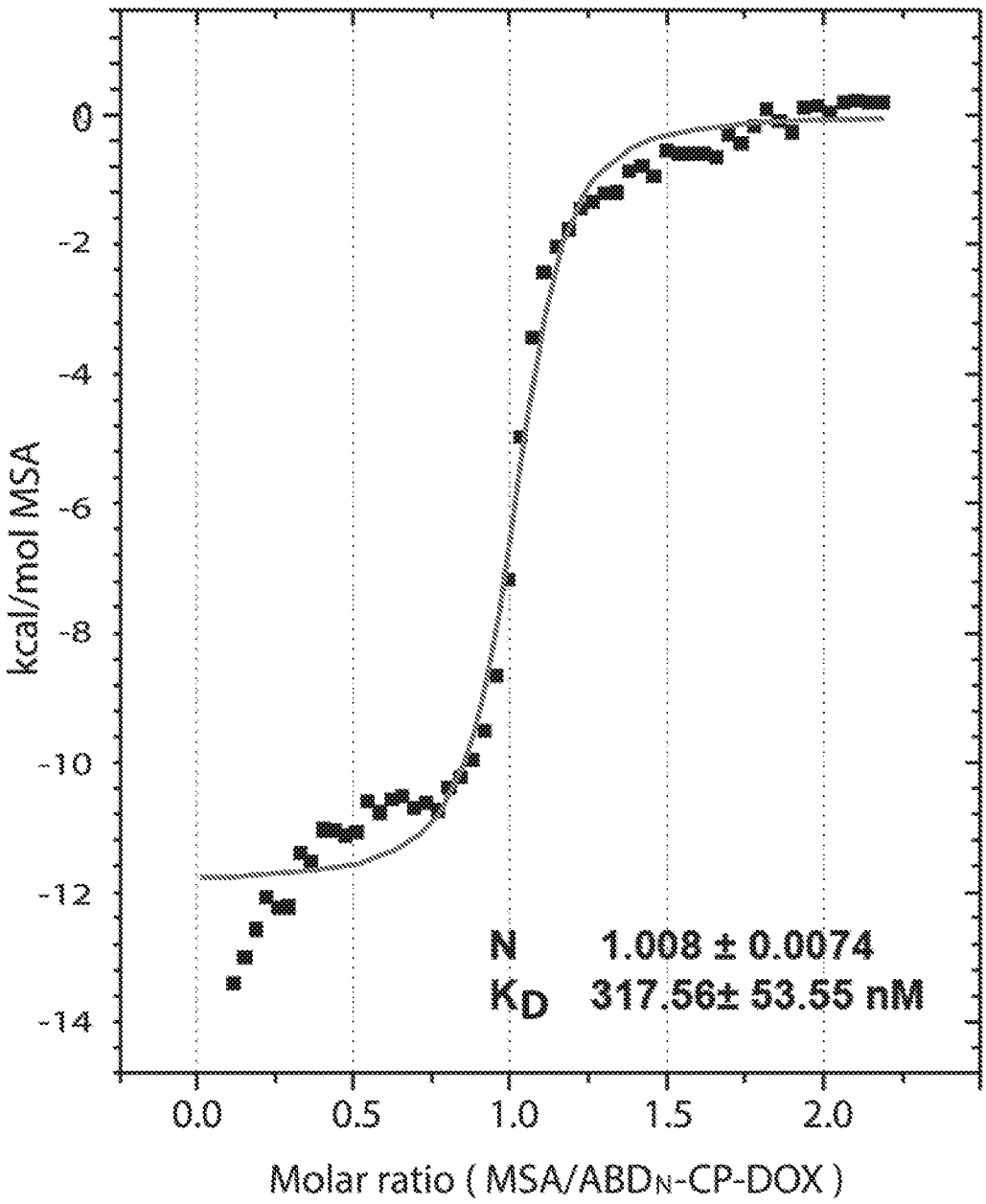
kcal/mol MSA
0
-2
-4
-6
-8
-10
-12
-14
0.0
0.5
1.0
1.5
2.0
Molar ratio (MSA/ABDN-CP-DOX)
N 1.008 ± 0.0074
KD 317.56± 53.55 nM

FIG. 7B

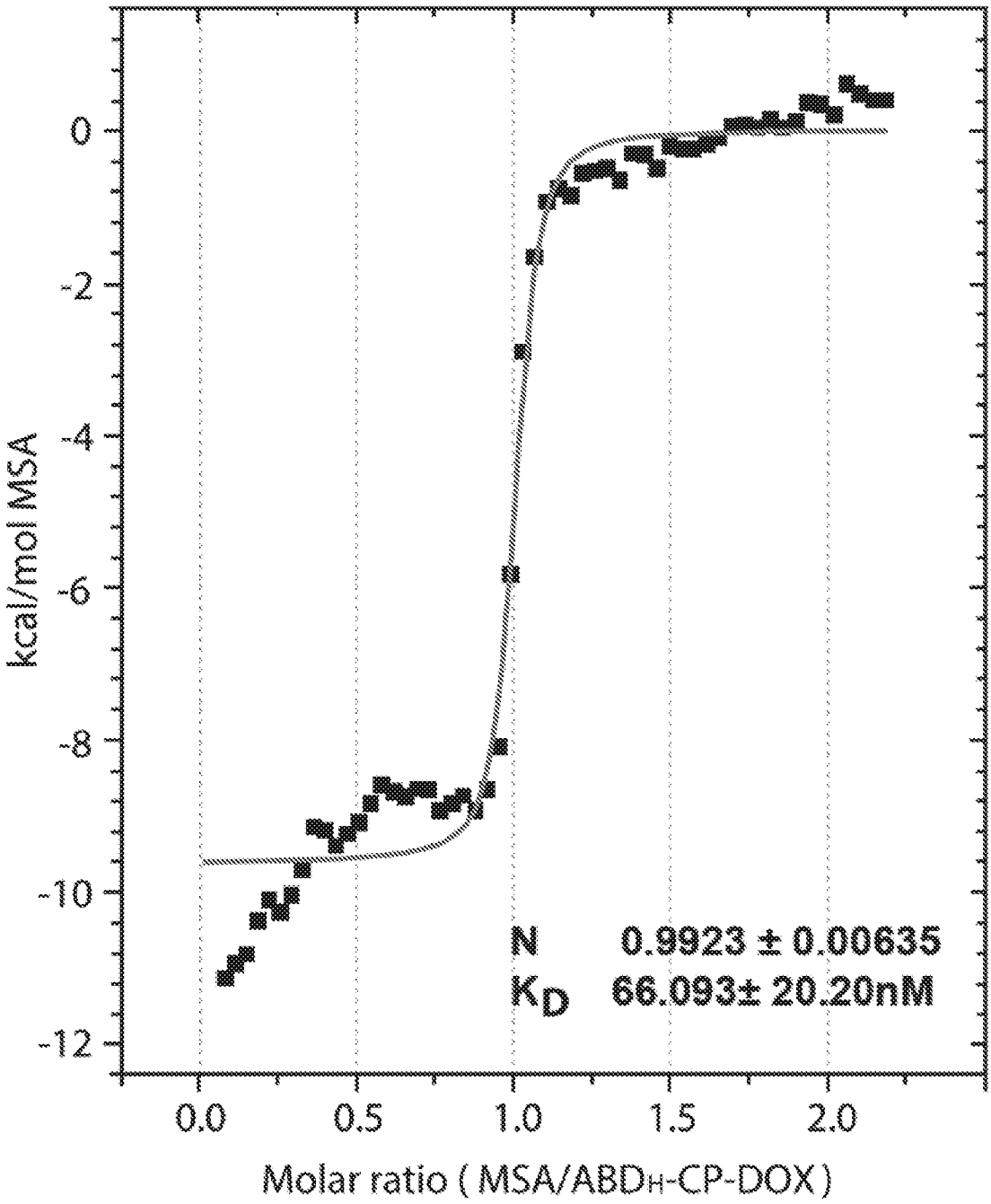
kcal/mol MSA
0
-2
-4
-6
-8
-10
-12
0.0
0.5
1.0
1.5
2.0
Molar ratio (MSA/ABDH-CP-DOX)
N 0.9923 ± 0.00635
KD 66.093± 20.20nM

FIG. 7C

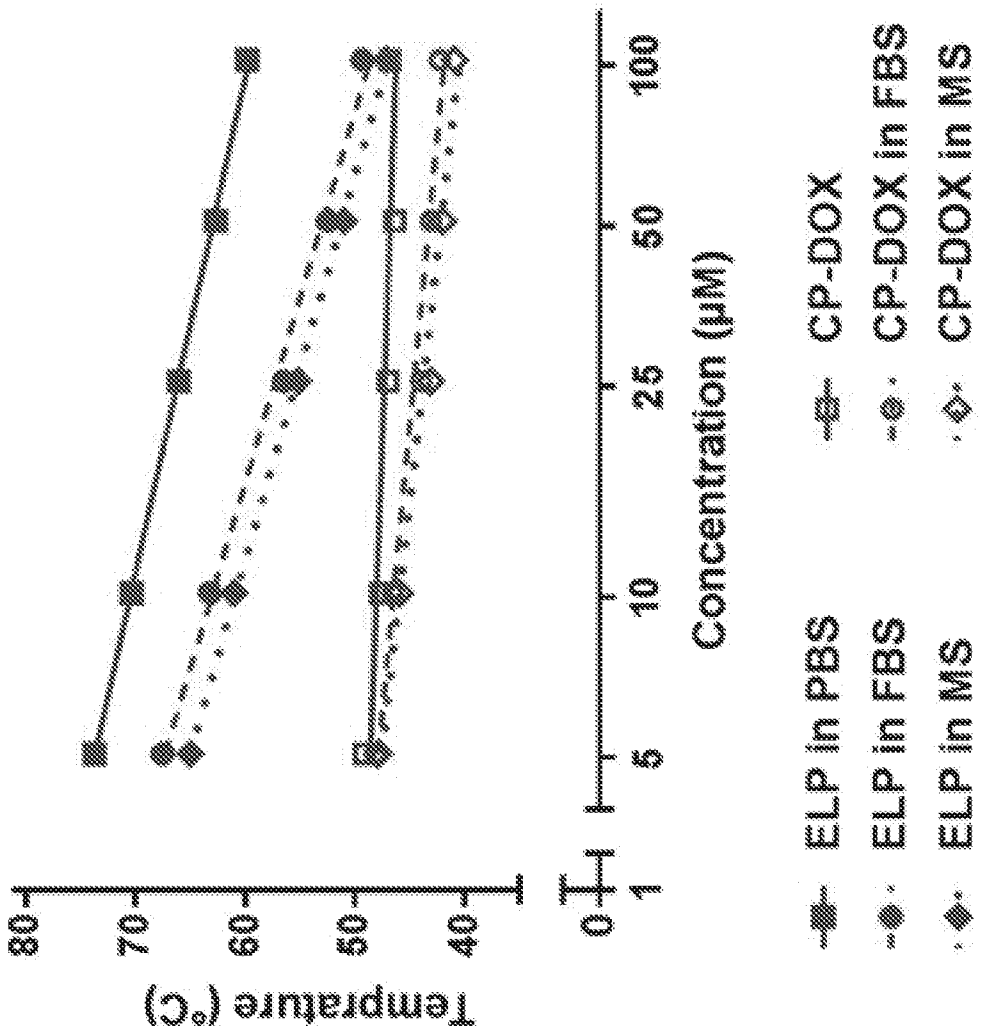
Temprature (°C)
80
70
60
50
40
0
1
5
10
25
50
100
Concentration (μM)
ELP in PBS
ELP in FBS
ELP in MS
CP-DOX
CP-DOX in FBS
CP-DOX in MS

FIG. 8A

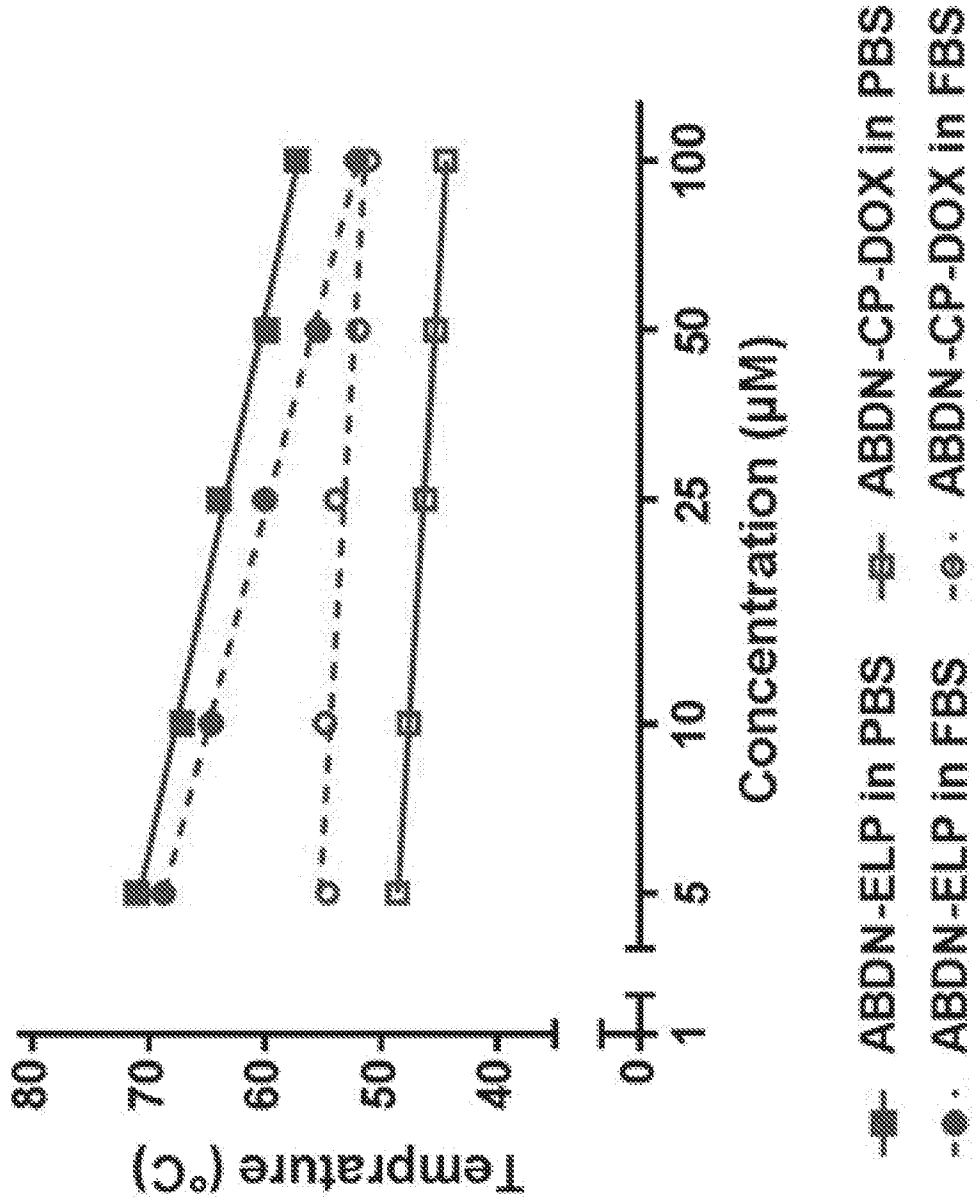
Temprature (°C)
80
70
60
50
40
0
1
5
10
25
50
100
Concentration (μM)
ABDN-ELP in PBS
ABDN-CP-DOX in PBS
ABDN-ELP in FBS
ABDN-CP-DOX in FBS

FIG. 8B

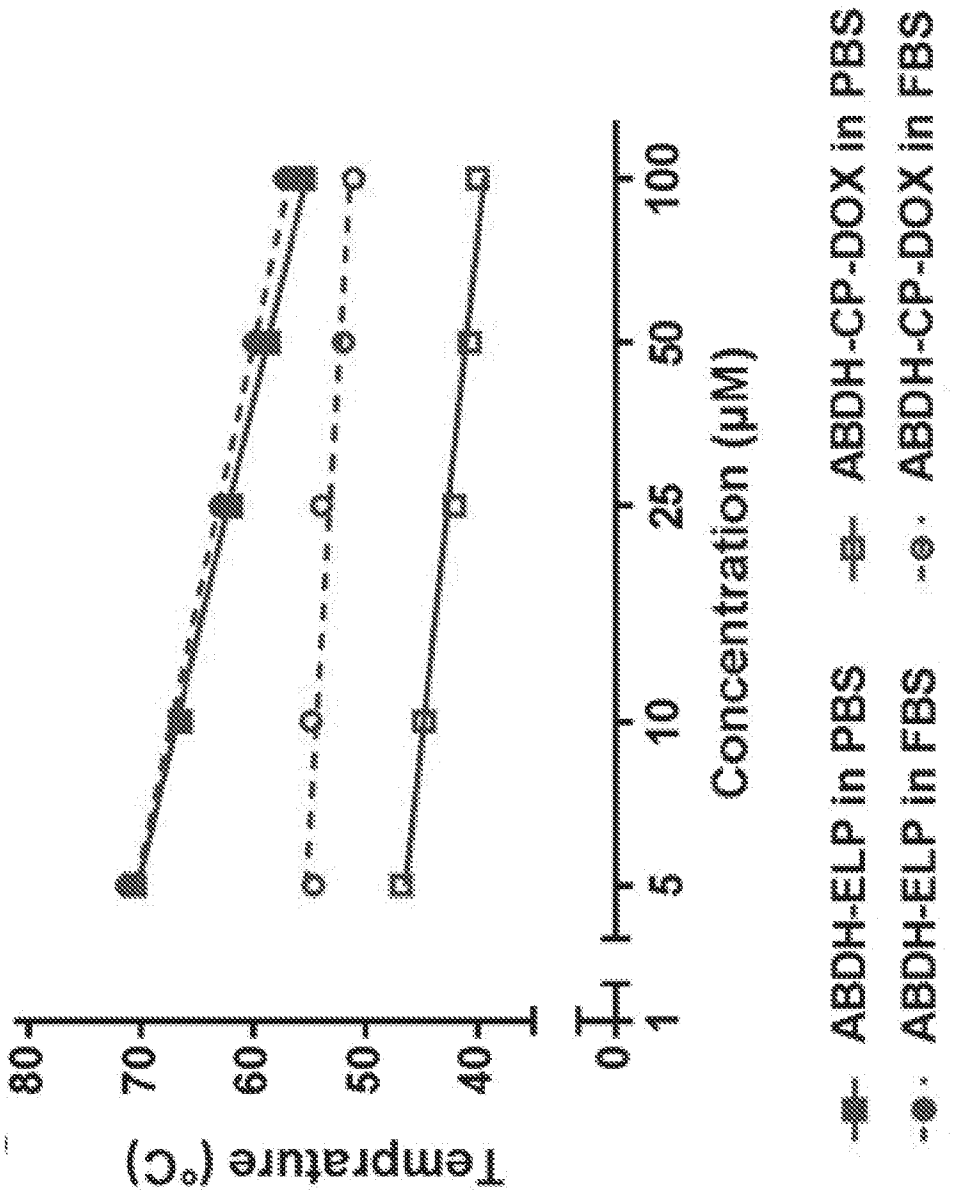
Temprature (°C)
80
70
60
50
40
0
1
5
10
25
50
100
Concentration (μM)
ABDH-ELP in PBS
ABDH-CP-DOX in PBS
ABDH-ELP in FBS
ABDH-CP-DOX in FBS

FIG. 8C

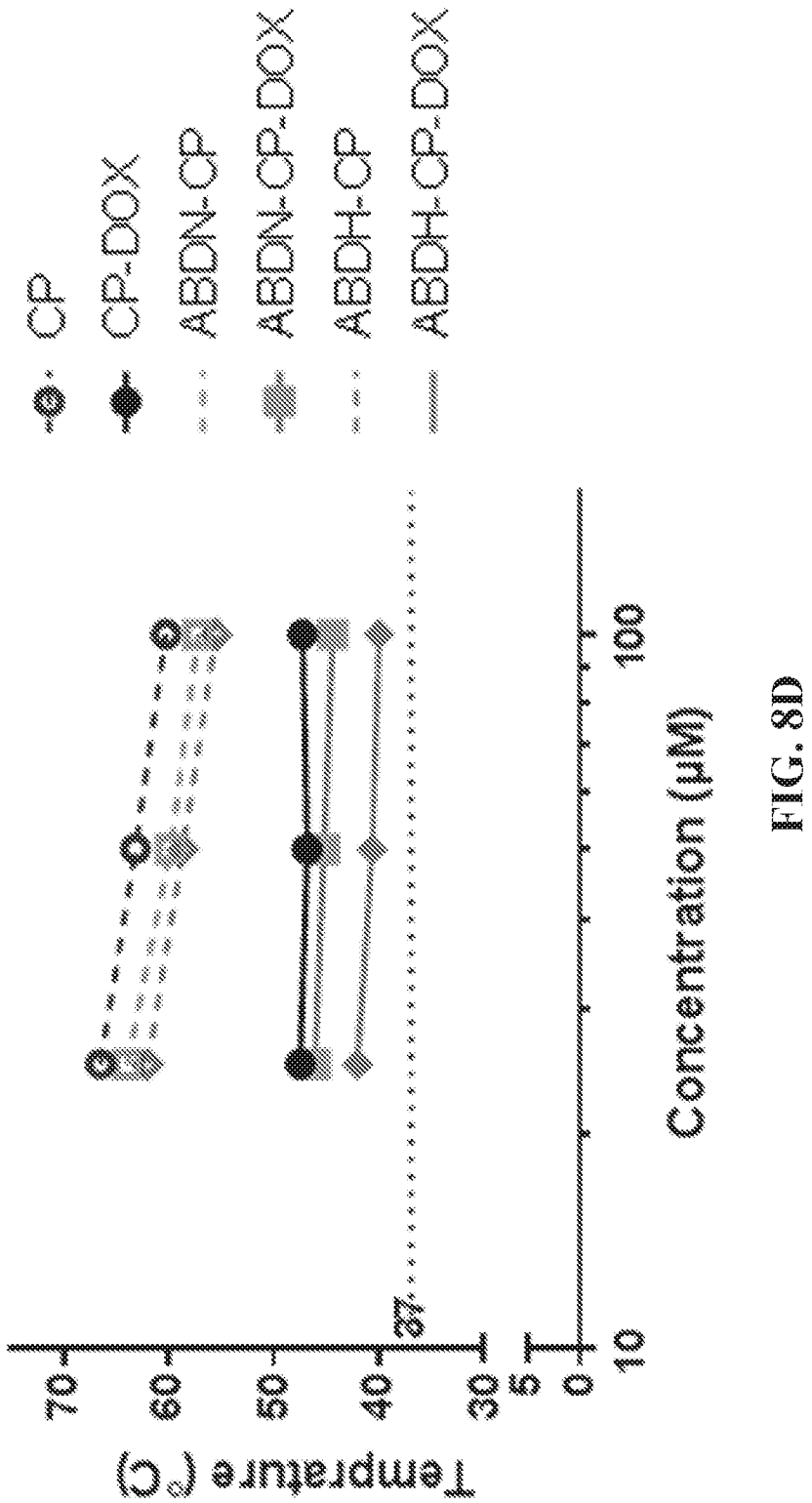
CP
CP-DOX
ABDN-CP
ABDN-CP-DOX
ABDH-CP
ABDH-CP-DOX
Temprature (°C)
70
60
50
40
37
30
0
5
10
100
Concentration (μM)

FIG. 8D

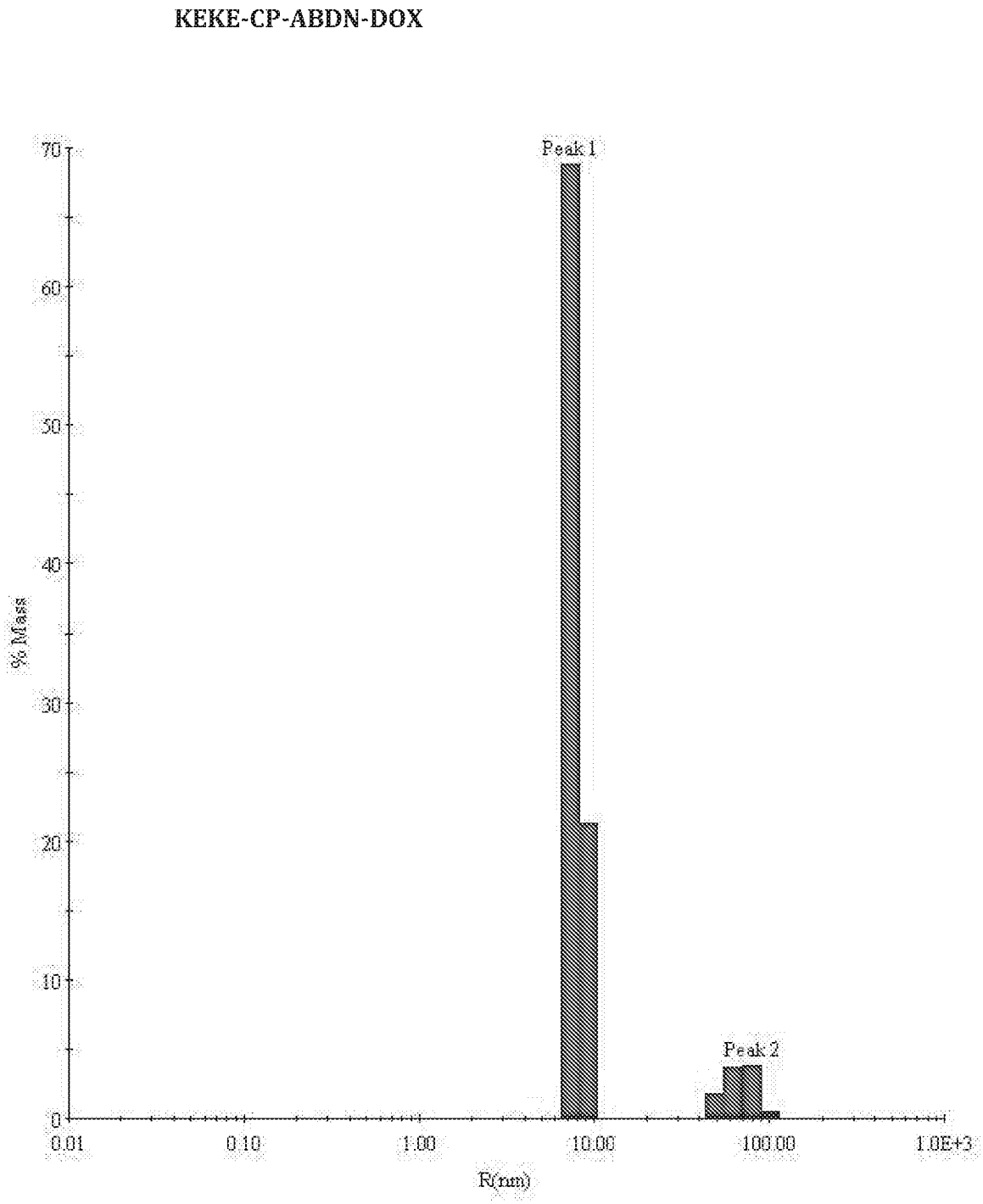
KEKE-CP-ABDN-DOX
Peak 1
Peak 2
% Mass
70
60
50
40
30
20
10
0
0.01
0.10
1.00
10.00
100.00
1.0E+3
R(nm)

FIG. 9A

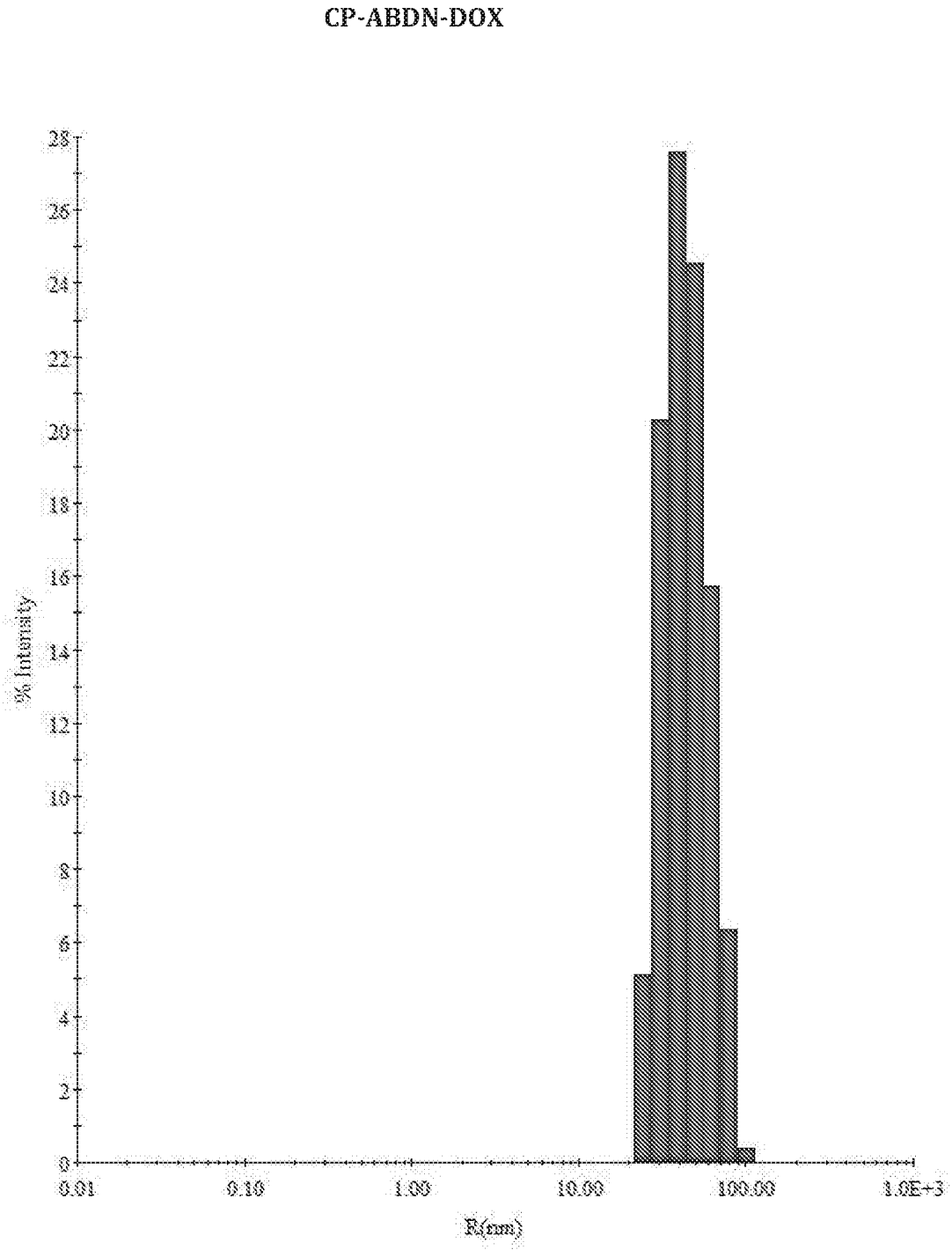
CP-ABDN-DOX
% Intensity
28
26
24
22
20
18
16
14
12
10
8
6
4
2
0
0.01
0.10
1.00
10.00
100.00
1.0E+3
R(nm)

FIG. 9B

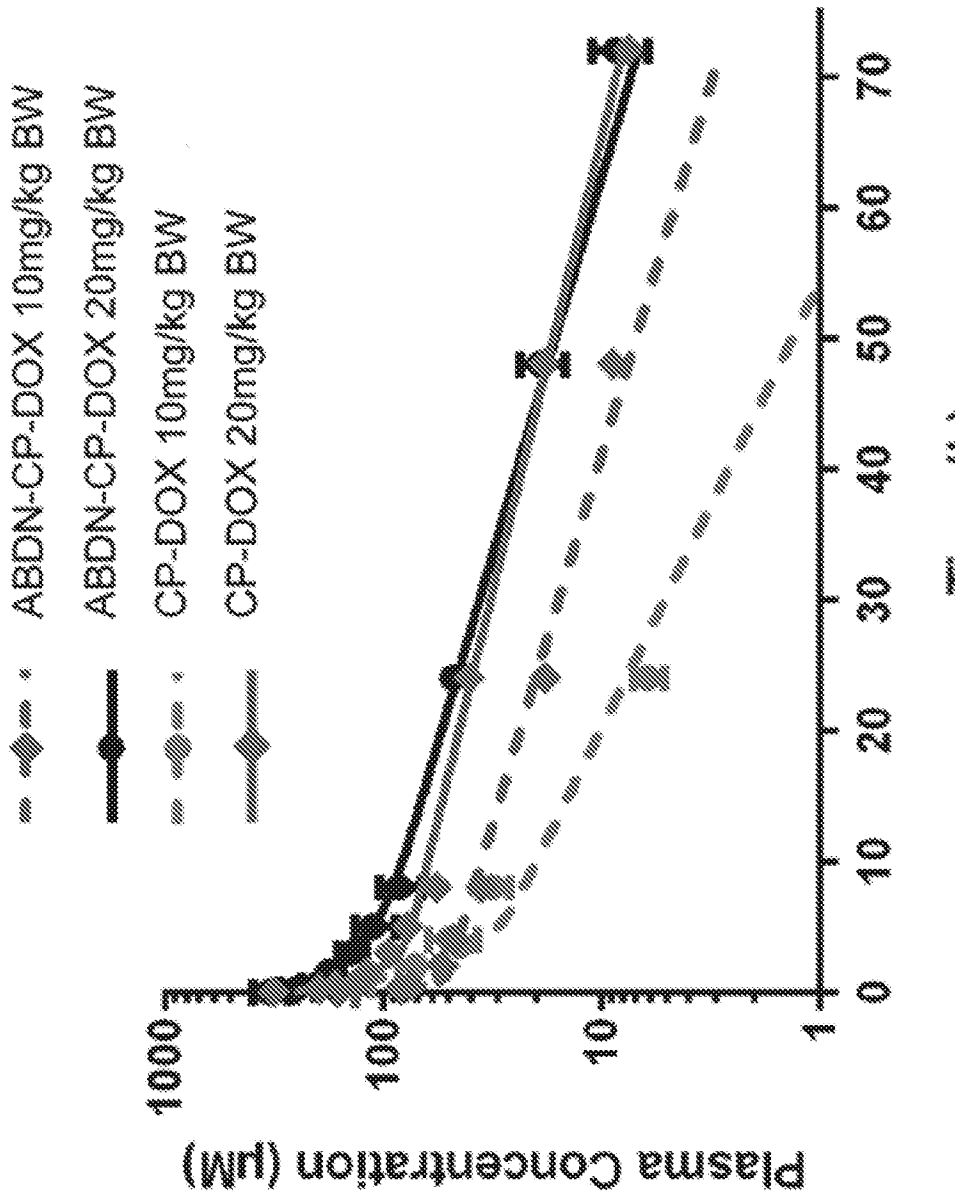
ABDN-CP-DOX 10mg/kg BW
ABDN-CP-DOX 20mg/kg BW
CP-DOX 10mg/kg BW
CP-DOX 20mg/kg BW
Plasma Concentration (μM)
1000
100
10
1
0
10
20
30
40
50
60
70
Time (h)

FIG. 10A

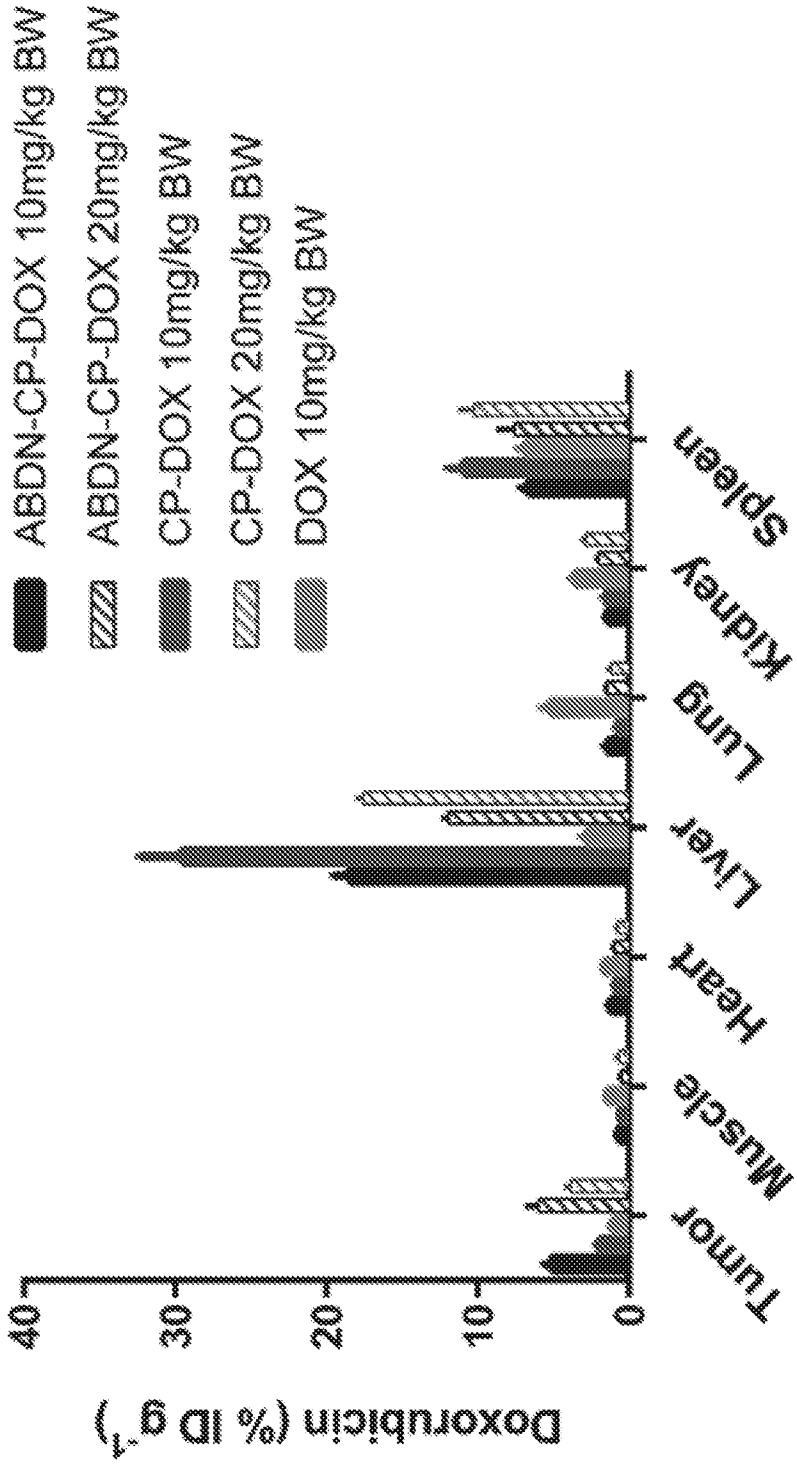
ABDN-CP-DOX 10mg/kg BW
ABDN-CP-DOX 20mg/kg BW
CP-DOX 10mg/kg BW
CP-DOX 20mg/kg BW
DOX 10mg/kg BW
Doxorubicin (% ID g-1)
40
30
20
10
0
Tumor
Muscle
Heart
Liver
Lung
Kidney
Spleen

FIG. 10B

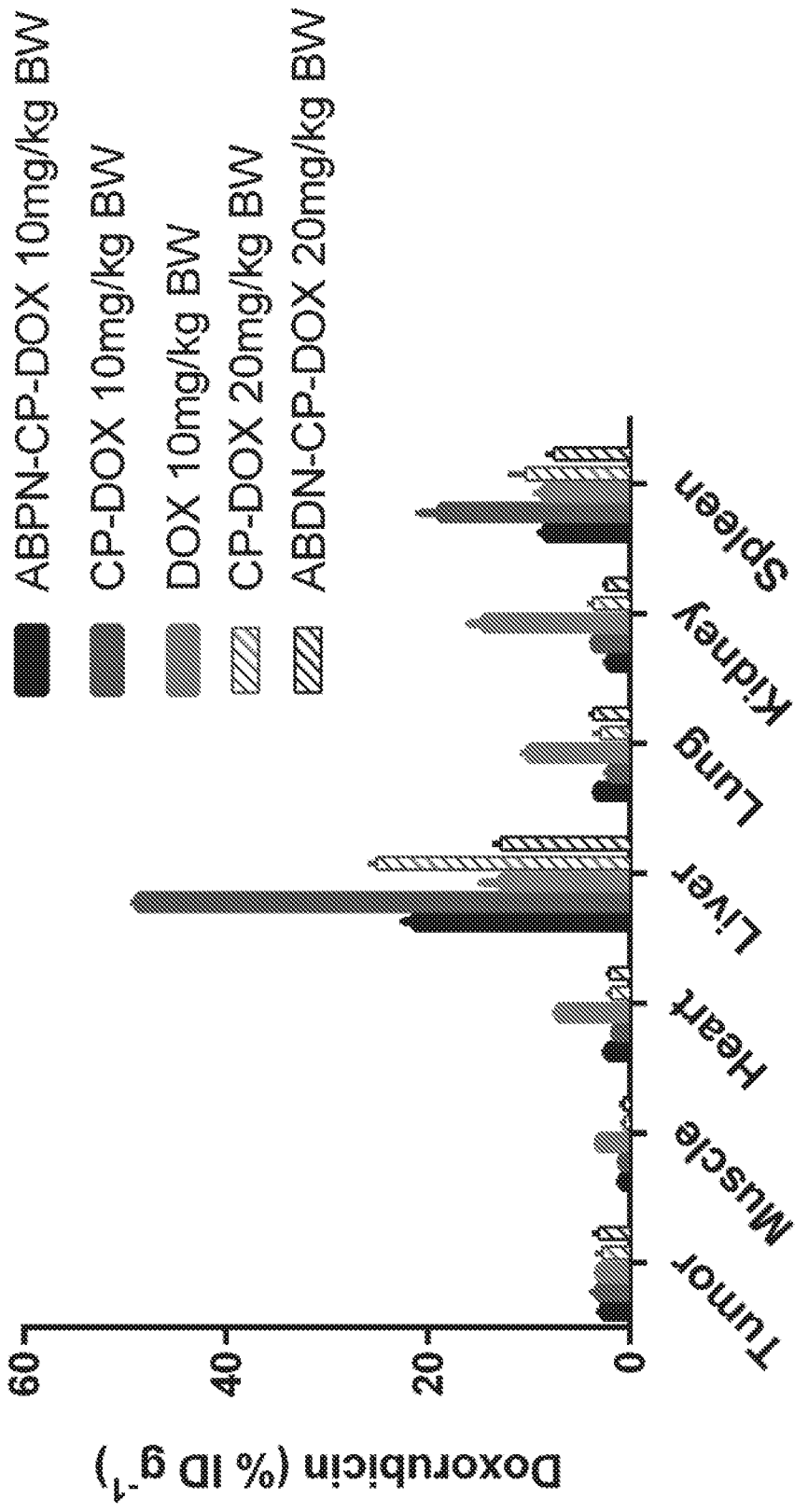
ABPN-CP-DOX 10mg/kg BW
CP-DOX 10mg/kg BW
DOX 10mg/kg BW
CP-DOX 20mg/kg BW
ABDN-CP-DOX 20mg/kg BW
Doxorubicin (% ID g-1)
60
40
20
0
Tumor
Muscle
Heart
Liver
Lung
Kidney
Spleen

FIG. 10C

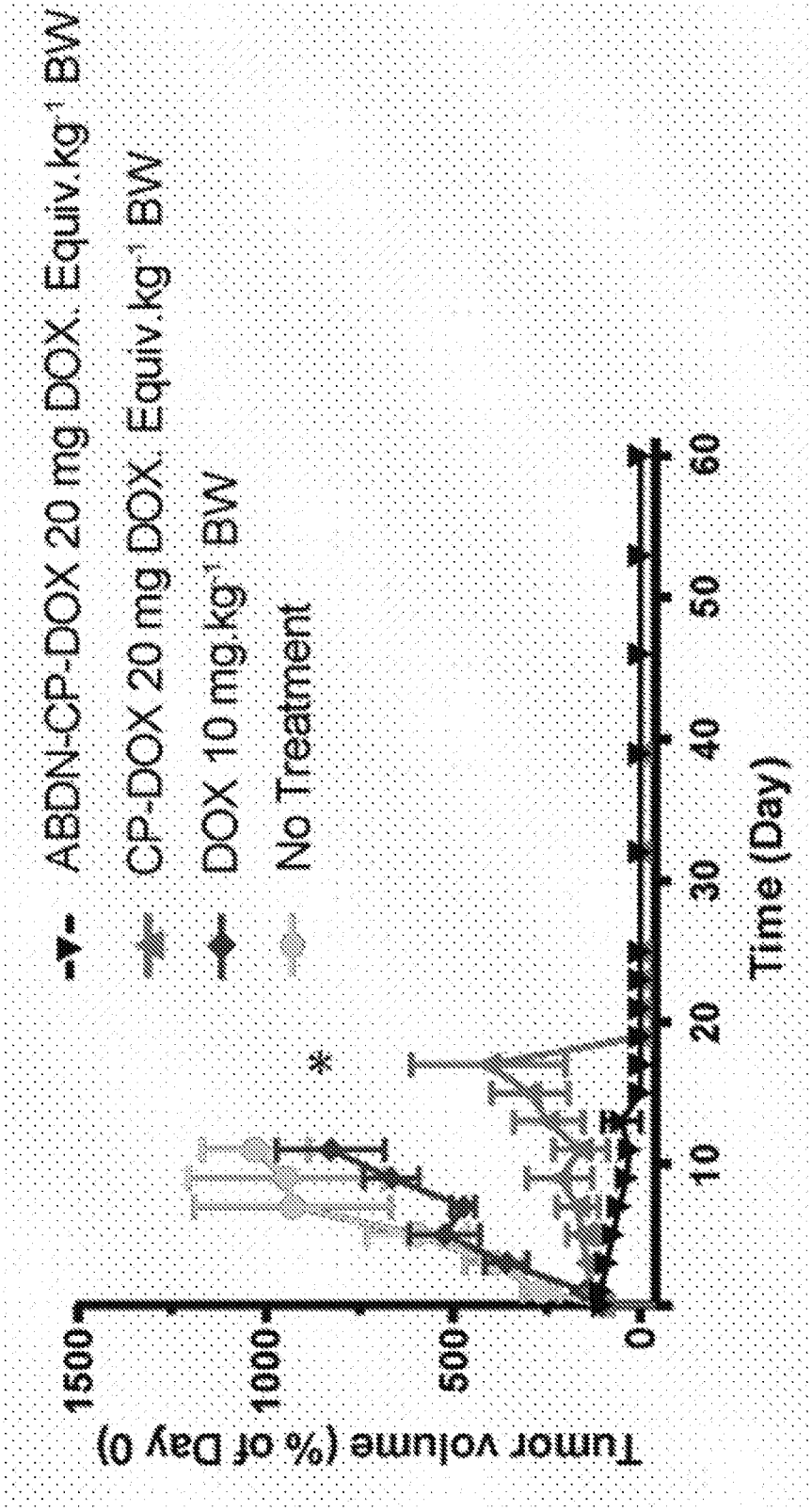
ABDN-CP-DOX 20 mg DOX. Equiv.kg-1 BW
CP-DOX 20 mg DOX. Equiv.kg-1 BW
DOX 10 mg.kg-1 BW
No Treatment
*
Tumor volume (% of Day 0)
1500
1000
500
0
10
20
30
40
50
60
Time (Day)

FIG. 10D

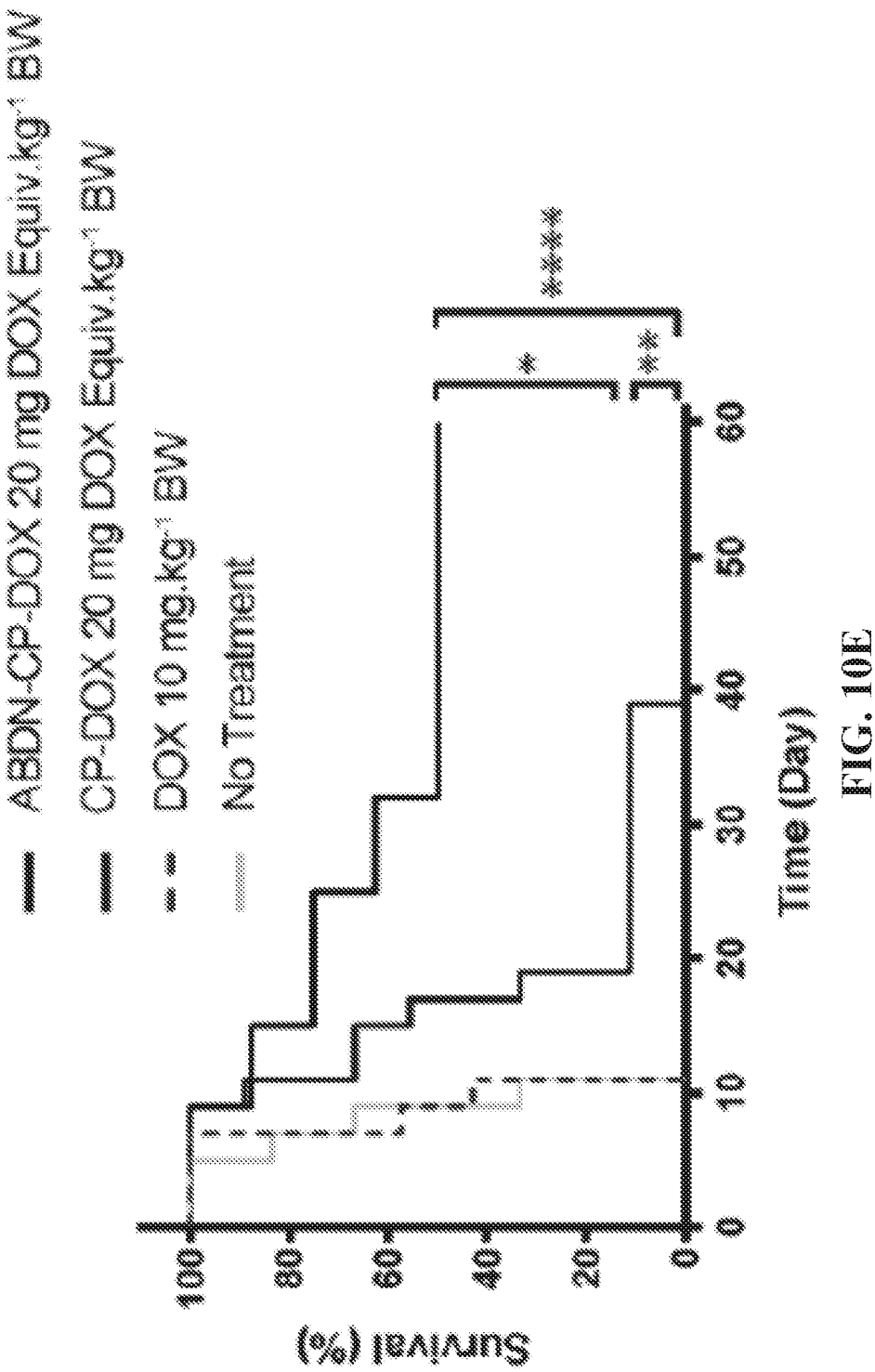
ABDN-CP-DOX 20 mg DOX Equiv.kg-1 BW
CP-DOX 20 mg DOX Equiv.kg-1 BW
DOX 10 mg.kg-1 BW
No Treatment
Survival (%)
100
80
60
40
20
0
0
10
20
30
40
50
60
Time (Day)
*
**
****

FIG. 10E

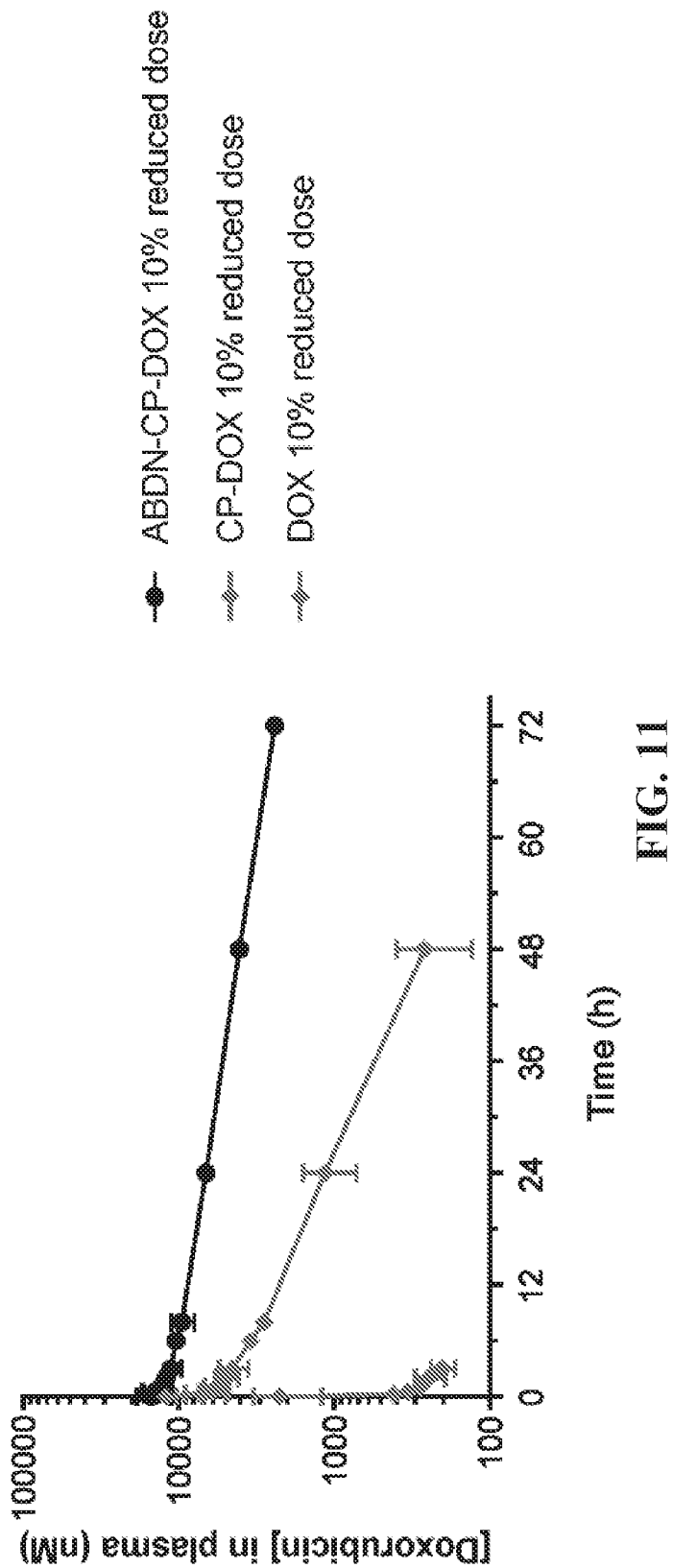
ABDN-CP-DOX 10% reduced dose
CP-DOX 10% reduced dose
DOX 10% reduced dose
[Doxorubicin] in plasma (nM)
100000
10000
1000
100
0
12
24
36
48
60
72
Time (h)

FIG. 11

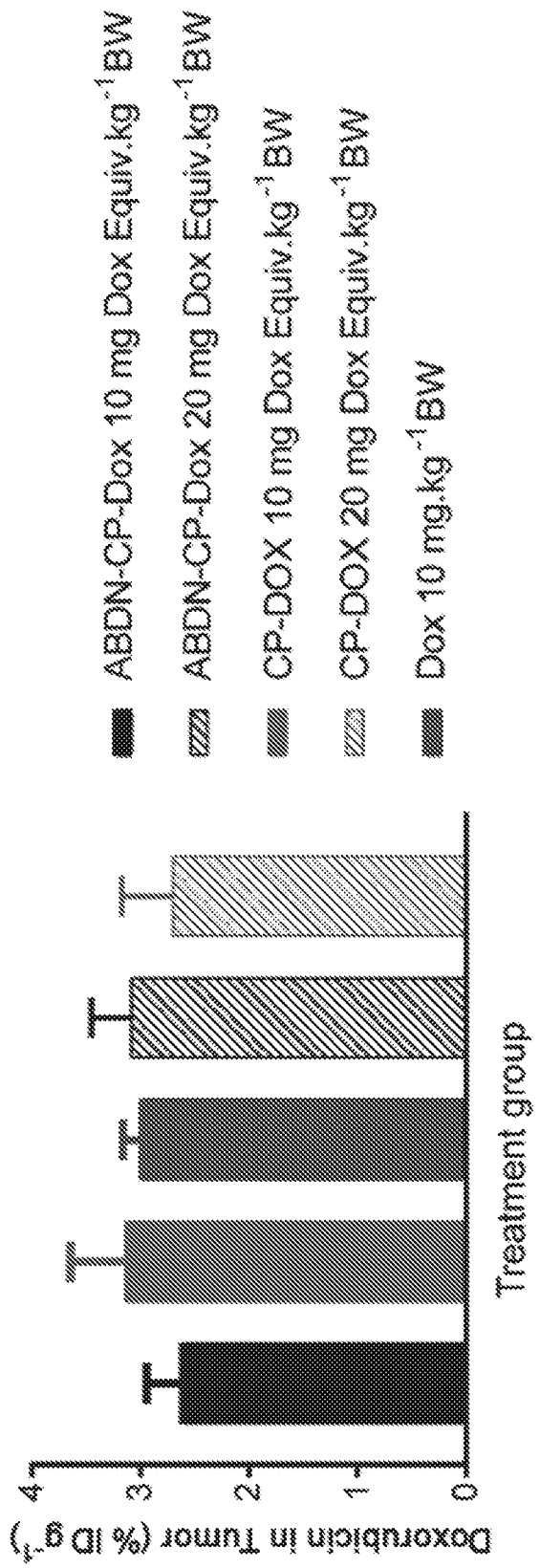
ABDN-CP-Dox 10 mg Dox Equiv.kg-1BW
ABDN-CP-Dox 20 mg Dox Equiv.kg-1BW
CP-DOX 10 mg Dox Equiv.kg-1BW
CP-DOX 20 mg Dox Equiv.kg-1BW
Dox 10 mg.kg-1BW
Doxorubicin in Tumor (% ID g-1)
0
1
2
3
4
Treatment group

FIG. 12A

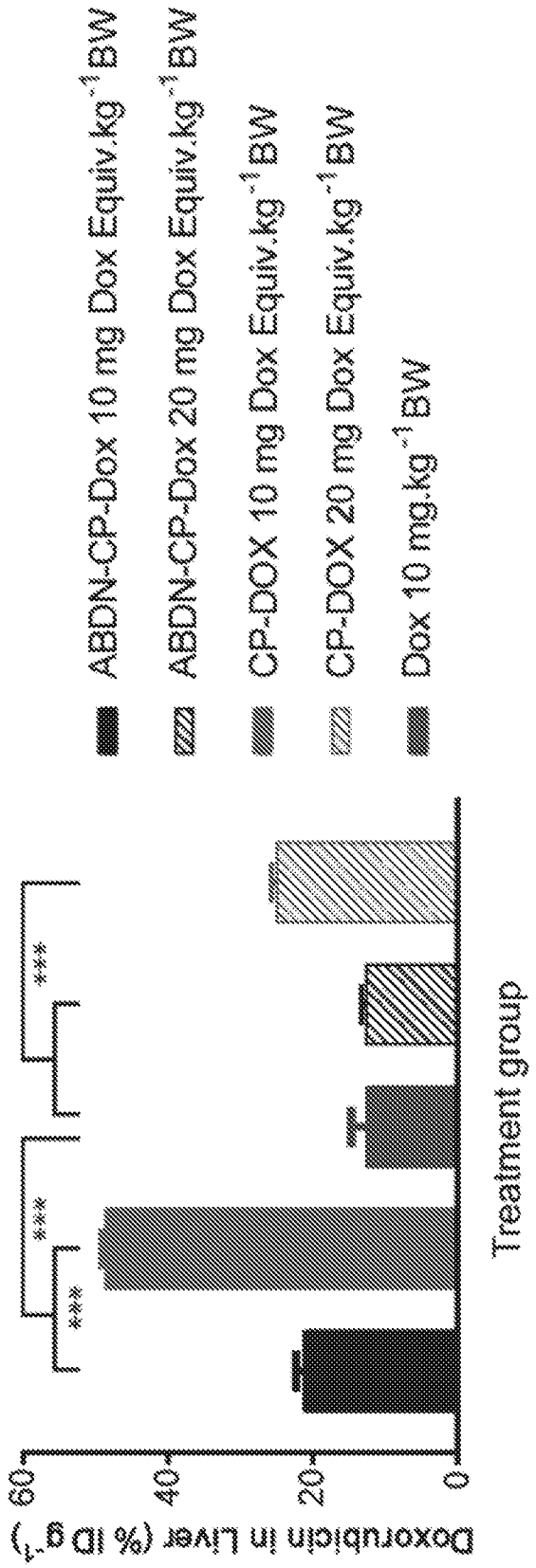
ABDN-CP-Dox 10 mg Dox Equiv.kg-1 BW
ABDN-CP-Dox 20 mg Dox Equiv.kg-1 BW
CP-DOX 10 mg Dox Equiv.kg-1 BW
CP-DOX 20 mg Dox Equiv.kg-1 BW
Dox 10 mg.kg-1 BW
***
***
***
Doxorubicin in Liver (% ID g-1)
0
20
40
60
Treatment group

FIG. 12B

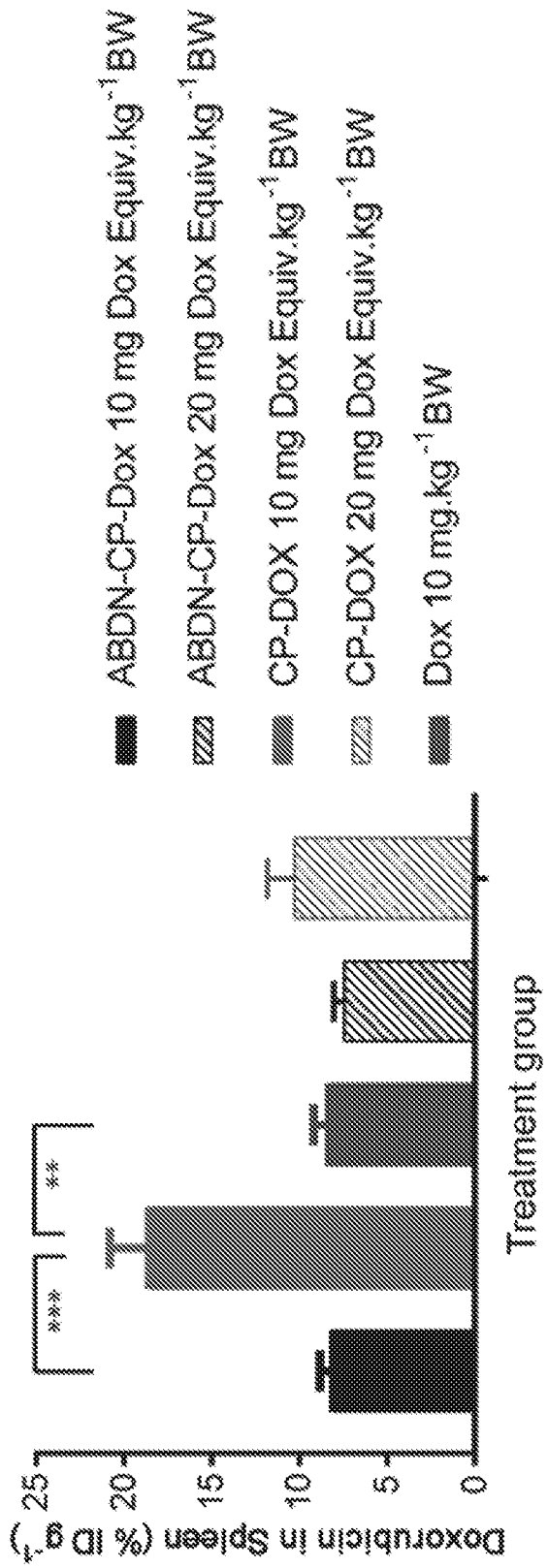
ABDN-CP-Dox 10 mg Dox Equiv.kg-1BW
ABDN-CP-Dox 20 mg Dox Equiv.kg-1BW
CP-DOX 10 mg Dox Equiv.kg-1BW
CP-DOX 20 mg Dox Equiv.kg-1BW
Dox 10 mg.kg-1BW
***
**
Doxorubicin in Spleen (% ID g-1)
0
5
10
15
20
25
Treatment group

FIG. 12C

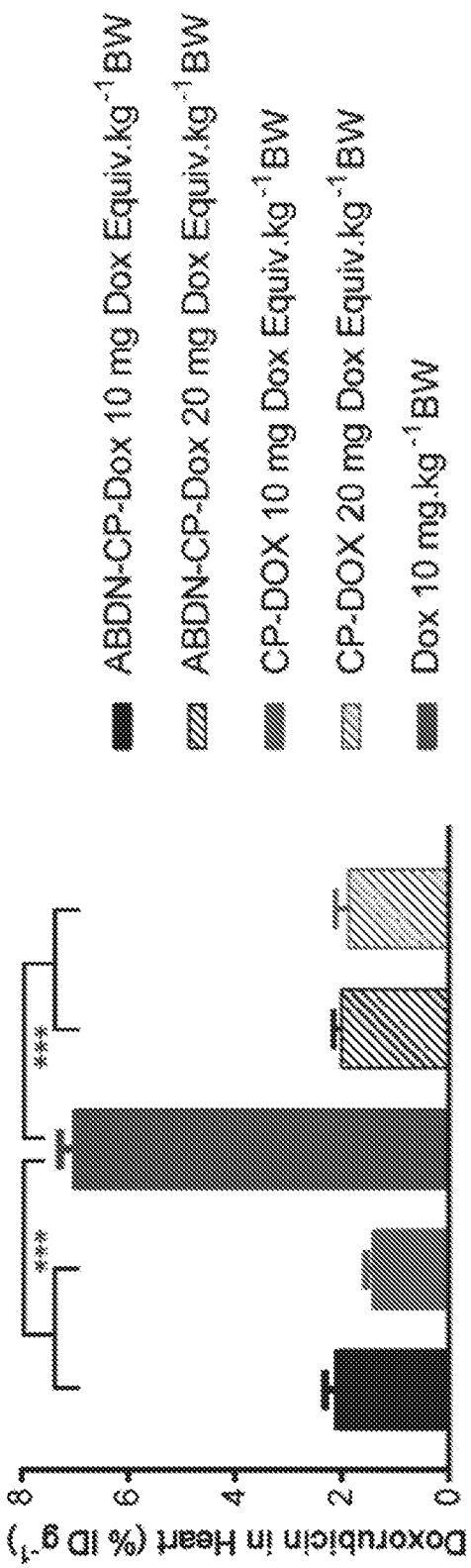
ABDN-CP-Dox 10 mg Dox Equiv.kg-1BW
ABDN-CP-Dox 20 mg Dox Equiv.kg-1BW
CP-DOX 10 mg Dox Equiv.kg-1BW
CP-DOX 20 mg Dox Equiv.kg-1BW
Dox 10 mg.kg-1BW
Doxorubicin in Heart (% ID g-1)
0
2
4
6
8
***
***
***
Treatment group

FIG. 12D

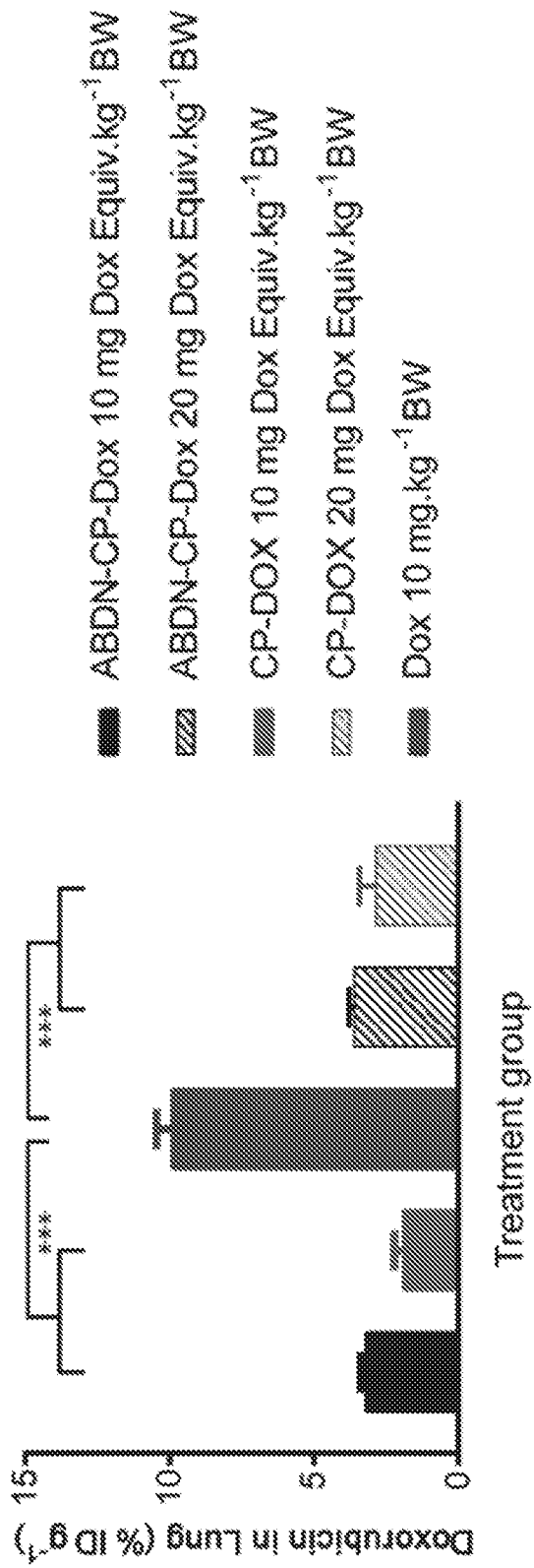
ABDN-CP-Dox 10 mg Dox Equiv.kg-1 BW
ABDN-CP-Dox 20 mg Dox Equiv.kg-1 BW
CP-DOX 10 mg Dox Equiv.kg-1 BW
CP-DOX 20 mg Dox Equiv.kg-1 BW
Dox 10 mg.kg-1 BW
***
***
Doxorubicin in Lung (% ID g-1)
15
10
5
0
Treatment group

FIG. 12E

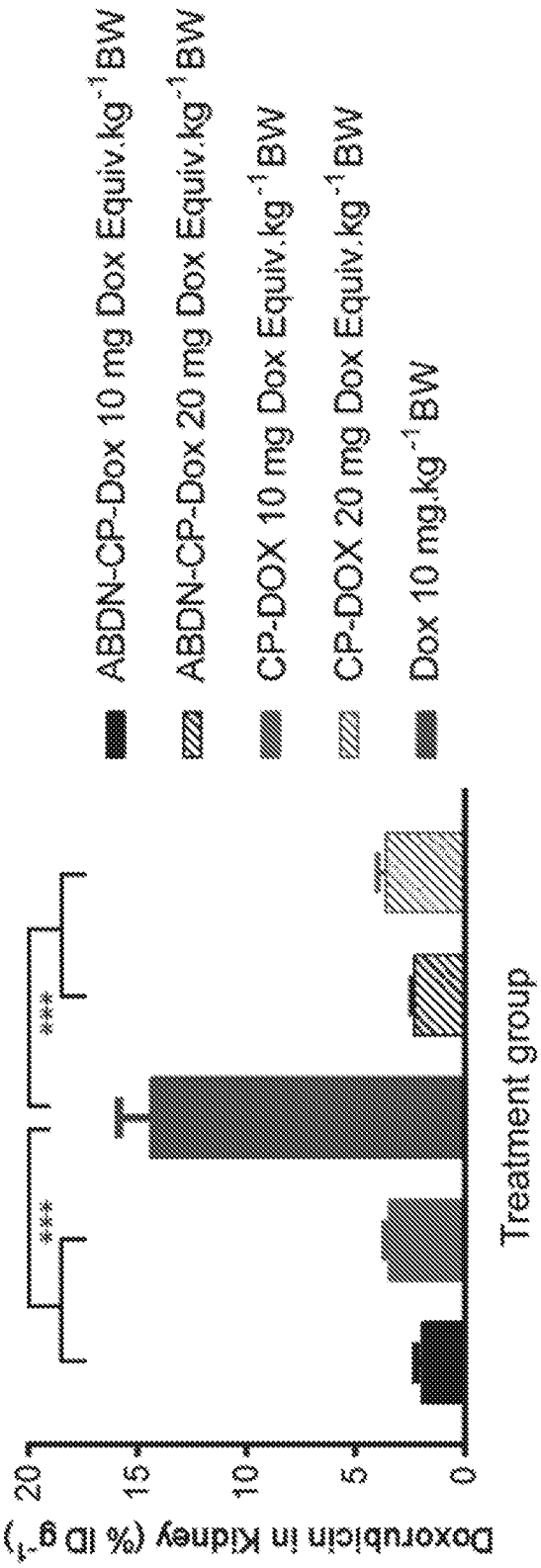
ABDN-CP-Dox 10 mg Dox Equiv.kg-1BW
ABDN-CP-Dox 20 mg Dox Equiv.kg-1BW
CP-DOX 10 mg Dox Equiv.kg-1BW
CP-DOX 20 mg Dox Equiv.kg-1BW
Dox 10 mg.kg-1BW
***
***
Doxorubicin in Kidney (% ID g-1)
20
15
10
5
0
Treatment group

FIG. 12F

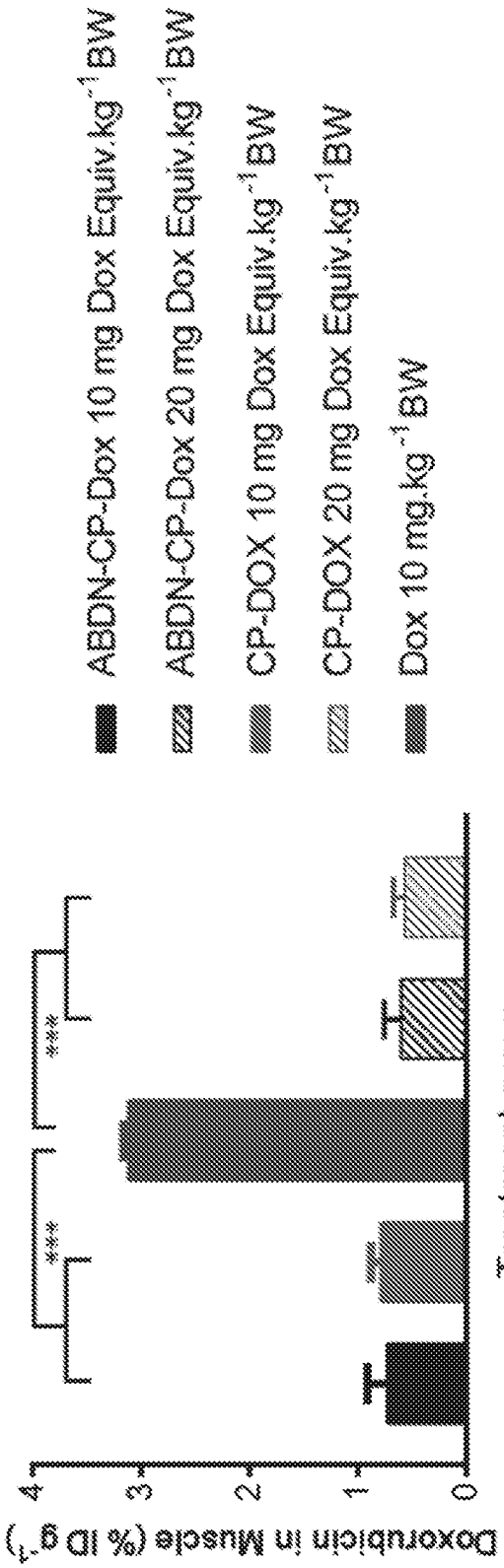
ABDN-CP-Dox 10 mg Dox Equiv.kg-1 BW
ABDN-CP-Dox 20 mg Dox Equiv.kg-1 BW
CP-DOX 10 mg Dox Equiv.kg-1 BW
CP-DOX 20 mg Dox Equiv.kg-1 BW
Dox 10 mg.kg-1 BW
Doxorubicin in Muscle (% ID g-1)
Treatment group
0
1
2
3
4
***
***

FIG. 12G

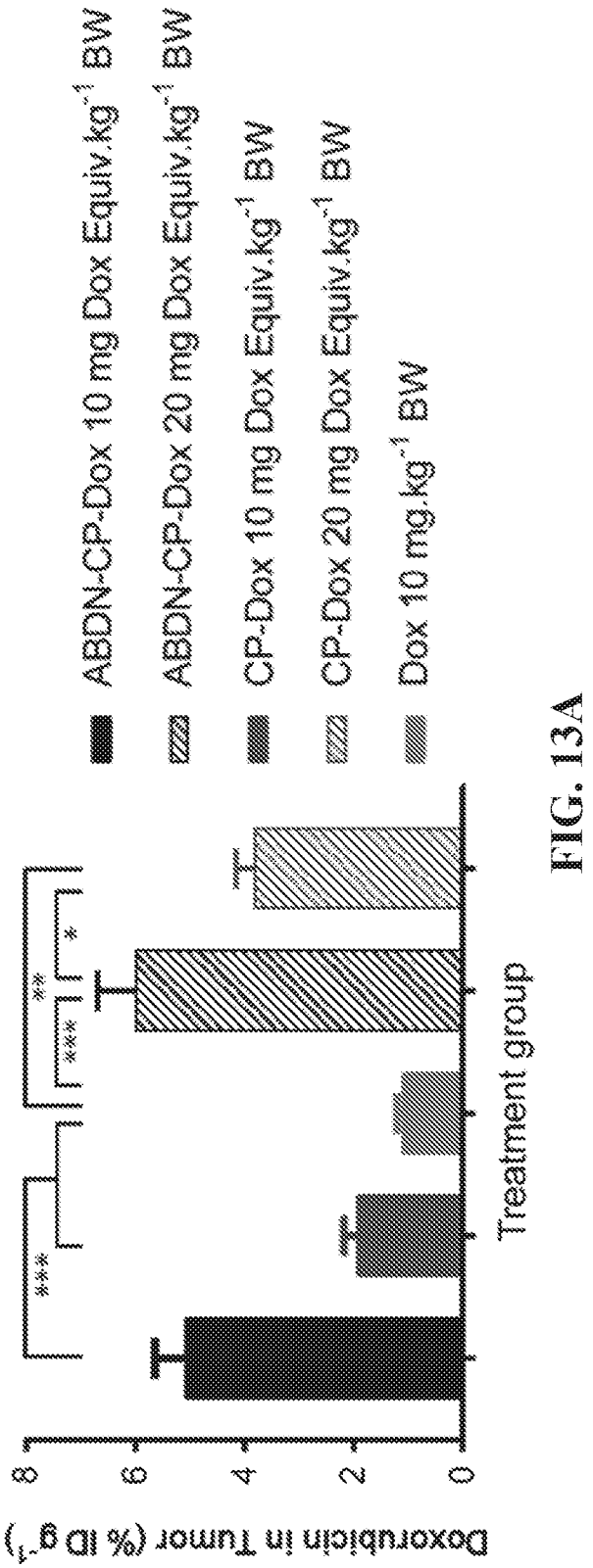
ABDN-CP-Dox 10 mg Dox Equiv.kg-1 BW
ABDN-CP-Dox 20 mg Dox Equiv.kg-1 BW
CP-Dox 10 mg Dox Equiv.kg-1 BW
CP-Dox 20 mg Dox Equiv.kg-1 BW
Dox 10 mg.kg-1 BW
Doxorubicin in Tumor (% ID g-1)
0
2
4
6
8
Treatment group
***
***
**
*

FIG. 13A

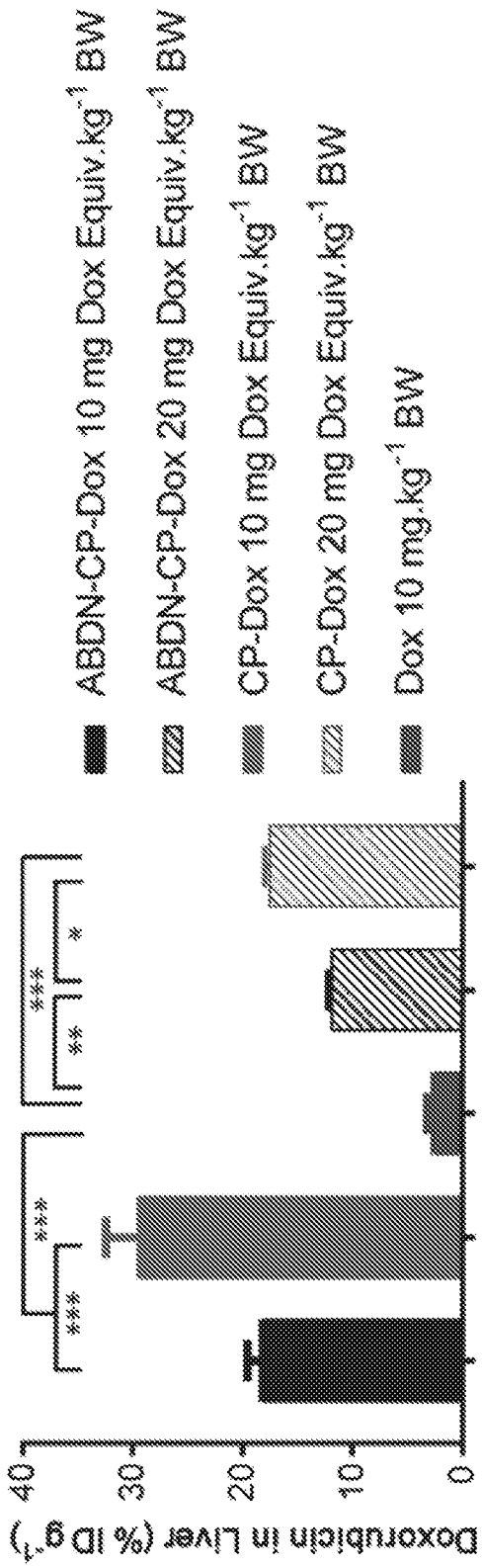
ABDN-CP-Dox 10 mg Dox Equiv.kg-1 BW
ABDN-CP-Dox 20 mg Dox Equiv.kg-1 BW
CP-Dox 10 mg Dox Equiv.kg-1 BW
CP-Dox 20 mg Dox Equiv.kg-1 BW
Dox 10 mg.kg-1 BW
Doxorubicin in Liver (% ID g-1)
0
10
20
30
40
***
***
**
*
Treatment group

FIG. 13B

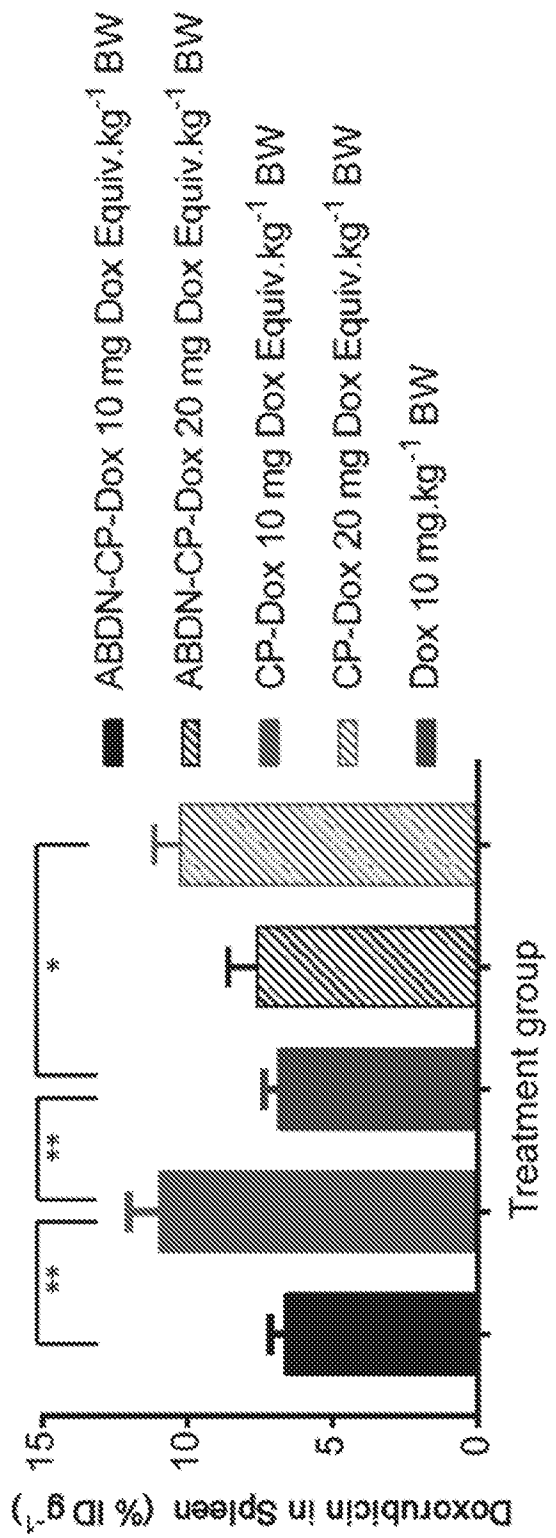
ABDN-CP-Dox 10 mg Dox Equiv.kg-1 BW
ABDN-CP-Dox 20 mg Dox Equiv.kg-1 BW
CP-Dox 10 mg Dox Equiv.kg-1 BW
CP-Dox 20 mg Dox Equiv.kg-1 BW
Dox 10 mg.kg-1 BW
Doxorubicin in Spleen (% ID g-1)
15
10
5
0
**
**
*
Treatment group

FIG. 13C

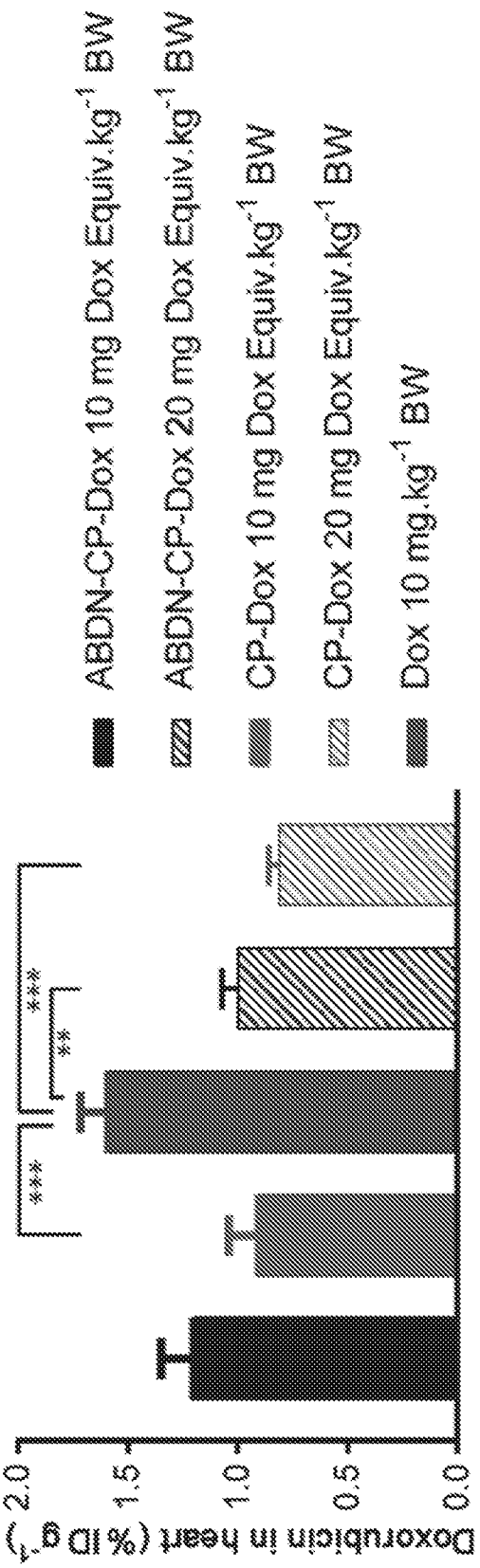
ABDN-CP-Dox 10 mg Dox Equiv.kg-1 BW
ABDN-CP-Dox 20 mg Dox Equiv.kg-1 BW
CP-Dox 10 mg Dox Equiv.kg-1 BW
CP-Dox 20 mg Dox Equiv.kg-1 BW
Dox 10 mg.kg-1 BW
***
**
***
2.0
1.5
1.0
0.5
0.0
Doxorubicin in heart (% ID g-1)
Treatment group

FIG. 13D

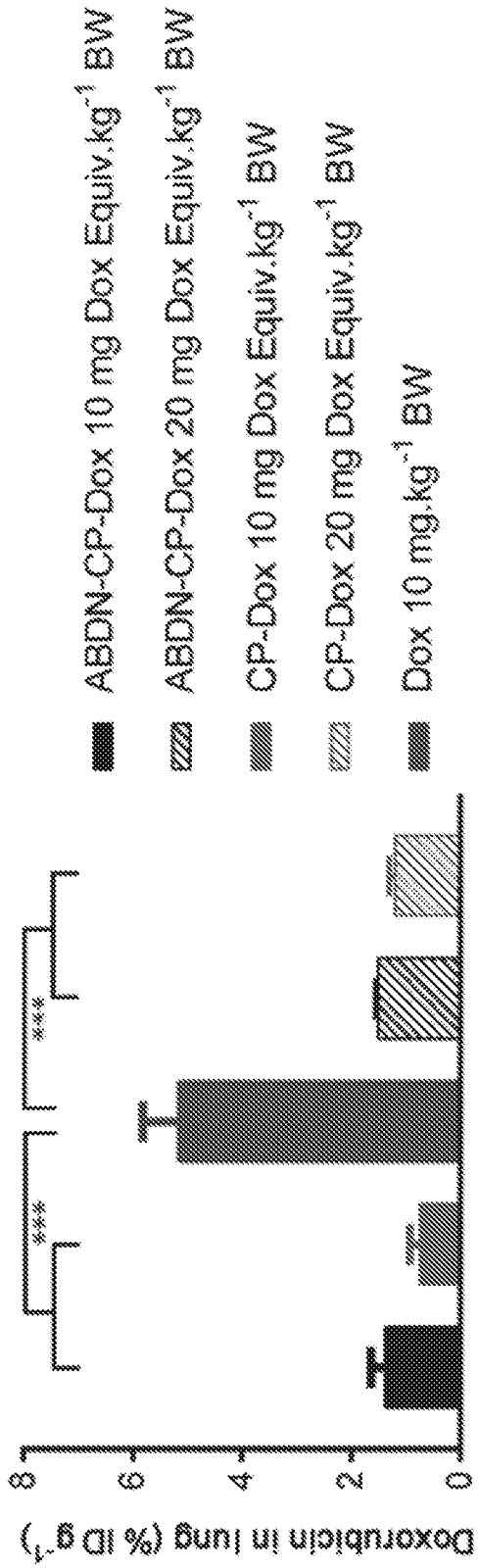
ABDN-CP-Dox 10 mg Dox Equiv.kg-1 BW
ABDN-CP-Dox 20 mg Dox Equiv.kg-1 BW
CP-Dox 10 mg Dox Equiv.kg-1 BW
CP-Dox 20 mg Dox Equiv.kg-1 BW
Dox 10 mg.kg-1 BW
***
***
Doxorubicin in lung (% ID g-1)
0
2
4
6
8
Treatment group

FIG. 13E

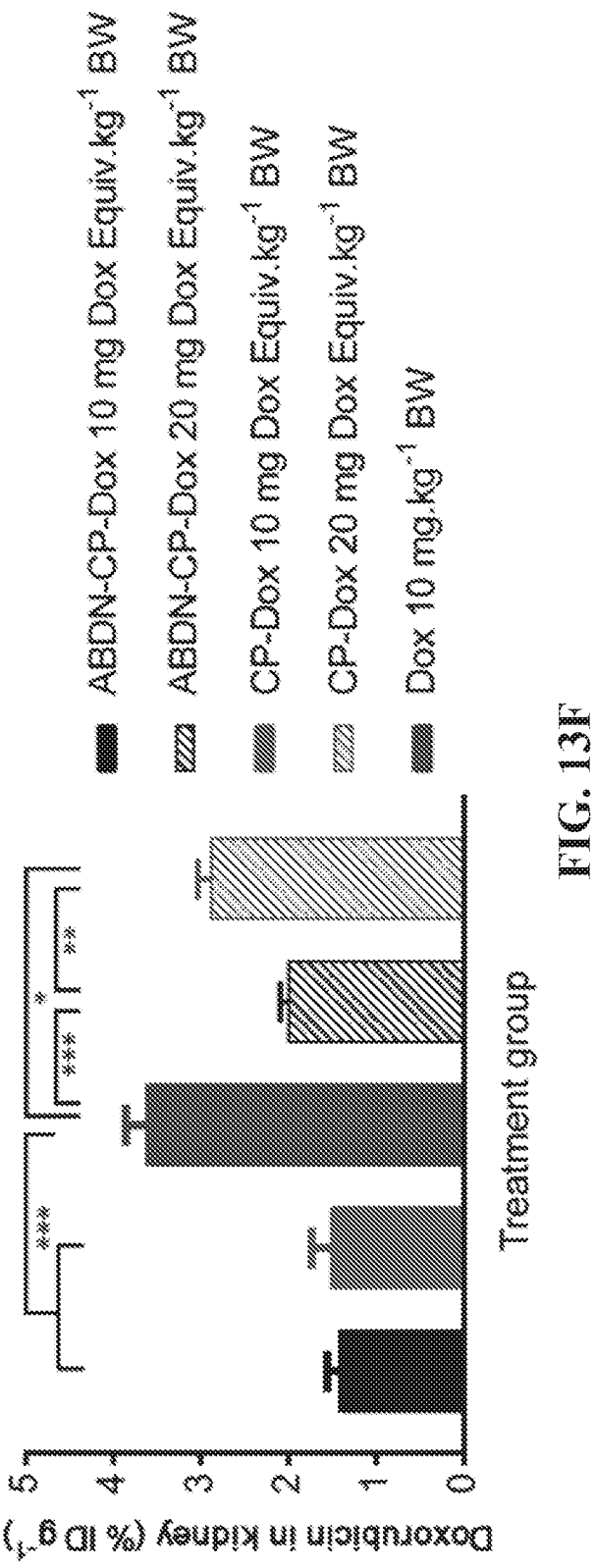
ABDN-CP-Dox 10 mg Dox Equiv.kg-1 BW
ABDN-CP-Dox 20 mg Dox Equiv.kg-1 BW
CP-Dox 10 mg Dox Equiv.kg-1 BW
CP-Dox 20 mg Dox Equiv.kg-1 BW
Dox 10 mg.kg-1 BW
Doxorubicin in kidney (% ID g-1)
0
1
2
3
4
5
Treatment group
***
***
*
**

FIG. 13F

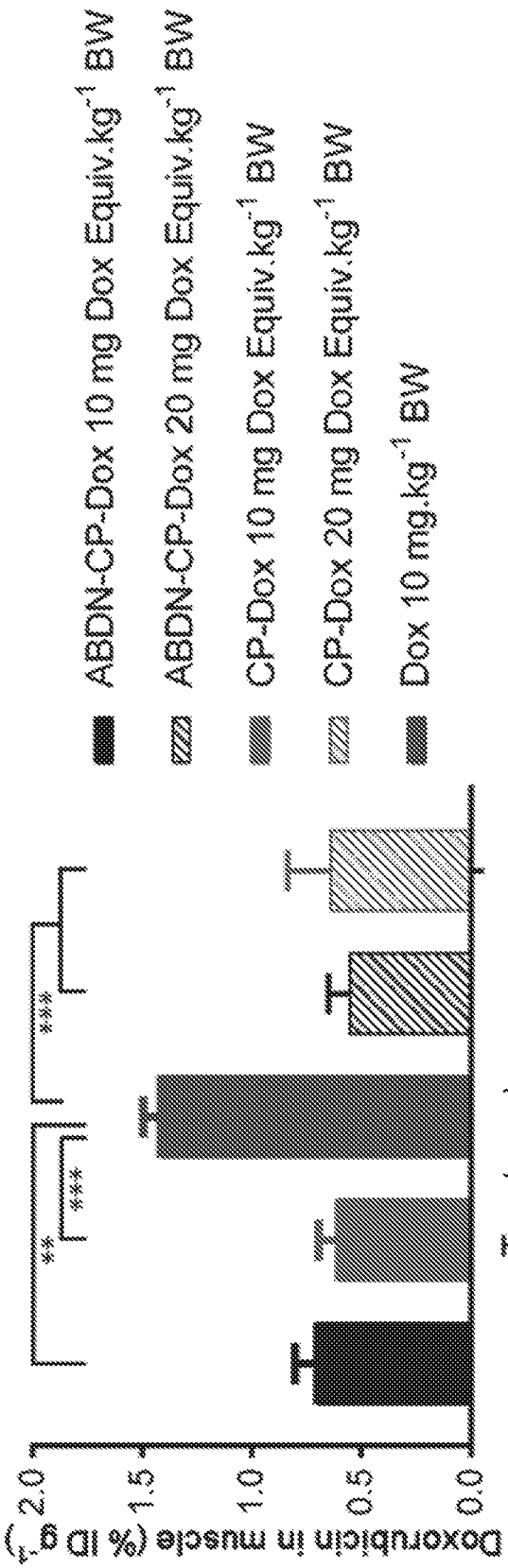
ABDN-CP-Dox 10 mg Dox Equiv.kg-1 BW
ABDN-CP-Dox 20 mg Dox Equiv.kg-1 BW
CP-Dox 10 mg Dox Equiv.kg-1 BW
CP-Dox 20 mg Dox Equiv.kg-1 BW
Dox 10 mg.kg-1 BW
Doxorubicin in muscle (% ID g-1)
2.0
1.5
1.0
0.5
0.0
**
***
***
Treatment group

FIG. 13G

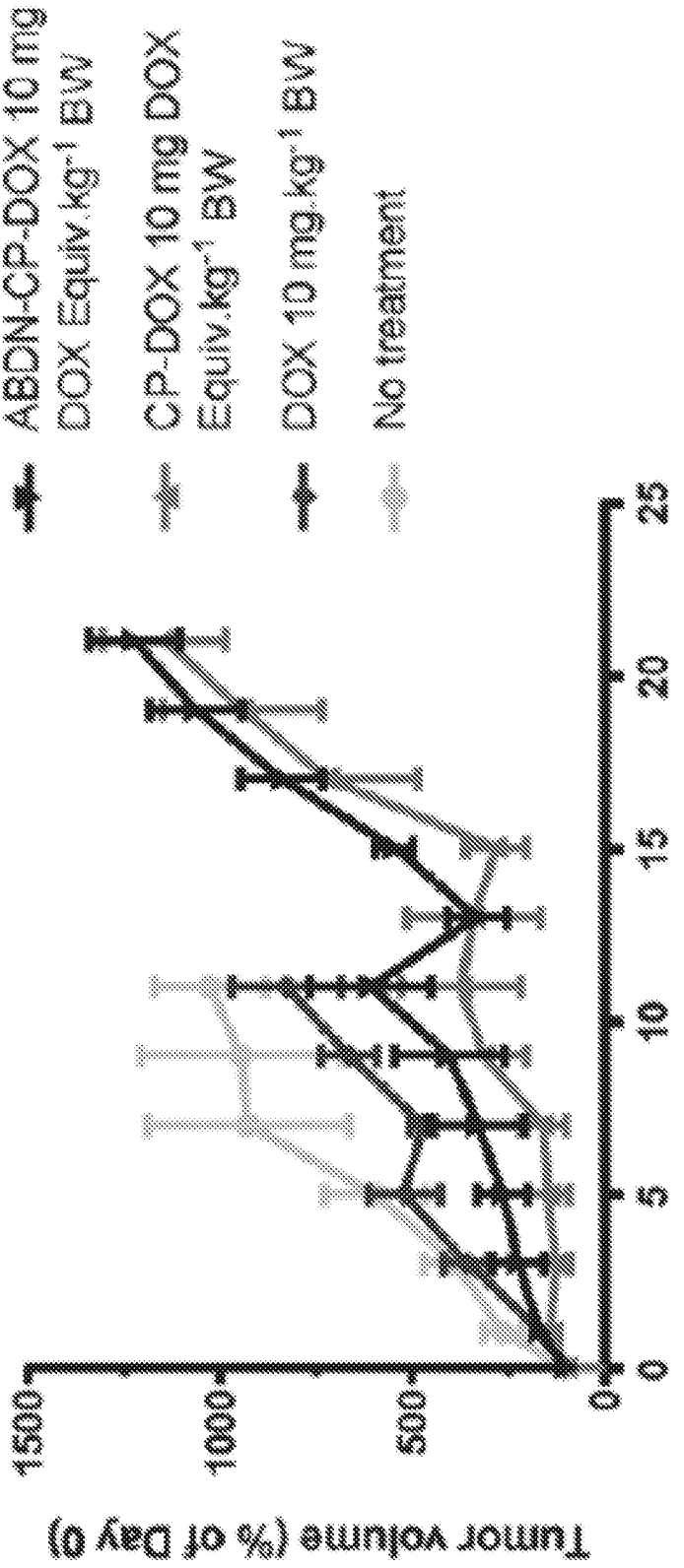
ABDN-CP-DOX 10 mg DOX Equiv.kg-1 BW
CP-DOX 10 mg DOX Equiv.kg-1 BW
DOX 10 mg.kg-1 BW
No treatment
Tumor volume (% of Day 0)
1500
1000
500
0
0
5
10
15
20
25
Time (Day)

FIG. 14A

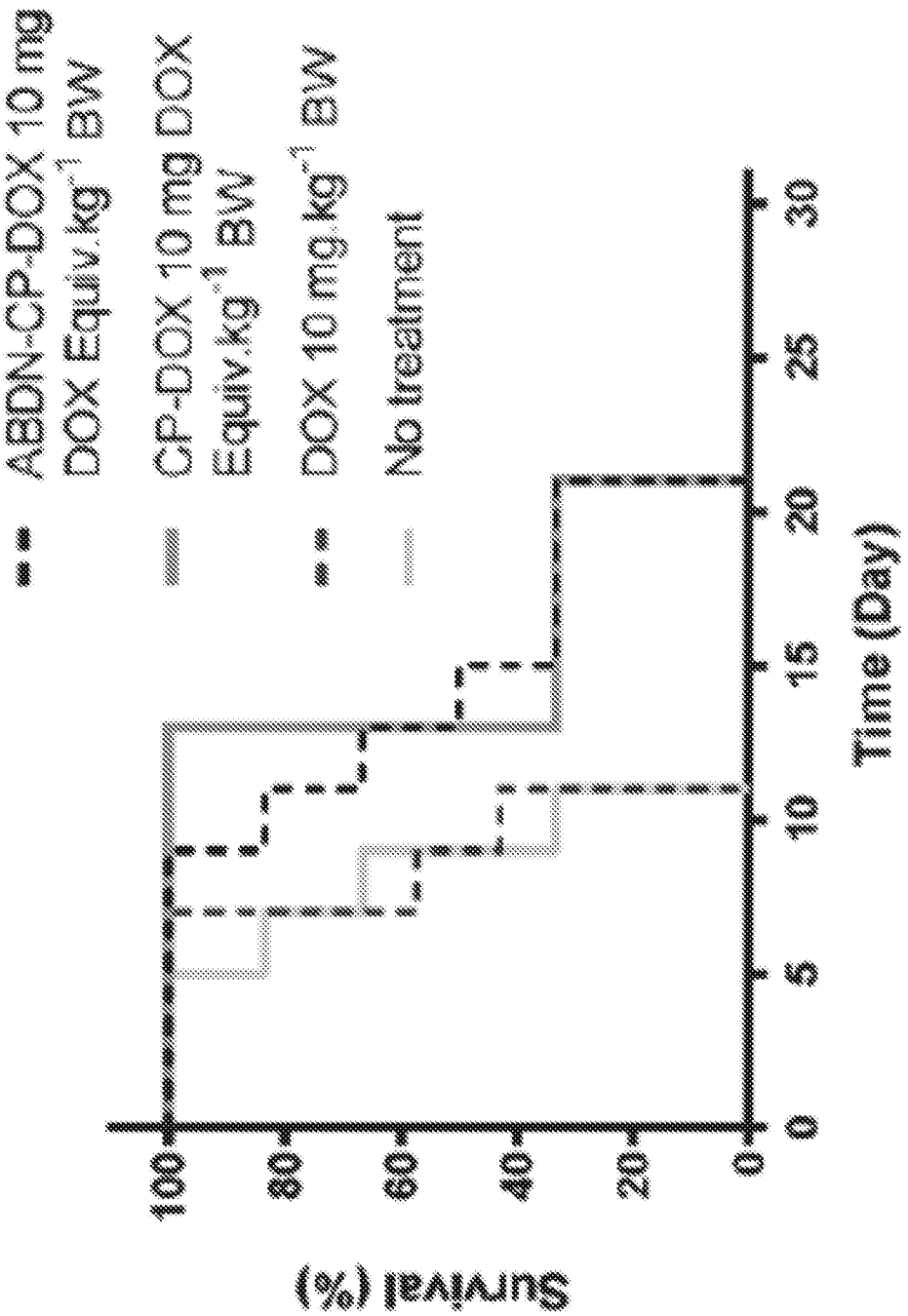
ABDN-CP-DOX 10 mg DOX Equiv.kg-1 BW
CP-DOX 10 mg DOX Equiv.kg-1 BW
DOX 10 mg.kg-1 BW
No treatment
Survival (%)
100
80
60
40
20
0
0
5
10
15
20
25
30
Time (Day)

FIG. 14B

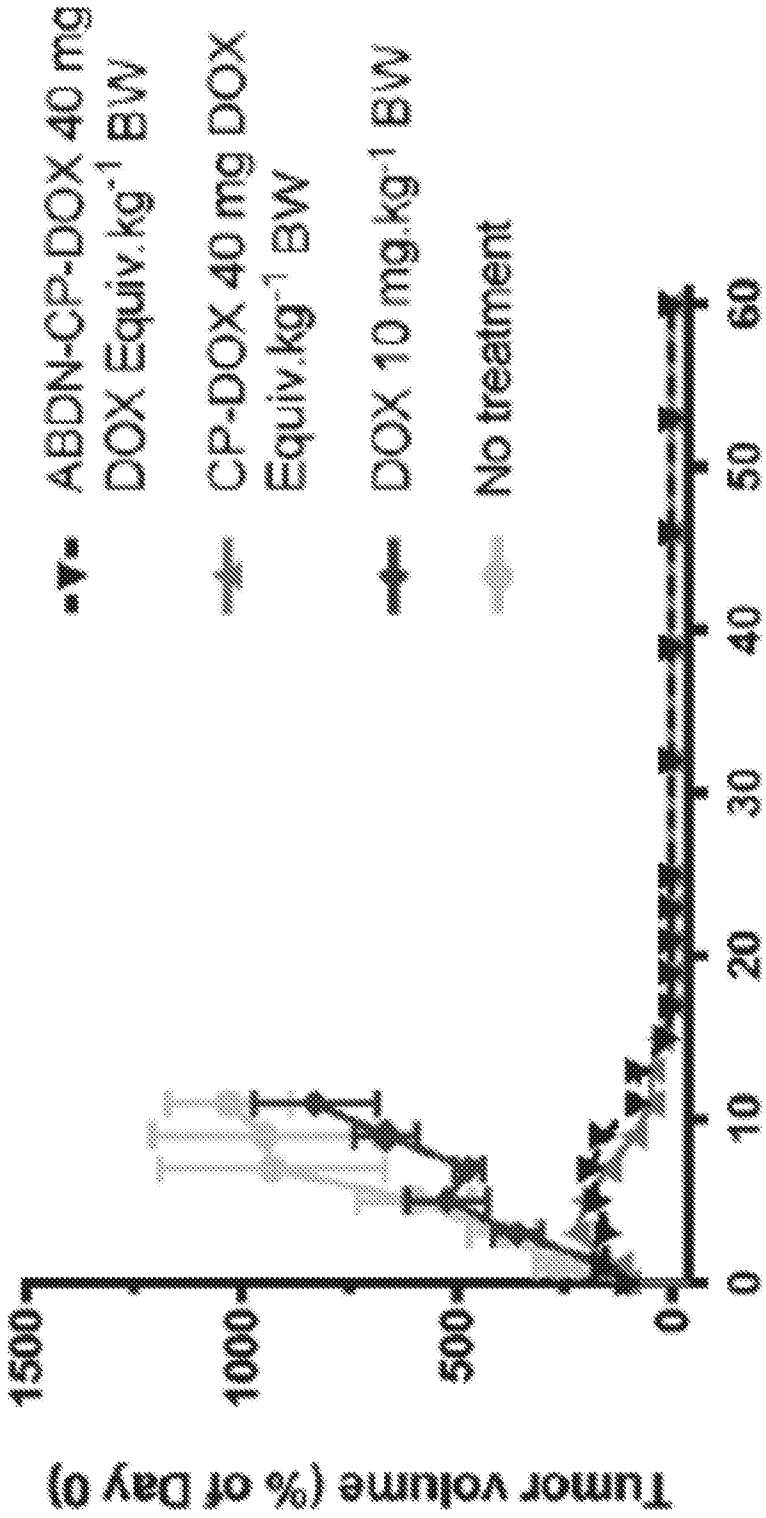
Tumor volume (% of Day 0)
1500
1000
500
0
0
10
20
30
40
50
60
Time (Day)
ABDN-CP-DOX 40 mg DOX Equiv.kg-1 BW
CP-DOX 40 mg DOX Equiv.kg-1 BW
DOX 10 mg.kg-1 BW
No treatment

FIG. 14C

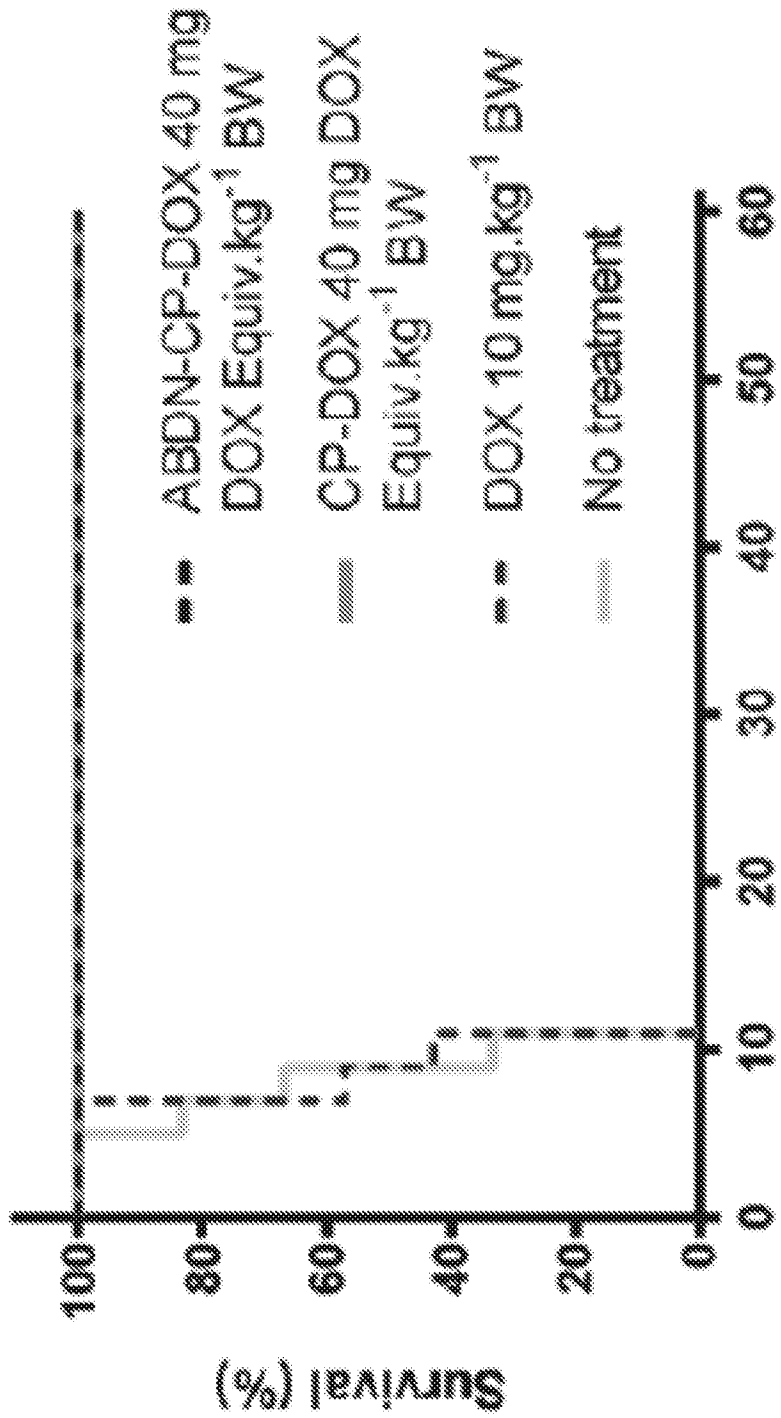
Survival (%)
100
80
60
40
20
0
0
10
20
30
40
50
60
Time (Day)
ABDN-CP-DOX 40 mg DOX Equiv.kg-1 BW
CP-DOX 40 mg DOX Equiv.kg-1 BW
DOX 10 mg.kg-1 BW
No treatment

FIG. 14D

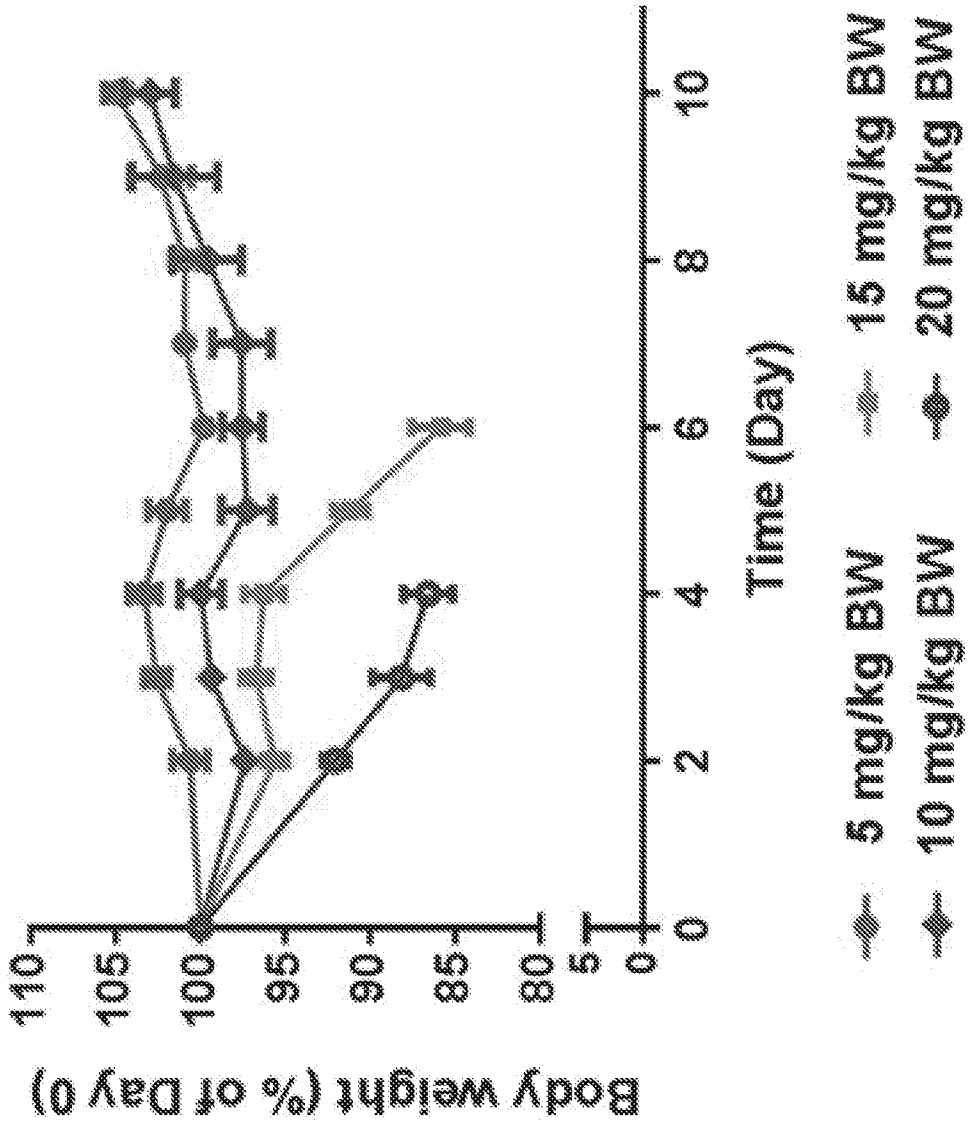
Body weight (% of Day 0)
110
105
100
95
90
85
80
0
2
4
6
8
10
Time (Day)
5 mg/kg BW
10 mg/kg BW
15 mg/kg BW
20 mg/kg BW

FIG. 15A

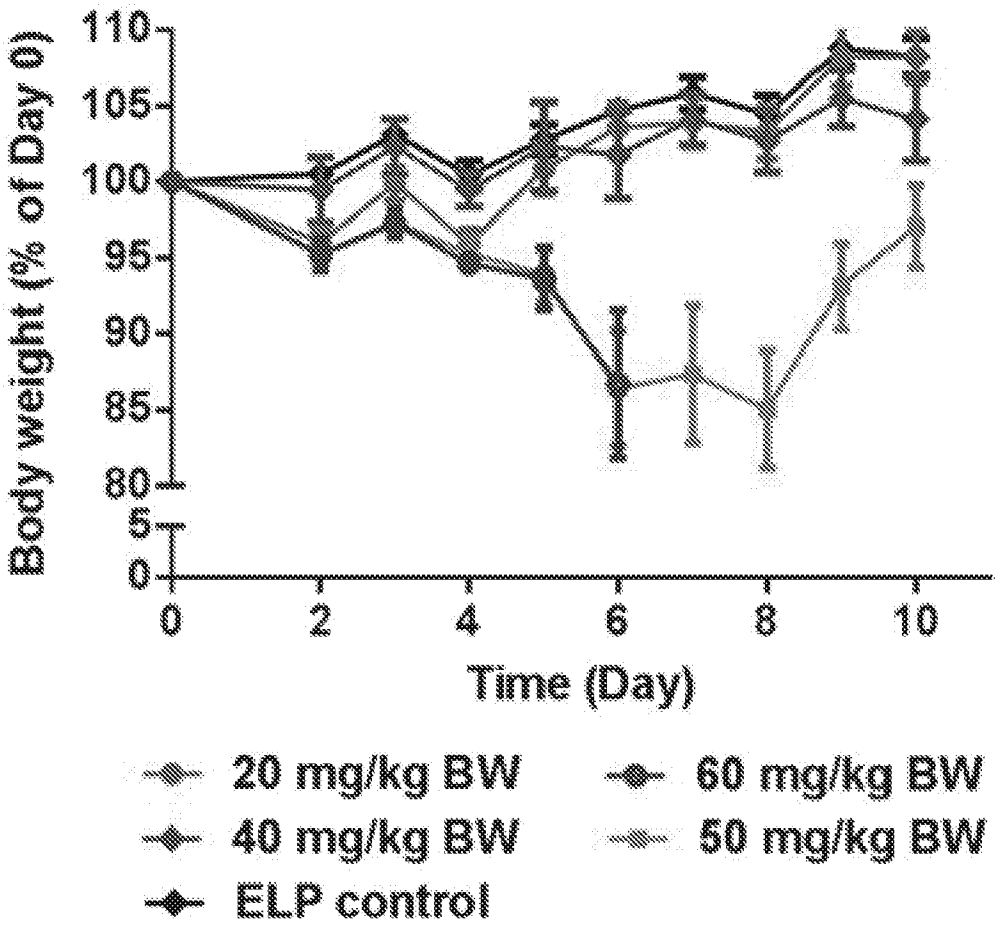
Body weight (% of Day 0)
110
105
100
95
90
85
80
5
0
0
2
4
6
8
10
Time (Day)
20 mg/kg BW
40 mg/kg BW
ELP control
60 mg/kg BW
50 mg/kg BW

FIG. 15B

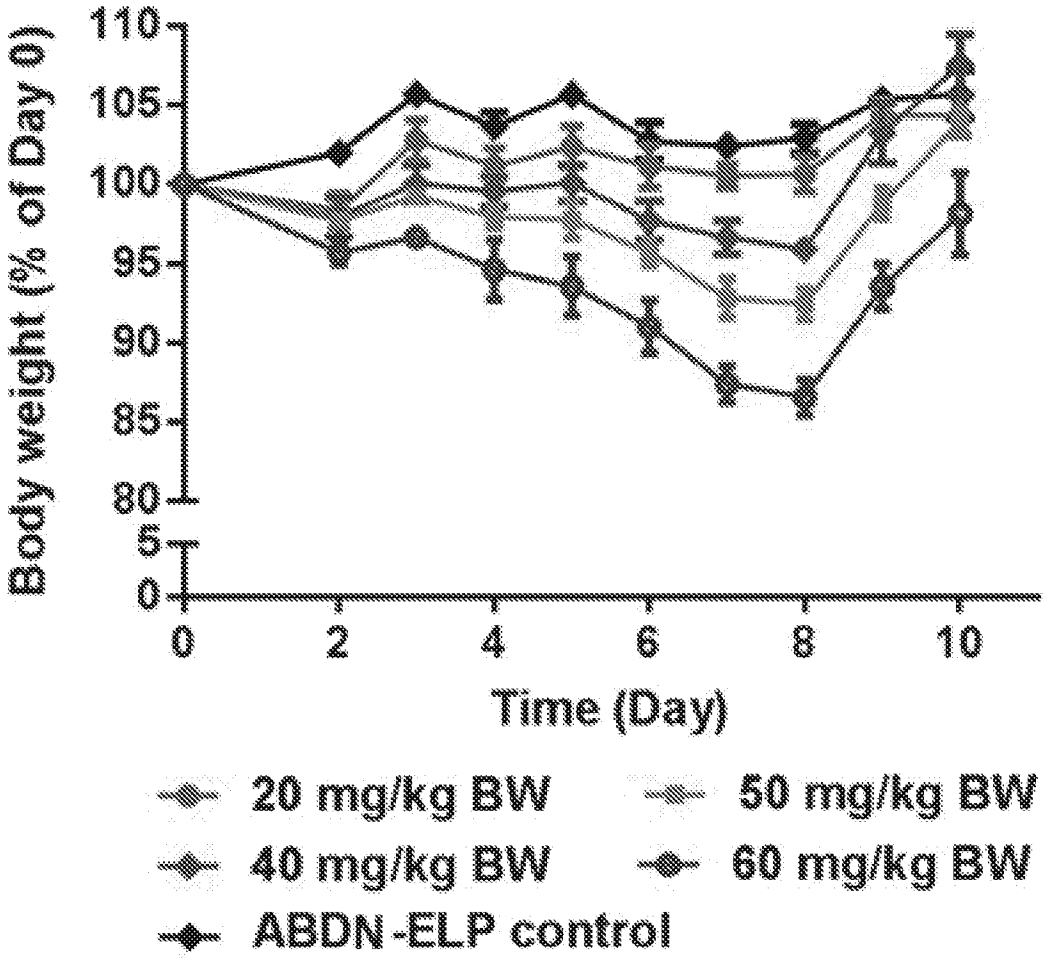
Body weight (% of Day 0)
110
105
100
95
90
85
80
5
0
0
2
4
6
8
10
Time (Day)
20 mg/kg BW
50 mg/kg BW
40 mg/kg BW
60 mg/kg BW
ABDN-ELP control

FIG. 15C

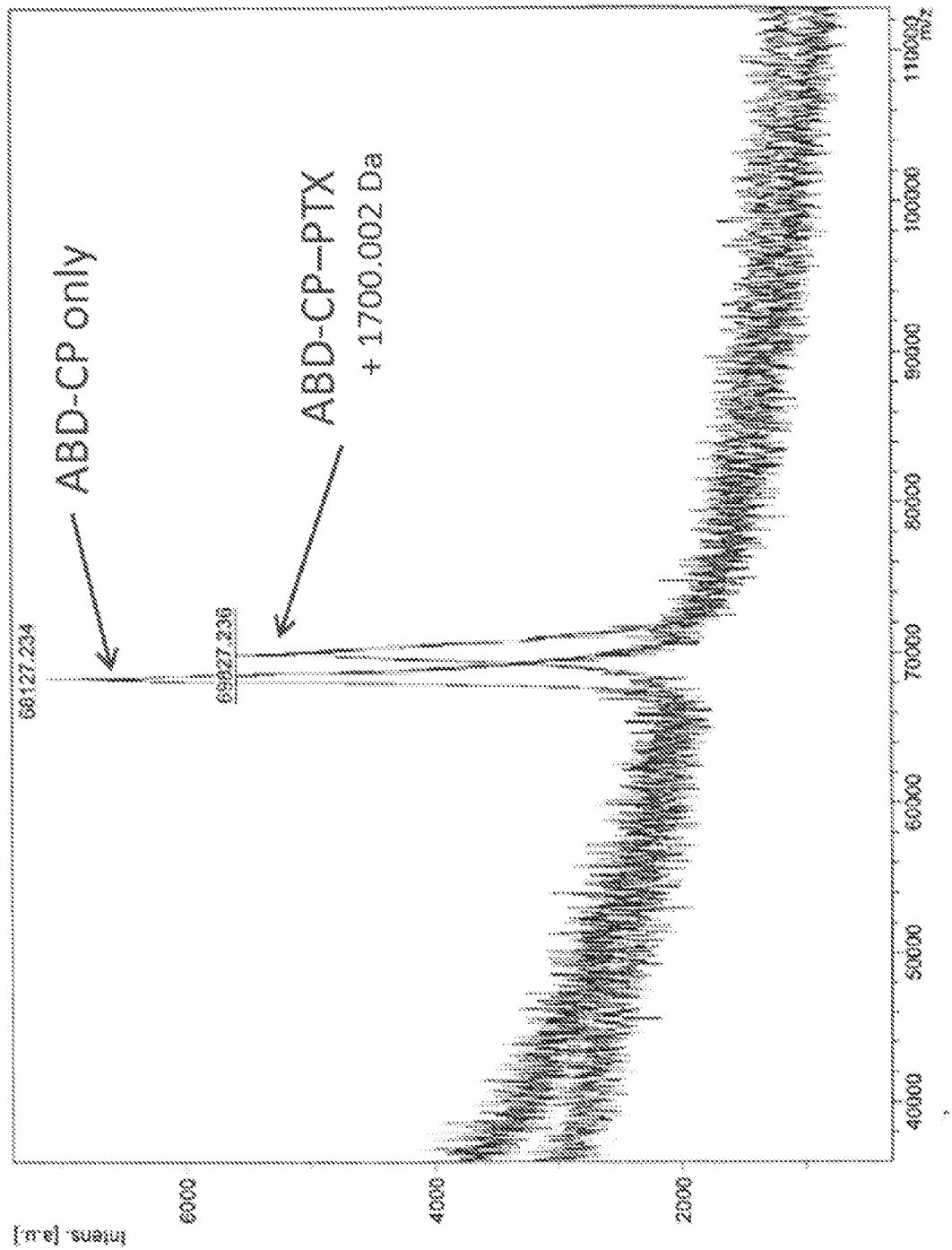
ABD-CP only
ABD-CP–PTX
+ 1700.002 Da
68127.234
69827.236
Intens. [a.u.]
6000
4000
2000
40000
50000
60000
70000
80000
90000
100000
110000
m/z

FIG. 16A

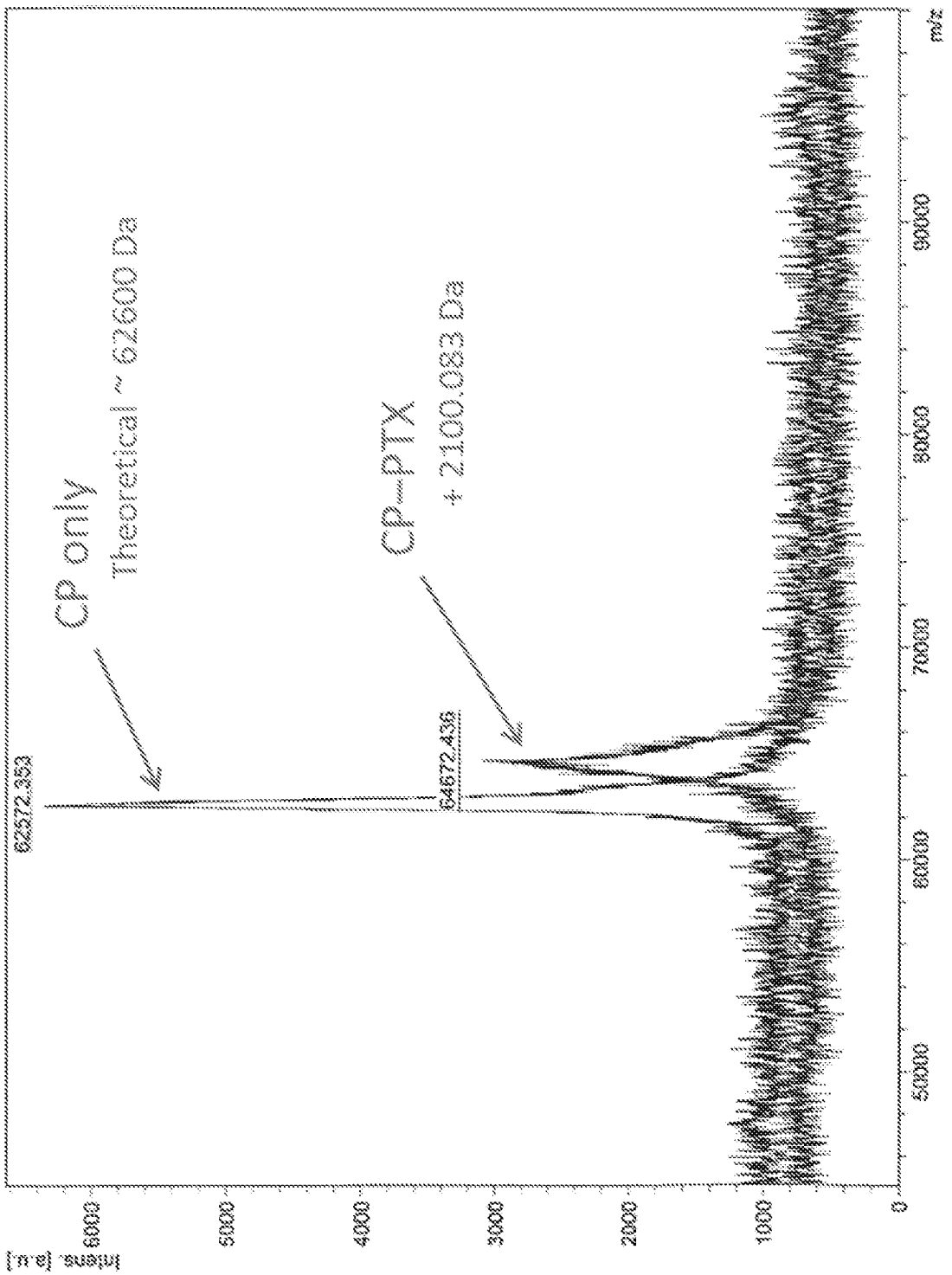
CP only
Theoretical ~ 62600 Da
CP–PTX
+ 2100.083 Da
62572.353
64672.436
Intens. [a.u.]
m/z
0
10000
20000
30000
40000
50000
60000
70000
80000
90000

FIG. 16B

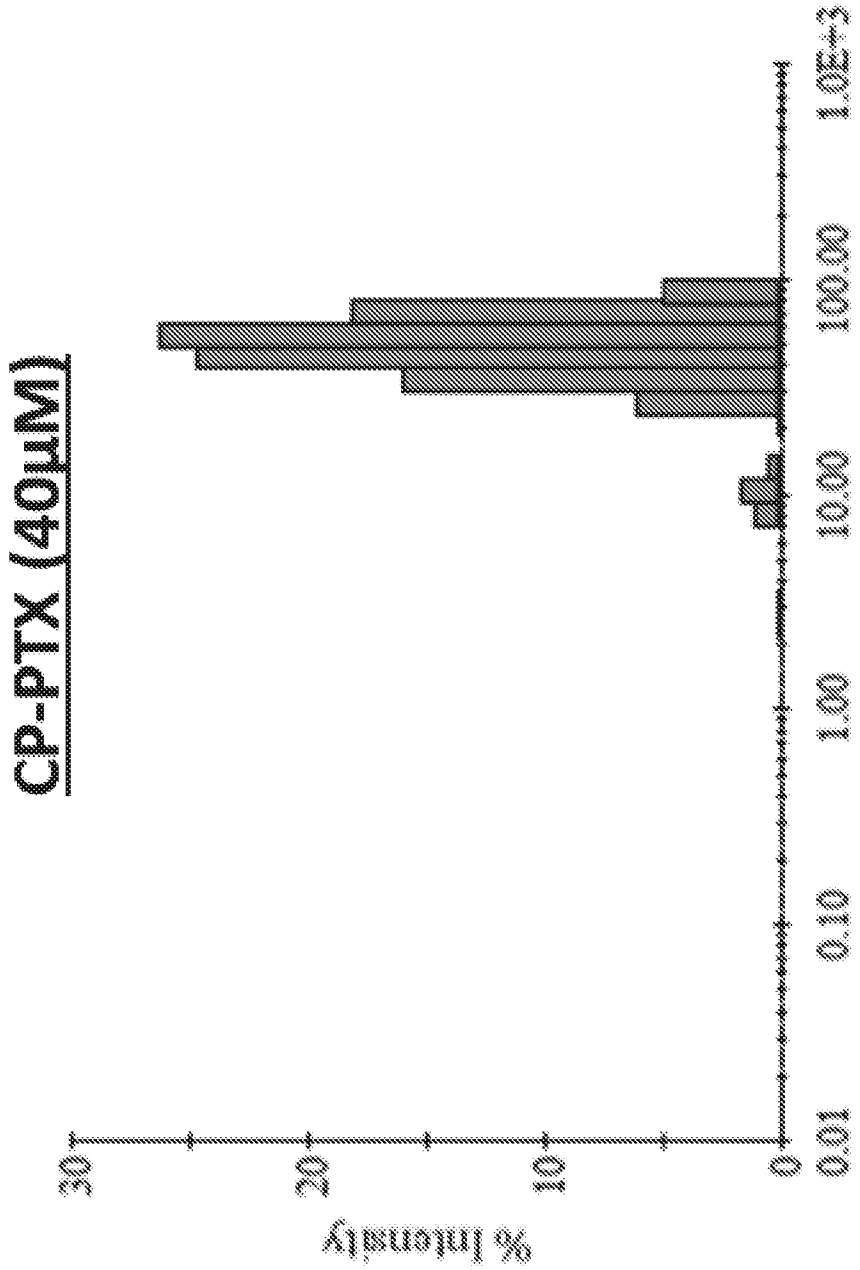
CP-PTX (40μM)
% Intensity
30
20
10
0
0.01
0.10
1.00
10.00
100.00
1.0E+3
R(nm)

FIG. 17A

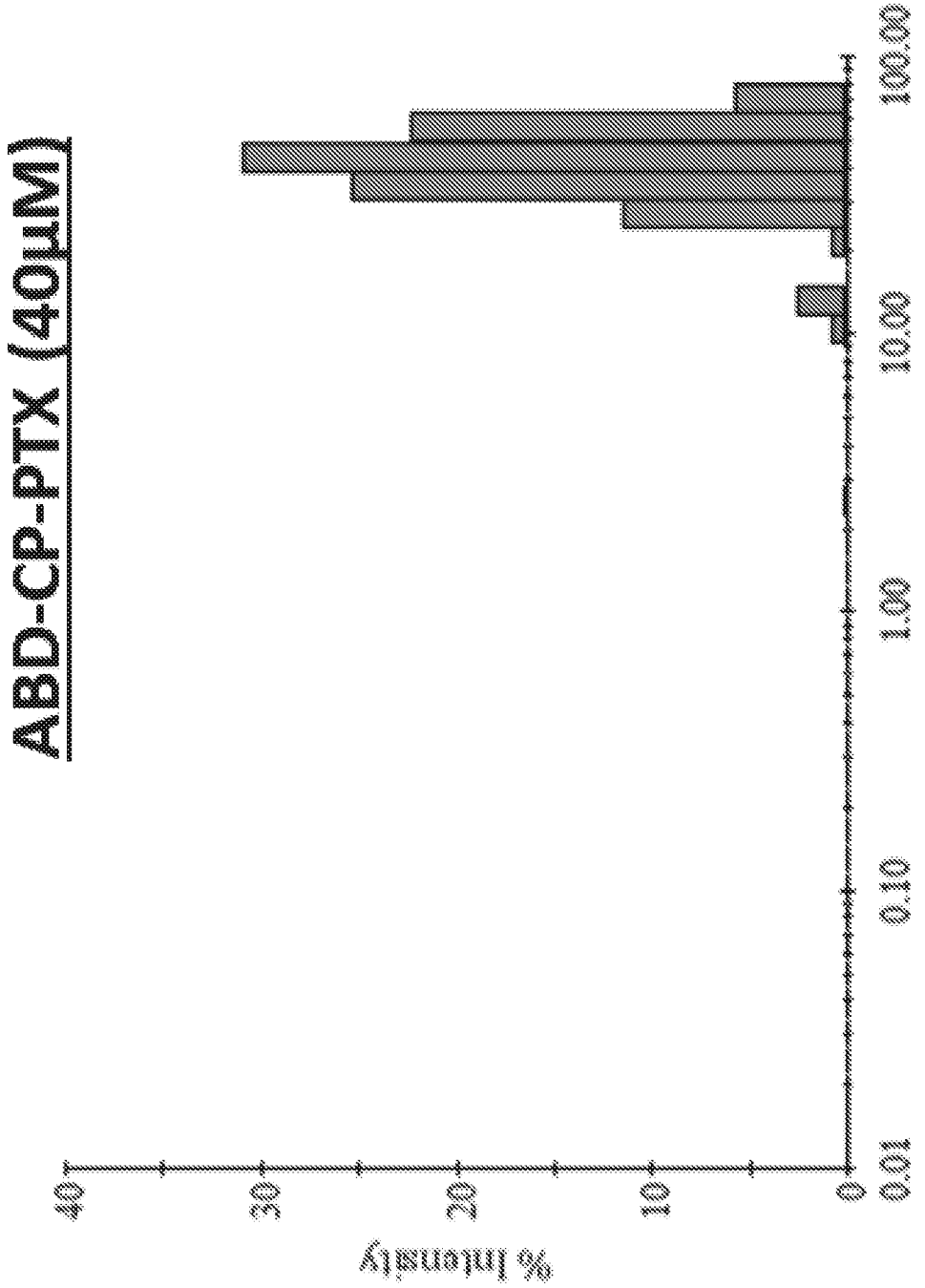
ABD-CP-PTX (40μM)
% Intensity
40
30
20
10
0
0.01
0.10
1.00
10.00
100.00
R(nm)

FIG. 17B

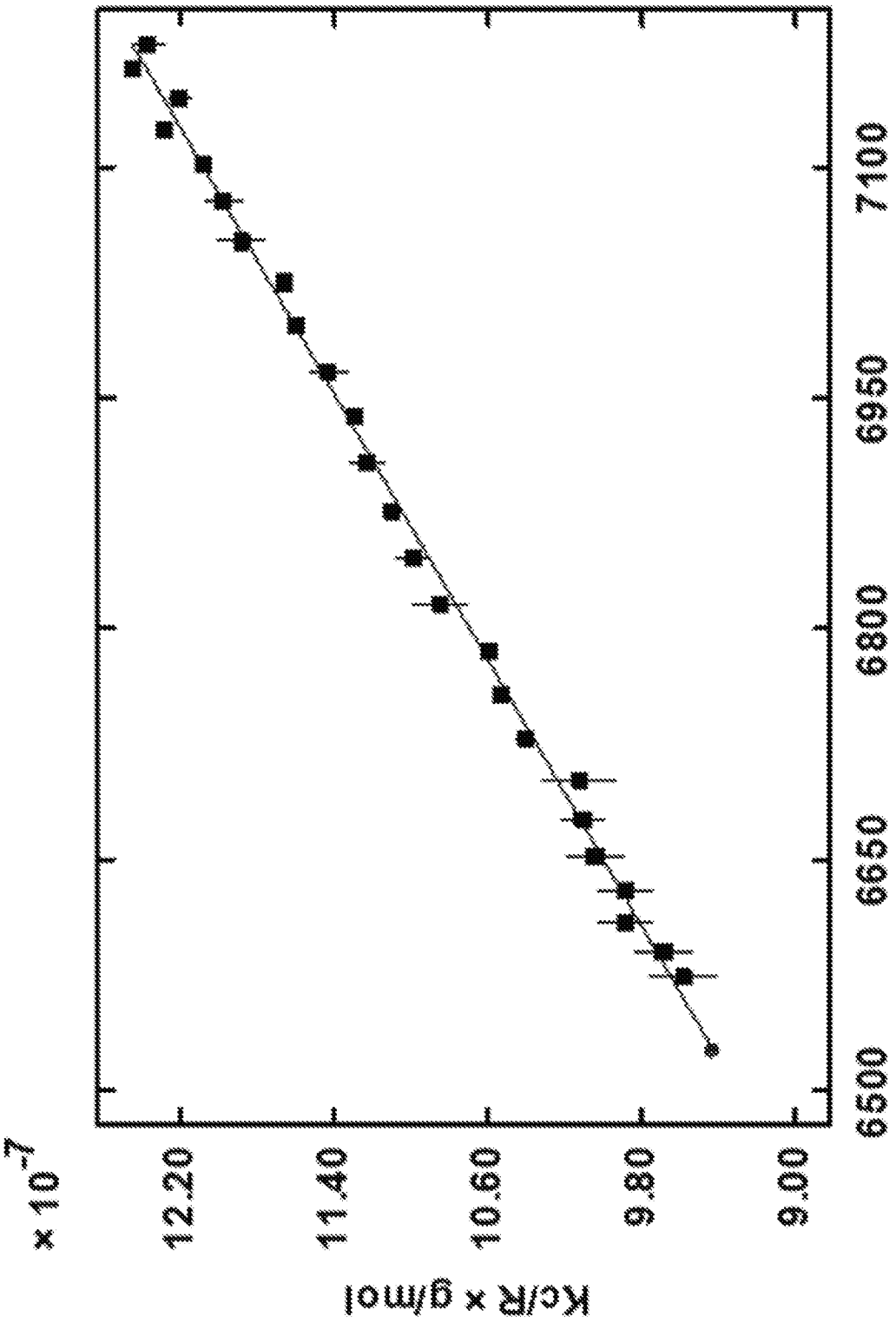
Kc/R x g/mol
x 10^-7
12.20
11.40
10.60
9.80
9.00
6500
6650
6800
6950
7100
(q²+k(c) x µm²

FIG. 18A

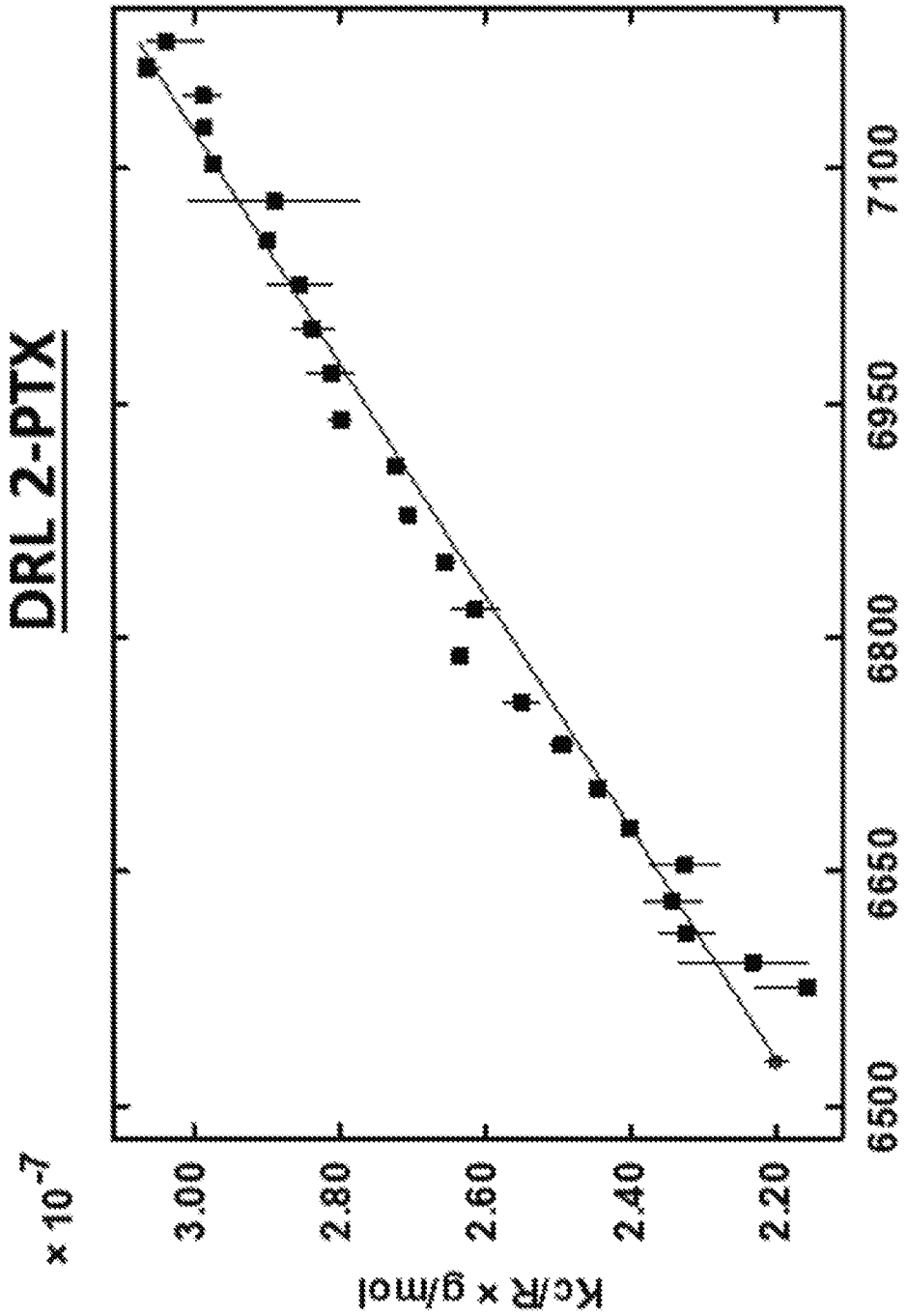
DRL 2-PTX
Kc/R x g/mol
x 10^-7
3.00
2.80
2.60
2.40
2.20
6500
6650
6800
6950
7100
(q²+kc) x µm²

FIG. 18B

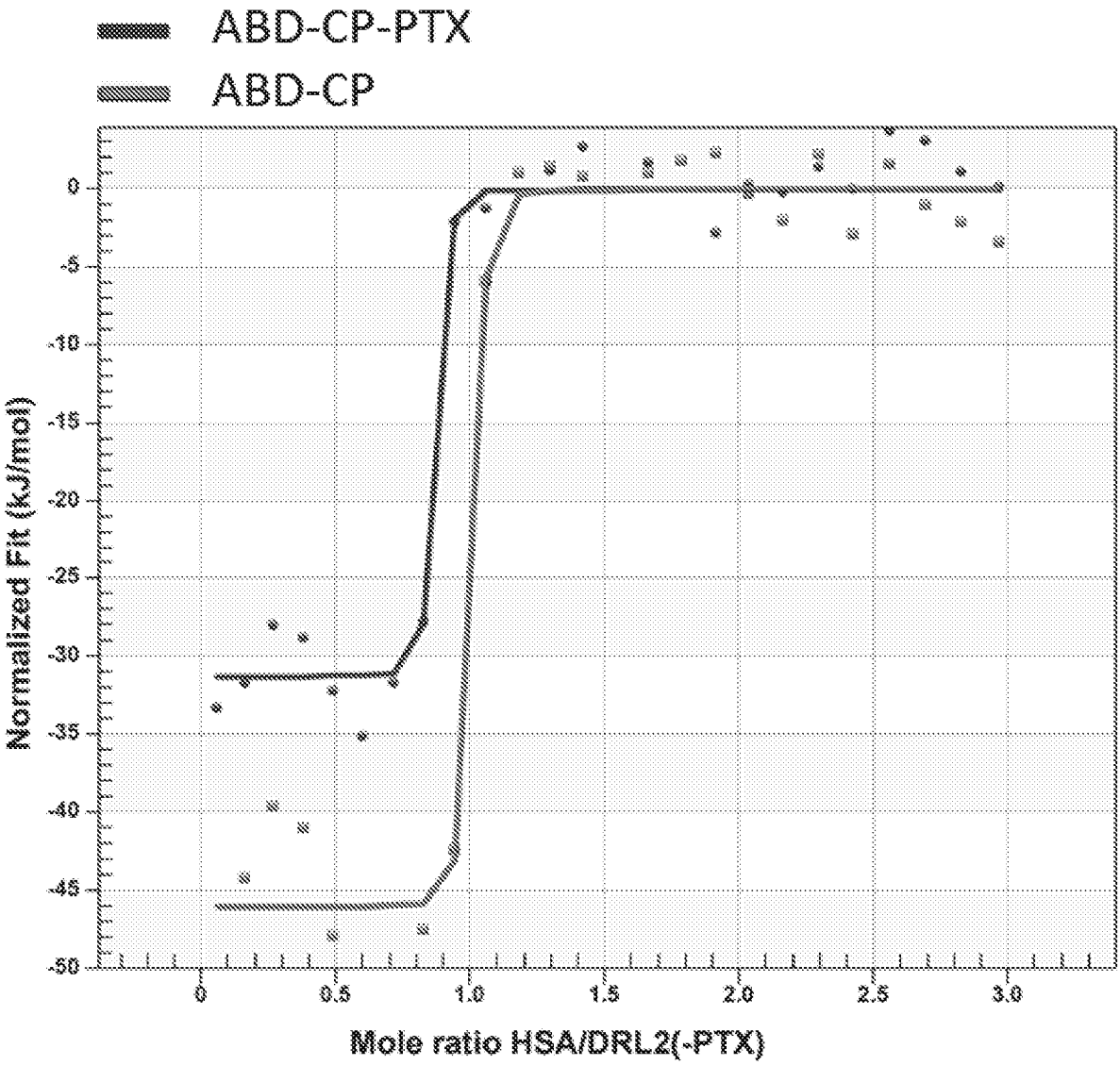
ABD-CP-PTX
ABD-CP
Normalized Fit (kJ/mol)
0
-5
-10
-15
-20
-25
-30
-35
-40
-45
-50
0
0.5
1.0
1.5
2.0
2.5
3.0
Mole ratio HSA/DRL2(-PTX)

FIG. 19A

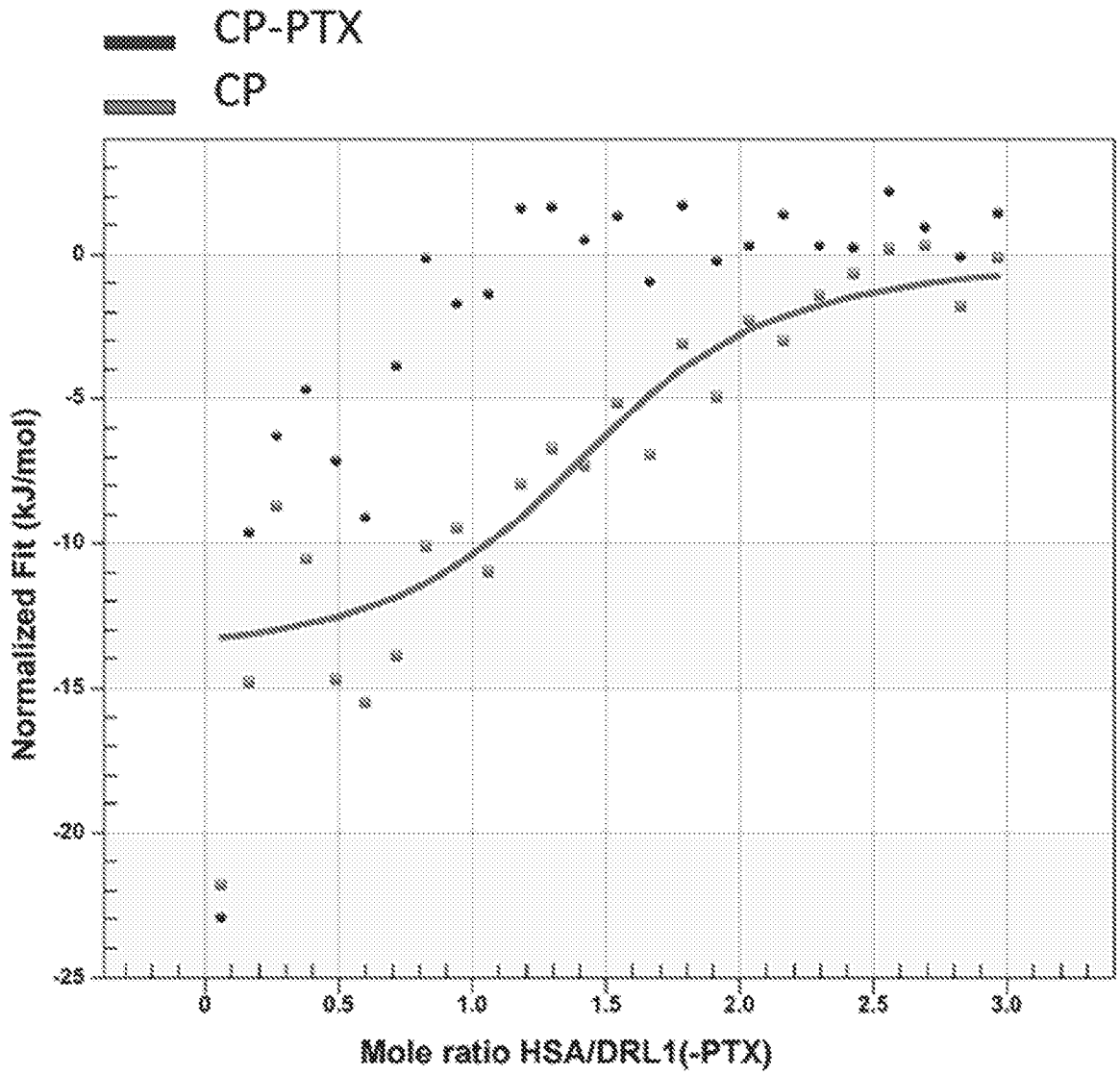
CP-PTX
CP
Normalized Fit (KJ/mol)
0
-5
-10
-15
-20
-25
0
0.5
1.0
1.5
2.0
2.5
3.0
Mole ratio HSA/DRL1(-PTX)

FIG. 19

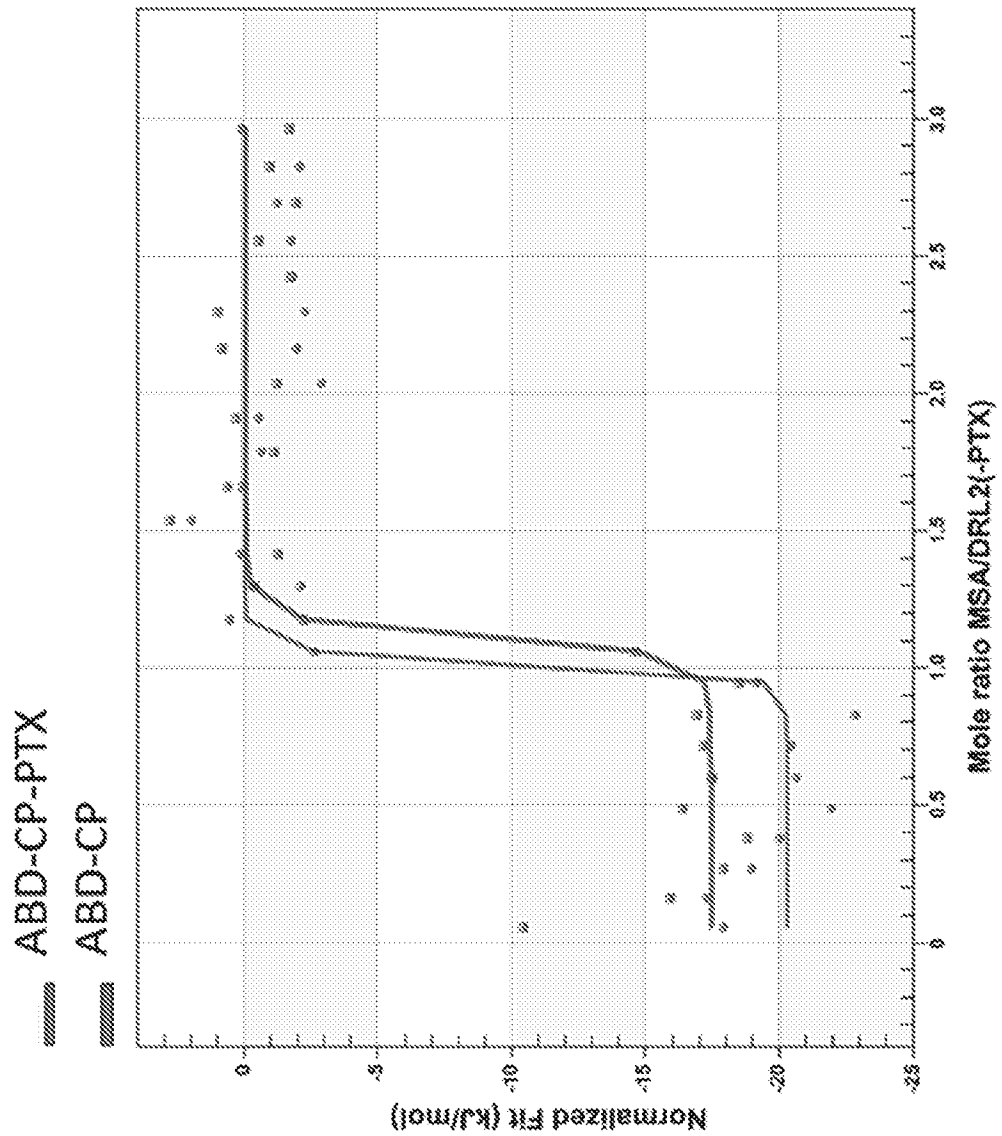
ABD-CP-PTX
ABD-CP
Normalized Fit (kJ/mol)
0
-5
-10
-15
-20
-25
0
0.5
1.0
1.5
2.0
2.5
3.0
Mole ratio MSA/DRL2(-PTX)

FIG. 20A

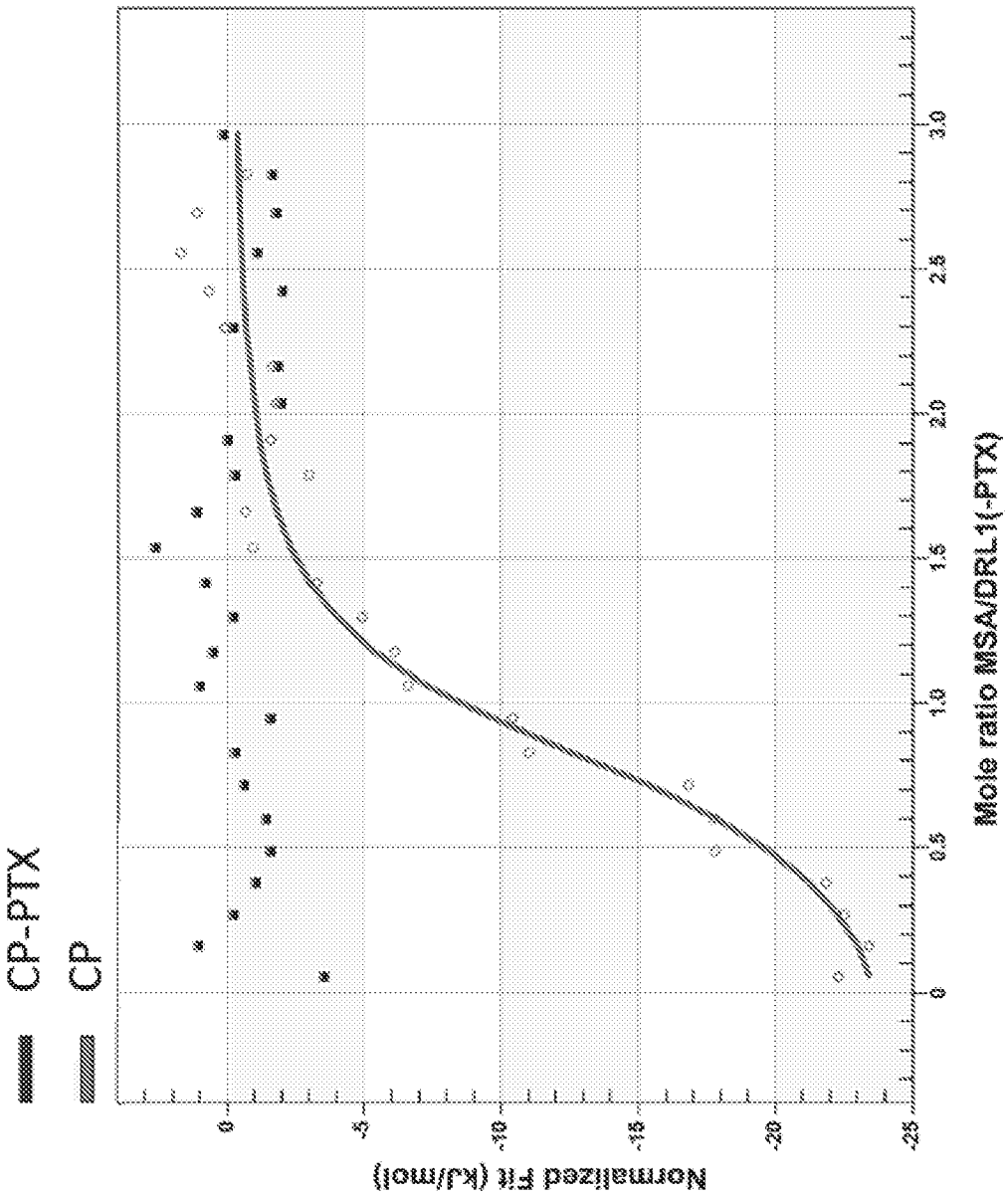
CP-PTX
CP
Normalized Fit (kJ/mol)
0
-5
-10
-15
-20
-25
0
0.5
1.0
1.5
2.0
2.5
3.0
Mole ratio MSA/DRL1(-PTX)

FIG. 20B

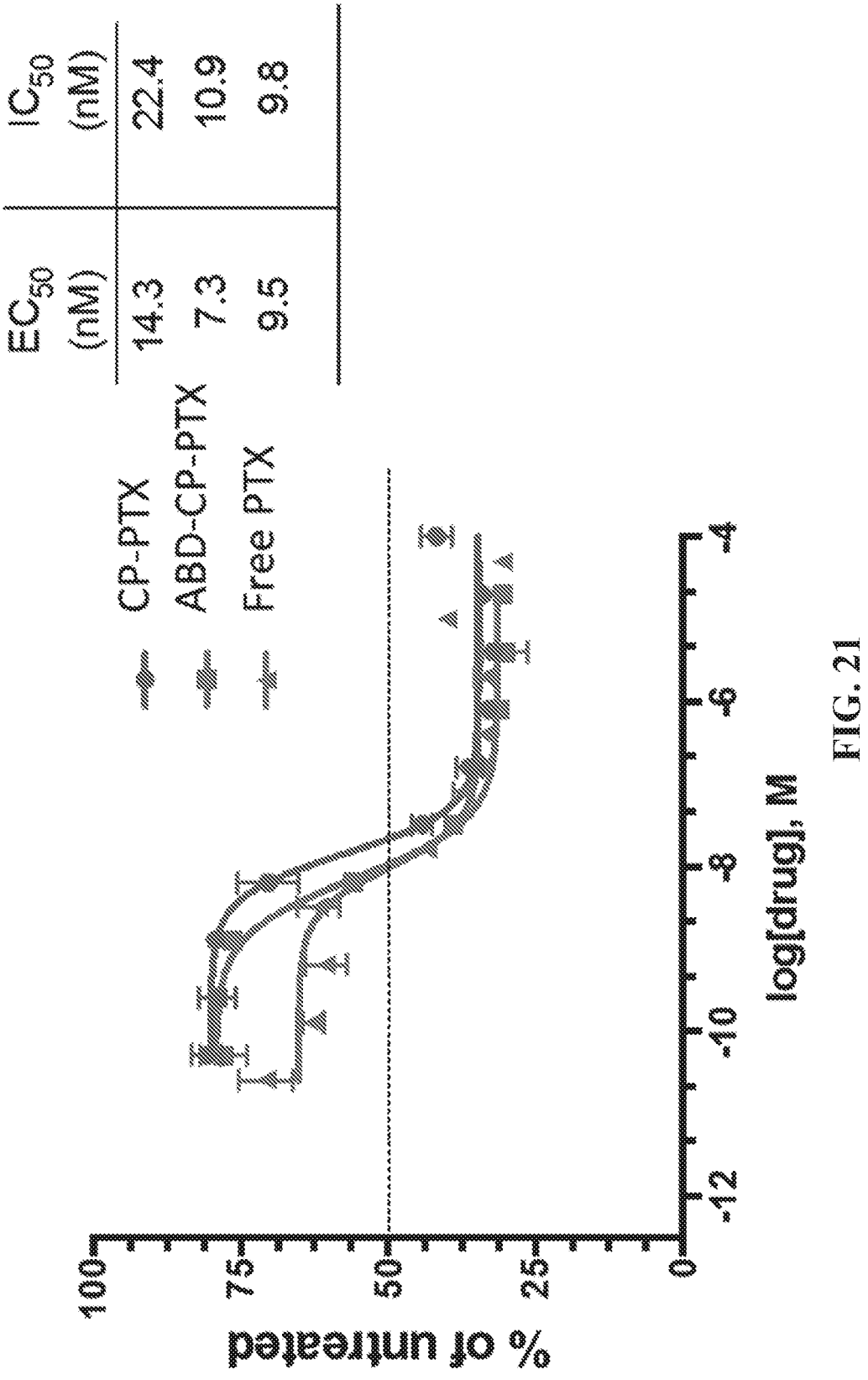
CP-PTX
ABD-CP-PTX
Free PTX
EC50 (nM)
14.3
7.3
9.5
IC50 (nM)
22.4
10.9
9.8
% of untreated
100
75
50
25
0
-12
-10
-8
-6
-4
log[drug], M

FIG. 21

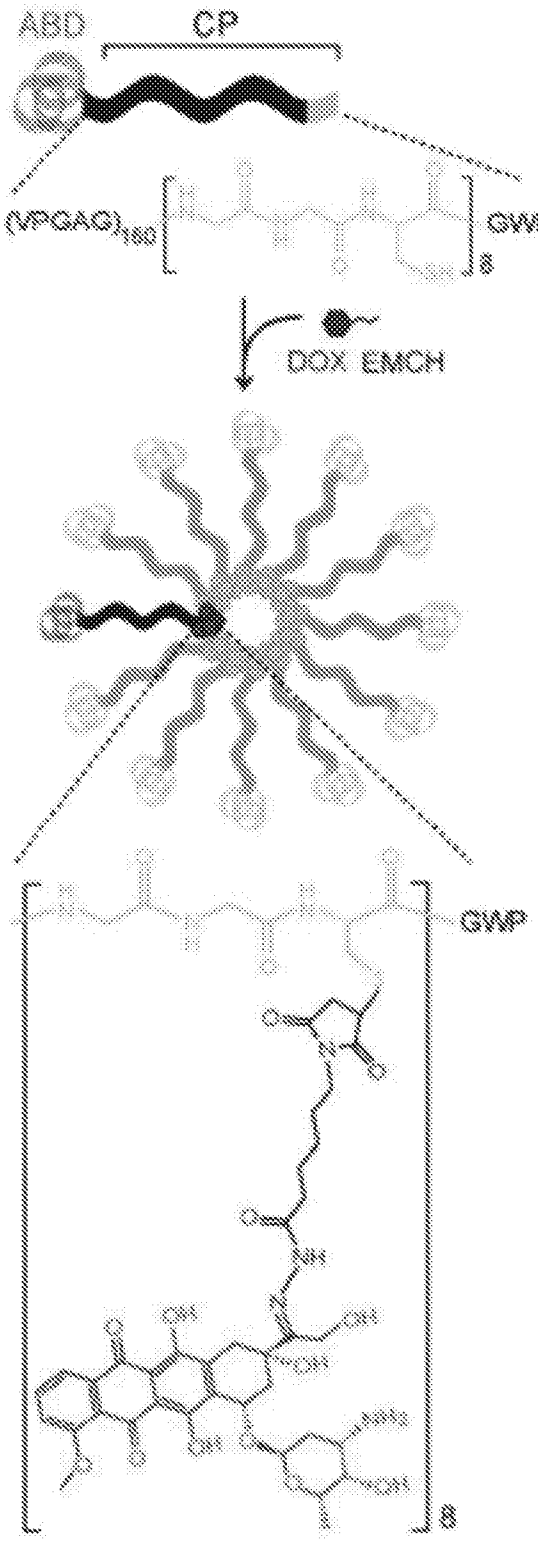

FIG. 22

INTERNATIONAL SEARCH REPORT

International application No.
PCT/US19/50077

A. CLASSIFICATION OF SUBJECT MATTER

IPC - A61K 47/64, 47/65, 47/66 (2019.01)

CPC - A61K 47/64, 47/65, 47/66

According to International Patent Classification (IPC) or to both national classification and IPC

B. FIELDS SEARCHED

Minimum documentation searched (classification system followed by classification symbols)
See Search History document

Documentation searched other than minimum documentation to the extent that such documents are included in the fields searched
See Search History document

Electronic data base consulted during the international search (name of data base and, where practicable, search terms used)
See Search History document

C. DOCUMENTS CONSIDERED TO BE RELEVANT

Category*	Citation of document, with indication, where appropriate, of the relevant passages	Relevant to claim No.
Y	(MCDANIEL, JR) Assembly of Highly Asymmetric Genetically-Encoded Amphiphiles for Thermally Targeted Delivery of Therapeutics. DUKE UNIVERSITY. 2013. Retrieved from the internet <https://pdfs.semanticscholar.org/cfda/165853d8947903efa8b8471a0aacd258252c.pdf>; pages 1-295; page 18, paragraph 1; page 21, paragraph 1; page 23, paragraph 1; page 59, paragraph 1; page 68, paragraph 2; page 95, paragraph 1; page 119, paragraph 1 – page 120, paragraph 1; page 133, paragraph 2 – page 134, paragraph 2; page 156, paragraph 1; page 180, paragraph 1; figures 26, 31A	1-2, 3/1-2, 4/1-2, 5/1-2, 6/1-2, 7/6/1-2, 8/1-2, 9/1-2, 10/1-2, 11/1-2, 12/1-2, 13/11/1-2, 14/11/1-2, 15/1-2, 16/15/1-2, 17/1-2, 18/17/1-2, 19/1-2, 20/19/1-2
Y	US 2014/0170142 A1 (MEDIMMUNE, LLC) 19 June 2014; paragraphs [0009], [0012]	1-2, 3/1-2, 4/1-2, 5/1-2, 6/1-2, 7/6/1-2, 8/1-2, 9/1-2, 10/1-2, 11/1-2, 12/1-2, 13/11/1-2, 14/11/1-2, 15/1-2, 16/15/1-2, 17/1-2, 18/17/1-2, 19/1-2, 20/19/1-2
Y	(MCDANIEL, JR et al.) Drug Delivery to Solid Tumors by Elastin-Like Polypeptides. Advanced Drug Delivery Reviews. 30 December 2010; Vol. 62, No. 15; pages 1-27; page 5, paragraph 3; DOI: 10.1016/j.addr.2010.05.004.	18/17/1-2

☒ Further documents are listed in the continuation of Box C. ☐ See patent family annex.

* Special categories of cited documents:
"A" document defining the general state of the art which is not considered to be of particular relevance
"D" document cited by the applicant in the international application
"E" earlier application or patent but published on or after the international filing date
"L" document which may throw doubts on priority claim(s) or which is cited to establish the publication date of another citation or other special reason (as specified)
"O" document referring to an oral disclosure, use, exhibition or other means
"P" document published prior to the international filing date but later than the priority date claimed
"T" later document published after the international filing date or priority date and not in conflict with the application but cited to understand the principle or theory underlying the invention
"X" document of particular relevance; the claimed invention cannot be considered novel or cannot be considered to involve an inventive step when the document is taken alone
"Y" document of particular relevance; the claimed invention cannot be considered to involve an inventive step when the document is combined with one or more other such documents, such combination being obvious to a person skilled in the art
"&" document member of the same patent family

Date of the actual completion of the international search	Date of mailing of the international search report
07 January 2020 (07.01.2020)	27 JAN 2020
Name and mailing address of the ISA/US Mail Stop PCT, Attn: ISA/US, Commissioner for Patents P.O. Box 1450, Alexandria, Virginia 22313-1450 Facsimile No. 571-273-8300	Authorized officer Shane Thomas Telephone No. PCT Helpdesk: 571-272-4300

INTERNATIONAL SEARCH REPORT

International application No.
PCT/US19/50077

Box No. II Observations where certain claims were found unsearchable (Continuation of item 2 of first sheet)

This international search report has not been established in respect of certain claims under Article 17(2)(a) for the following reasons:

1. ☐ Claims Nos.:
because they relate to subject matter not required to be searched by this Authority, namely:

2. ☐ Claims Nos.:
because they relate to parts of the international application that do not comply with the prescribed requirements to such an extent that no meaningful international search can be carried out, specifically:

3. ☐ Claims Nos.:
because they are dependent claims and are not drafted in accordance with the second and third sentences of Rule 6.4(a).

Box No. III Observations where unity of invention is lacking (Continuation of item 3 of first sheet)

This International Searching Authority found multiple inventions in this international application, as follows:

-***- Please See the Next Supplemental Page-***-

1. ☐ As all required additional search fees were timely paid by the applicant, this international search report covers all searchable claims.

2. ☐ As all searchable claims could be searched without effort justifying additional fees, this Authority did not invite payment of additional fees.

3. ☐ As only some of the required additional search fees were timely paid by the applicant, this international search report covers only those claims for which fees were paid, specifically claims Nos.:

4. ☒ No required additional search fees were timely paid by the applicant. Consequently, this international search report is restricted to the invention first mentioned in the claims; it is covered by claims Nos.:

Groups I+, Claims 1-20, a polypeptide encompassing (AGVPG)x (polypeptide), and a molecule encompassing a chemotherapeutic (molecule)

Remark on Protest

☐ The additional search fees were accompanied by the applicant's protest and, where applicable, the payment of a protest fee.

☐ The additional search fees were accompanied by the applicant's protest but the applicable protest fee was not paid within the time limit specified in the invitation.

☐ No protest accompanied the payment of additional search fees.

INTERNATIONAL SEARCH REPORT

International application No.
PCT/US19/50077

C (Continuation). DOCUMENTS CONSIDERED TO BE RELEVANT

Category*	Citation of document, with indication, where appropriate, of the relevant passages	Relevant to claim No.
A	US 2016/0120952 A1 (DUKE UNIVERSITY) 05 May 2016; paragraphs [0005], [0008], [0047], [0049], [0094], [0121], [0124]	1-2, 3/1-2, 4/1-2, 5/1-2, 6/1-2, 7/6/1-2, 8/1-2, 9/1-2, 10/1-2, 11/1-2, 12/1-2, 13/11/1-2, 14/11/1-2, 15/1-2, 16/15/1-2, 17/1-2, 18/17/1-2, 19/1-2, 20/19/1-2
P, X	WO 2019/147954 A1 (DUKE UNIVERSITY) 01 August 2019; whole document	1-2, 3/1-2, 4/1-2, 5/1-2, 6/1-2, 7/6/1-2, 8/1-2, 9/1-2, 10/1-2, 11/1-2, 12/1-2, 13/11/1-2, 14/11/1-2, 15/1-2, 16/15/1-2, 17/1-2, 18/17/1-2, 19/1-2, 20/19/1-2

INTERNATIONAL SEARCH REPORT
Information on patent family members

International application No.
PCT/US19/50077

-***-Continued from Box III Observations where unity of invention is lacking -***-

This application contains the following inventions or groups of inventions which are not so linked as to form a single general inventive concept under PCT Rule 13.1. In order for all inventions to be examined, the appropriate additional examination fees must be paid.

Groups I+, Claims 1-20, a polypeptide encompassing (AGVPG)x (polypeptide), and a molecule encompassing a chemotherapeutic (molecule) are directed toward a composition and methods associated therewith.

The composition and methods will be searched to the extent they encompass a conjugate encompassing a polypeptide encompassing (AGVPG)x (first exemplary polypeptide), and a molecule encompassing a chemotherapeutic (first exemplary molecule). Applicant is invited to elect additional polypeptide(s), with specified SEQ ID NO: for each, or with specified substitution(s) at specified site(s) of a SEQ ID NO:, such that the sequence of each elected species is fully specified (i.e. no optional or variable residues or substituents), and/or additional molecule(s), to be searched. Additional polypeptide sequence(s), and/or molecule(s) will be searched upon the payment of additional fees. It is believed that claims 1-3, 4 (in-part), 5 (in-part), 6, 7, 8 (in-part), and 9-20 encompass this first named invention and thus these claims will be searched without fee to the extent that they encompass (AGVPG)x (polypeptide), and a chemotherapeutic (molecule). Applicants must specify the searchable claims that encompass any additionally elected polypeptide sequence(s) and/or molecule(s). Applicants must further indicate, if applicable, the claims which encompass the first named invention, if different than what was indicated above for this group. Failure to clearly identify how any paid additional invention fees are to be applied to the "+" group(s) will result in only the first claimed invention to be searched/examined. An exemplary election would be (CGVPG)x (polypeptide).
Groups I+ share the technical features including: a composition comprising: an assembly of self-assembling conjugates, each self-assembling conjugate comprising a polypeptide having a transition temperature (Tt) above 50C when the polypeptide is not attached to the conjugate; an albumin binding domain (ABD) attached to a first end of the polypeptide, wherein: i) the ABD attached to the polypeptide lowers the Tt of the polypeptide no more than 5C relative to the polypeptide's Tt when the polypeptide is not attached to the ABD or the conjugate; or ii) wherein the conjugate has a Tt above 40C at a concentration of 100 microM; and at least one molecule attached to a second end of the polypeptide through a cysteine group, wherein the molecule has an octanol-water distribution coefficient (logD) of greater than or equal to 1.5 at a pH of 7.4 when the molecule is not attached to the conjugate; a method of treating a disease or disorder in a subject comprising administering to the subject the composition; a method of localizing a molecule to a tissue or organ in a subject, the method comprising administering to the subject the composition, wherein following administration of the composition the amount of the molecule localized in the tissue or organ is decreased when compared to the molecule in a self-assembling conjugate without an albumin binding domain and wherein the tissue or organ is a kidney, liver, spleen or any combination thereof; a method of localizing a molecule to a tumor in a subject, the method comprising administering to the subject the composition, wherein following administration of the composition the amount of the molecule localized to the tumor is increased when compared to the molecule in a self-assembling conjugate without an albumin binding domain.

However, these shared technical features are previously disclosed by US 2016/0120952 A1 to Duke University (hereinafter "Duke'952"), in view of US 2016/0114053 A1 to Duke University (hereinafter "Duke'053").

Duke'952 discloses a composition comprising: an assembly of self-assembling conjugates (aggregates (an assembly) of self-assembling conjugates; paragraphs [0008], [0047], [0049]), each self-assembling conjugate comprising a polypeptide (each self-assembling conjugate comprising a polypeptide; paragraphs [0008], [0049]) having a transition temperature (Tt) above 50C when the polypeptide is not attached to the conjugate (having a transition temperature (Tt) above 50C when the polypeptide is not attached to the conjugate; paragraph [0073]); an albumin binding domain (ABD) attached to a first end of the polypeptide (an albumin binding domain (ABD) attached to a first end of the polypeptide; paragraphs [0047], [0094]), wherein: i) the ABD attached to the polypeptide lowers the Tt of the polypeptide no more than 5C relative to the polypeptide's Tt when the polypeptide is not attached to the ABD or the conjugate (wherein the albumin is attached to the polypeptide (wherein: i) the ABD attached to the polypeptide lowers the Tt of the polypeptide no more than 5C relative to the polypeptide's Tt when the polypeptide is not attached to the ABD or the conjugate); paragraphs [0047], [0094]; absent evidence to the contrary, the polypeptide with and without the albumin attached meet the claimed Tt specifications); and at least one molecule attached to a second end of the polypeptide through a cysteine group (at least one molecule attached to a second end of the polypeptide through a cysteine group; paragraphs [0008], [0158]); a method of treating a disease or disorder in a subject comprising administering to the subject the composition (a method of treating a disease or disorder in a subject comprising administering to the subject the composition; paragraph [0011]); a method of localizing a molecule to a tissue or organ in a subject, the method comprising administering to the subject the composition (a method of treating a disease or disorder in a subject (a method of localizing a molecule to a tissue or organ in a subject), the method comprising administering to the subject the composition; paragraph [0011]). Duke'952 further discloses wherein the charge distribution and size of albumin prevent filtering through the kidney glomerulus (wherein the charge distribution and size of albumin prevent filtering through the kidney glomerulus; paragraph [0047]); and wherein therapeutic proteins fused to albumin exhibit extended serum half-lives when compared to proteins in the unfused state (wherein therapeutic proteins fused to albumin exhibit extended serum half-lives when compared to proteins in the unfused state; paragraph [0005]).

Duke'952 does not disclose wherein the molecule has an octanol-water distribution coefficient (logD) of greater than or equal to 1.5 at a pH of 7.4 when the molecule is not attached to the conjugate; wherein following administration of the composition the amount of the molecule localized in the tissue or organ is decreased when compared to the molecule in a self-assembling conjugate without an albumin binding domain and wherein the tissue or organ is a kidney; and a method of localizing a molecule to a tumor in a subject, the method comprising administering to the subject the composition, wherein following administration of the composition the amount of the molecule localized to the tumor is increased when compared to the molecule in a self-assembling conjugate without an albumin binding domain.

It would have been obvious to a person of ordinary skill in the art at the time the invention was made to have modified the disclosure of Duke'952 to have compared the localization of the molecule in the absence of the self-assembling conjugate, with and without albumin; wherein, based on the avoidance of glomerular filtration, and increased lifetime of the albumin conjugate, as disclosed by Duke'952, a decrease in the distribution of the albumin conjugate in the kidney would have been a logical result, and thus obvious. It further would have been obvious to a person of ordinary skill in the art at the time the invention was made to have modified the disclosure of Duke'952 to have included the production and use of conjugates including chemotherapeutic agents, such as doxorubicin, as disclosed by Duke'053, in order to effect enhanced treatment of cancers, by enhancing the localization of the drug molecule to the tumor, as disclosed by Duke'053.

Since none of the special technical features of the Groups I+ inventions is found in more than one of the inventions, and since all of the shared technical features are previously disclosed by the Duke'952 and Duke'053 references, unity of invention is lacking.